# Probabilistic Modelling of Plug-in Hybrid Electric Vehicle Impacts on Distribution Networks in British Columbia

by

Liam Kelly

B.A.Sc, University of Waterloo, 2005

A Thesis Submitted in Partial Fulfillment

of the Requirements for the Degree of

MASTER OF APPLIED SCIENCE

in the Department of Mechanical Engineering

# Supervisory Committee

**Probabilistic Modelling of Plug-in Hybrid Electric Vehicle Impacts on Distribution Networks in British Columbia**

by

Liam Kelly

B.A.Sc., University of Waterloo, 2005

**Supervisory Committee**

Dr. Andrew Rowe (Department of Mechanical Engineering)
**Supervisor**

Dr. Peter Wild (Department of Mechanical Engineering
**Co-Supervisor**

Dr. Curran Crawford (Department of Mechanical Engineering)
**Departmental Member**

# Abstract

**Supervisory Committee**

Dr. Andrew Rowe (Department of Mechanical Engineering)
**Supervisor**

Dr. Peter Wild (Department of Mechanical Engineering
**Co-Supervisor**

Dr. Curran Crawford (Department of Mechanical Engineering)
**Departmental Member**

Plug-in hybrid electric vehicles (PHEVs) represent a promising future direction for the personal transportation sector in terms of decreasing the reliance on fossil fuels while simultaneously decreasing emissions. Energy used for driving is fully or partially shifted to electricity leading to lower emission rates, especially in a low carbon intensive generation mixture such as that of British Columbia's. Despite the benefits of PHEVs for vehicle owners, care will need to be taken when integrating PHEVs into existing electrical grids. For example, there is a natural coincidence between peak electricity demand and the hours during which the majority of vehicles are parked at a residence after a daily commute. This research aims to investigate the incremental impacts to distribution networks in British Columbia imposed by the charging of PHEVs.

A probabilistic model based on Monte Carlo Simulations is used to investigate the impacts of uncontrolled PHEV charging on three phase networks in the BC electricity system. A model simulating daily electricity demand is used to estimate the residential and commercial demand on a network. A PHEV operator model simulates the actions of drivers throughout a typical day in order to estimate the demand for vehicle charging imposed on networks. A load flow algorithm is used to solve three phase networks for voltage, current and line losses. Representative three

phase networks are investigated typical of suburban, urban and rural networks. Scenarios of increasing PHEV penetration on the network and technological advancement are considered in the absence of vehicle charging control.

The results are analyzed in terms of three main categories of impacts: network demands, network voltage levels and secondary transformer overloading. In all of the networks, the PHEV charging adds a large amount of demand to the daily peak period. The increase in peak demand due to PHEV charging increases at a higher rate than the increase in energy supplied to the network as a result of vehicles charging at 240V outlets. No significant voltage drop or voltage unbalance problems occur on any of the networks investigated. Secondary transformer overloading rates are highest on the suburban network. PHEVs can also contribute to loss of transformer life specifically for transformers that are overloaded in the absence of PHEV charging. For the majority of feeders, uncontrolled PHEV charging should not pose significant problems in the near term. Recommendations are made for future studies and possible methods for mitigating the impacts.

# Table of Contents

# List of Tables

# List of Figures

# Nomenclature

| | | |
|---|---|---|
| $D$ | Distance of a trip or commuting distance | [km] |
| $E$ | Energy | [kWh] |
| $G$ | Gasoline used | [L] |
| $I$ | Complex current | [A] |
| $M$ | Total number of iterations | |
| $N$ | Total number of transformers | [-] |
| $pf$ | Power factor of the load | [-] |
| $P$ | Real Power | [kW] |
| $Q$ | Reactive Power | [kVAr] |
| $r$ | Uniformly distributed number between 0 and 1 | [-] |
| $S$ | Complex Power Demand | [kVA, MVA] |
| $\dot{S}$ | Normalized power demand | [-] |
| $S^*$ | Peak power demand | [kVA] |
| $U$ | Probability value | [-] |
| $V$ | Complex voltage | [V] |
| $Y$ | Branch admittance | [S] |
| $Z$ | Branch Impedance | [Ω] |
| $\bar{P}$ | Average power | [-] |
| $\sigma$ | Standard deviation | [-] |
| $\mu$ | Mean value | [-] |
| $\eta$ | Efficiency | [-] |

*Subscripts*

| | |
|---|---|
| $a,b,c$ | Phase of a branch or load |
| $n, m$ | Secondary transformer |
| $h$ | Half-hour interval |
| $i$ | Iteration |
| $k$ | Branch or line section |

*Superscripts*

| | |
|---|---|
| *B* | Battery |
| *c* | Customer type |
| *cap* | Capacity |
| *CD* | Charge depleting mode |
| *CR* | Charge rate |
| *CS* | Charge sustaining mode |
| *d* | Day |
| *high* | Highest value in a range |
| *loss* | Energy or Power Loss |
| *low* | Lowest value in a range |
| *PHEV* | Total number of PHEVs |
| *PR* | Penetration rate |
| *T* | Total |
| *trip* | Simulated vehicle trip |
| *WC* | Work charging |
| *WE* | Work end time |
| *wo* | Without |
| *WS* | Work start time |
| *x* | Customer index number |

*Abbreviations*

| | | | |
|---|---|---|---|
| FBS | Forward-backward sweep | NREL | National renewable energy laboratory |
| KCL/KVL | Kirchhoff's current law/Kirchhoff's voltage law | NPTS | National personal transportation survey |
| MCS | Monte Carlo simulations | USABC | US advanced battery consortium |
| p.u | Per unit | AER | All electric range |
| PHEV | Plug-in Hybrid Electric Vehicle | GHG | Greenhouse gas |
| SOC | State of Charge | | |

# Acknowledgements

There are a number of people who I would like to thank for their support and contribution to this work.

First, I would like to thank my supervisors Dr. Andrew Rowe and Dr. Peter Wild for providing valuable guidance and insight into my work. I would also like to thank Dr. Curran Crawford for his support and valuable criticism during the course of my study. Because of all three of you my presentation and writing styles have greatly improved beyond my expectations.

I would next like to thank all the professionals at BC Hydro who took the time to help me. Specifically, thanks to Calin Micu and Adrien Tennent for their valuable modelling advice and guiding discussions. Thanks to Kelly Stich for finding great input data and helping to explain the inner workings of distribution networks to me. Thanks are also due to Alec Tsang who supervised the MITACS program that made this study possible.

Finally, I would like to thank Lily for providing me constant inspiration and reassurance as well as my parents for their support and understanding. I couldn't have done it without you.

# 1 Introduction

Recent attention to the issues of fossil fuel use such as greenhouse gas emissions, cost and supply security have led governments and automobile manufacturers to explore electric vehicle technologies in an attempt to decrease emissions from passenger vehicles and reduce reliance on fossil fuels. In the province of British Columbia, Canada (BC), a recent greenhouse gas inventory estimated that 14% of the total emissions came from the use of passenger vehicles [1].The vast majority of these vehicles derived their energy from gasoline or diesel, with little or no alternative to the type of fuel used.

Plug-in Hybrid Electric Vehicles (PHEVs) represent a promising direction in the personal transportation sector for decreasing the reliance on fossil fuels while simultaneously decreasing emissions [2]. Taking the concept of the hybrid electric vehicle (HEV) a step further with the addition of a larger battery, PHEVs have the ability to travel on electricity derived from the electrical grid for small distances. The inclusion of a small gas engine or generator increases the range of the vehicle, thus maintaining the reliability of the familiar internal combustion engine. Currently, most of the major automobile manufacturers are considering or designing a PHEV or a full electric vehicle (EV). While there are a number of vehicle technologies and drive train arrangements being considered by manufacturers, this thesis will focus on near-term PHEV technologies.

Advantages for PHEV owners will be reduced fuel costs and emissions as driving on electricity has been found to be less expensive per mile and typically produces less emissions than a conventional vehicle, even in highly fossil based systems [3]. In fact, the emissions per

mile were found to be similar to a hybrid electric vehicle when charging on a generation mixture consisting mostly of coal and natural gas [4]. In British Columbia, electricity is generated by large hydroelectric dams with low emission intensities and thus PHEVs are an attractive option for reducing emissions in the transportation sector in the province. The wide availability of existing charging infrastructure in the form of 120/240V outlets at homes and offices is another strong argument for a transition to PHEVs, over other alternative vehicle technologies such as fuel cells.

Despite the potential benefits for PHEV owners when compared to conventional vehicles, reconciliation will be needed between vehicle owners and grid operators [5]. For example, there is a natural coincidence between peak electricity demand and vehicles returning to a residence after a daily commute. This coincidence between vehicle charging demand and existing peak demand is the principle near-term concern from the utility point of view. Previous studies have called for some form of control over vehicle charging to avoid adding to the peak demand [3,6].

For the utility operator in the long term, PHEVs present the possibility of a distributed energy storage mechanism that can be controlled to increase the efficiency of the grid [7]. First, and most likely in the near term, PHEVs may operate as a responsive load where the time of day when the vehicles charge would be controlled. This would shift vehicle charging to off-peak hours. Second, and requiring a more complicated integration, the PHEVs' batteries may be able to supply power back to the grid in an operating mode known as Vehicle-to-Grid or V2G. This scheme may prove more useful in terms of economic and technical operation of the grid [5].

This research investigates the impacts that are likely to be seen on the electricity system due to the charging of PHEVs, specifically focussing on distribution networks. It is unlikely that

large-scale dispatch of generators or operation of transmission systems will be greatly affected by small penetrations of PHEVs. However, even with low penetrations of PHEVs across a province or transmission system, certain neighbourhoods or areas could have higher penetration rates; such an effect has been seen with the aggregation of hybrid electric vehicles [8]. Thus, distribution networks are where the first impacts from PHEVs are likely to occur and these systems are therefore the focus of this research. Also, it will be some time before proper time-of-use incentives or charging control infrastructure is in place to encourage vehicle charging during the low demand hours, thus, this study will focus on impacts in the absence of vehicle charging control methods.

To investigate the impacts of PHEVs on distribution networks, an analogy can be drawn between electric vehicles and distributed energy resources (DERs), such as distributed generation. For example, the vehicles will be distributed in a random fashion and connect to the customer side of the meter, similar to many distributed generators such as rooftop photovoltaics. The action of PHEV drivers connecting to the grid will be somewhat predictable, but will contain elements of randomness much like many distributed renewable energy generators. It is also very important to understand how people use their vehicles and what actions they will take to charge their vehicles. The behaviour of vehicle operators is an important aspect for understanding the connection of PHEVs to the grid, similar to understanding how the weather or season may affect a renewable generator's output.

The considerations for connection of PHEVs to distribution networks are similar to that of other DERs and should be subject to the same technical, economic and regulatory challenges. Technical challenges may include large voltage drops, increased losses, voltage unbalance and other issues related to power quality [9]. Economic challenges include costs of infrastructure,

maintenance and shifting the operation of distribution networks toward active instead of passive management [10]. The third and perhaps most important challenge is a regulatory one; without clear policy from both governments and utilities, it is unlikely that PHEVs will have the impact that some researchers are suggesting is possible [11].

The aim of this research is to investigate the impacts of PHEV charging on distribution networks in the absence of vehicle charging control strategies. A probabilistic model based on Monte Carlo simulations is developed and used to achieve this objective. The model uses a simulation of daily residential and commercial loads on representative three-phase distribution networks within the BC transmission system. A PHEV operator simulation model is coupled to the load model to estimate the demand for vehicle charging and the emissions from driving. A direct concern is to estimate the impacts on certain power quality aspects of the network such as voltage and current constraints as well as to determine the emissions from operation of PHEVs. These impacts are investigated under scenarios of PHEV penetration and technology advancement.

Chapter 2 of this thesis contains a literature review, where methods of analyzing distributed energy resources and examining PHEV impacts are summarized. The literature review highlights the necessity of using a probabilistic approach for this research as well as summarizing some of the recent studies investigating PHEV impacts on the grid. In Chapter 3, a model framework outlining the probabilistic load flow model using Monte Carlo simulations is provided, with a discussion of the three phase aspects of distribution networks and the load flow algorithm used. The method for simulating the residential and commercial loads that are used as inputs to the probabilistic load flow model and the techniques used for simulating the vehicle charging aspects are also described in Chapter 3. Following this, Chapter 4 presents three representative

distribution networks from the BC grid and summarizes the scenarios used as inputs to the model, including the assumptions for battery sizes, charging rates and PHEV penetration. The modelling results follow in Chapter 5, starting with the impact that PHEV charging may have on the network demand in terms of power and energy. The network voltage drop, voltage unbalance, network energy losses and secondary transformer overloads are investigated to examine the frequency and probability of impacts caused by PHEV charging. The fuel consumption of vehicles in the network is analyzed including the emissions released from driving on gasoline and an estimate of the emissions created from vehicle charging. In the discussion and conclusions sections of Chapters 6 and 7, the key results and insights are highlighted with recommendations for future work concluding the thesis.

# 2 Literature Review

This chapter reviews previous research related to distribution network modelling and PHEV impacts on the grid. The first section reviews aspects of modelling distribution networks and the integration of distributed generation. The need for a probabilistic analysis is highlighted. The second section reviews some of the recent large scale studies conducted to investigate potential environmental and grid related impacts of PHEVs.

## 2.1   Probabilistic Modelling of Distribution Networks

The traditional method for operation of distribution networks has been challenged in recent years by the concept of distributed energy resources (DERs). These resources could include distributed generation (DG), combined heat and power systems, responsive loads or energy storage systems [12]. Recent attention has been given to shifting the architecture of energy systems away from centralized power plants located large distances from load centers toward many small electric power sources connected throughout distribution networks, often on the customers side of the meter. Lopes et al. [11] review the economic, technical and environmental challenges of integrating a variety of DERs into distribution networks. The review highlights the commercial, regulatory and environmental drivers causing the shift towards DERs. Emphasis is placed on the notion that these resources should not be regarded in a *fit and forget* manner but should be *integrated* into the larger system for maximum benefit.

A load flow (or power flow) algorithm solves the non-linear relationships among complex power demand, line currents, bus voltages and angles with the network constants provided in terms of circuit parameters such as impedance and network structure [13]. Traditionally, distribution networks are radial, passively operated systems that were designed using load flow

studies to capture the critical or high demand cases. Typically, the design was aided through deterministic studies that contained no elements of randomness. Only the maximum power demand expected from groups of customers needed to be specified, and a single solution was enough to capture the absolute voltage drop and maximum line currents expected to occur on a network.

When considering the connection of DG to a distribution network, load flow calculations can be used to assess the maximum number of generators allowed in order to ensure the voltage and line current carrying capacities are not exceeded. Because DG may be based on renewable energy sources such as wind and solar, a deterministic load flow may not capture the intermittency and random nature of these sources and may be an inadequate approach to assessing the true impacts on the distribution network. Conti and Raiti [14], show that the use of a traditional deterministic load flow leads to an overestimation of the maximum photovoltaic (PV) power that can be installed. They also outlined a probabilistic load flow (PLF) algorithm with appropriate statistical models for loads and PV generator productions that provides a more accurate evaluation of PV integration.

Monte Carlo Simulation (MCS) is a modelling technique that involves repetition of a simulation process using a set of probability distributions defining the random variables of interest. MCS methods are commonly used for PLF studies. In the case of distribution networks these variables are usually consumer loads and DG production [11]. In a MCS, the random variables are sampled at each repetition from a probability density function and used as inputs to the load flow program. The output from a PLF estimates the frequency of adverse events such as overvoltage, voltage drop and transformer overloads.

McQueen et al. [15] used MCS to model residential electricity demand and its application to low voltage regulation problems. Their predicted voltage distributions were compared to actual voltage readings showing a good match between modelled and measured voltages. El-Khattam et al. [16] presented a MCS algorithm that used a single phase representation of a distribution network to estimate the impacts of DG units on the steady-state system behaviour. They estimated the power loss savings and the impacts to bus voltage variation due to the presence of DG. An interesting application of the MCS approach to probabilistic network modelling by Mendez et al. [9] studied the use of DG for the deferral of capital investment. Their results find that once some initial network reinforcements for DG connection are in place, significant investment in feeder and/or transformer reinforcements can be deferred. In the context of distribution networks, MCS have also been applied to study reliability improvements due to energy storage systems [17] and to examine the impact of harmonic distortions [18].

Often in the PLF literature, the load on a three phase network is assumed to be fully balanced and a single phase representation of the network is applied. In real distribution systems, the lines are unbalanced and sections can carry a mixture of single, double or three phases. This mixture of lines and the presence of single and three phase loads causes imbalances where the voltage phase angles are not always $120^0$ displaced and the magnitude of the voltages between lines are not always equal. Caramia et al. [19] used a three phase representation of a distribution network to investigate a PLF with MCS considering only phase-load demands and network configurations. They recently extended this work to incorporate the effects of wind farms with asynchronous machines on the unbalance of the network [20]. The three phase model provides a more realistic evaluation of the network operation as phase unbalance in distribution networks can cause increased losses, upstream problems to the transmission network and increases the

likelihood of a fault. The impacts on the unbalance of the system should therefore be taken into account when performing a PLF where possible.

## 2.2    Summary of Plug-in Hybrid Electric Vehicle Studies

In contrast to the work being done in the field of integration of DG, no research has been published that focuses on the integration of PHEVs into distribution networks. The majority of PHEV studies so far have been aimed at two aspects of PHEVs: (1) the long term impacts of large penetrations of PHEVs on existing power systems and the effects on the dispatch of generation assets and (2) assessing the environmental impacts, upstream emissions and battery technology.

An environmental assessment of PHEVs performed by the electric power research institute (EPRI) examined the emissions from vehicles and the electric sector under various scenarios of electric sector $CO_2$ intensity and electric vehicle penetrations from 2010 to 2050 [4]. The study found that annual and cumulative $CO_2$ reductions were possible in every scenario analyzed, ranging from reductions of 163 to 612 million metric tons of $CO_2$ annually by the year 2050. Vehicle emissions per mile were calculated based on the upstream electric sector $CO_2$ emissions and upstream gasoline emissions (well-to-tank). They found that PHEVs or EVs have similar or less emissions than regular hybrid electric vehicles (HEVs) in all scenarios of carbon intensity.

A study performed at the National Renewable Energy Laboratory (NREL) [21] investigated the costs and emissions associated with PHEV charging in a Colorado service area. The authors created aggregate charging profiles for a 30% penetration of PHEVs and, using a generation dispatch algorithm to optimally dispatch power, they investigated the operation with and without the charging of vehicles. This study found that no additional generating capacity would be

required even for massive penetrations of vehicles assuming some form of vehicle charging control is in place. Similar to the study by EPRI, they concluded that PHEVs would allow for significant emissions reductions, even in the highly fossil based system under study.

Another large scale scoping study [22] estimated the regional percentages of the energy requirements for the US light duty vehicle (LDV) stock that could be supported by the existing infrastructure in 12 NERC (North American Energy Reliability Council) regions. They found that up to 73% of LDVs energy requirement could be supported without the need for additional capacity. Similarly, Denholm and Short [6] found that for six regions in the U.S., large-scale deployment of PHEVs will have limited negative impacts on the electric power systems in terms of the need for more additional generation capacity. The studies discussed above have all assumed some form of utility or third party control over vehicle charging to avoid charging during the peak demand periods. These large-scale utility studies have shown that proper control of vehicle charging can lead to benefits to the grid and to the transportation sector in terms of operational costs and emissions.

A recent survey of drivers of hybrid vehicles converted to PHEVs performed by Kurani et al [23] showed some interesting results, despite a small number of respondents. They found that very few drivers, if any, considered the impact that their vehicle charging had on the grid. Also, upwards of 80% of drivers plugged their vehicles in whenever possible, especially at routine locations such as home and work. This brief study, while not statistically significant due to the limited sample size, shows that the behaviour of PHEV owners is an important aspect that must be considered and that a wide range of actions is likely to occur when examining vehicle charging in the near-term.

To the author's knowledge, there has yet to be any literature published that has examined the impact of PHEVs on the operation of distribution networks. As PHEVs slowly enter the market, it will be some time before proper charging control mechanisms are realized and put in place. Until then, it is unlikely that many vehicle owners will consider the impacts to the grid when charging their vehicles and will likely plug their cars in at every opportunity. The stochastic nature of human decisions for vehicle operation can be thought of as similar to intermittent renewable energy, and thus a probabilistic approach to modelling should be undertaken when considering PHEVs connection to distribution networks.

# 3 Model Overview

This chapter provides a background on distribution networks and a description of the probabilistic model. The processes for load modelling and PHEV simulation are also explained. All modelling work in this thesis is performed in the Matlab™ environment.

## 3.1 Three Phase Distribution Networks in BC

A simplified one-line example of a distribution network is shown in Figure 3.1. The distribution system starts with a substation that is fed by a high-voltage transmission line or sub-transmission line. The substations serve primary "feeders", the vast majority of which are radial, meaning there is only one flow path for the power from substation to customer [24]. The substation's main function is to reduce the voltage down to the primary distribution voltage level. The primary feeder distributes the power throughout the network to the secondary transformers where the voltage is further decreased to the customer level of 120/240V. It should be noted that all networks considered in this thesis are 4-wire "wye" systems; the line voltages are separated into three phases displaced by an angle of $120^0$, with a single neutral return wire.

Every distribution network is designed to meet the specific requirements of the area it serves. An attempt is made at the design stage to balance the load amongst the phases to ensure efficient operation; however, the loading on a network is inherently unbalanced because of the presence of unequal single phase loads. Thus, a single phase representation as is typically useful for transmission systems analysis is not adequate, and a full three-phase analysis should be employed [25]. When the load is unbalanced on the network, current will flow in the neutral wire increasing the system losses. For customers connected to a three phase secondary transformer, unbalanced voltages can cause three phase induction motors to function improperly.
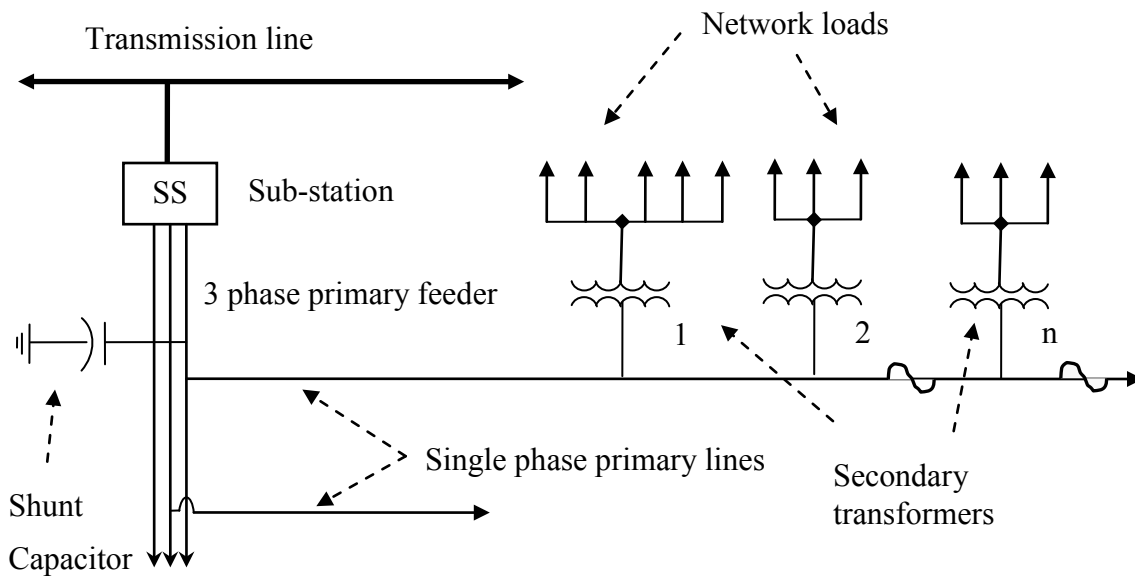
**Figure 3.1 Simplified one line diagram of a three phase distribution network**

## 3.2    Model Description

As mentioned previously, the model presented here is a probabilistic load flow model using Monte Carlo simulations to capture the stochastic nature of loads and PHEV charging to estimate the impacts on distribution networks. A detailed flow chart is shown in Figure 3.2, outlining the general steps taken in the algorithm. The model begins by selecting a distribution network to study and selecting a scenario that provides the input parameters to be used in the model, such as: the penetration rate of PHEVs, the amount of office and retail charging, size of PHEV batteries, etc. The scenarios are explained in Chapter 4.
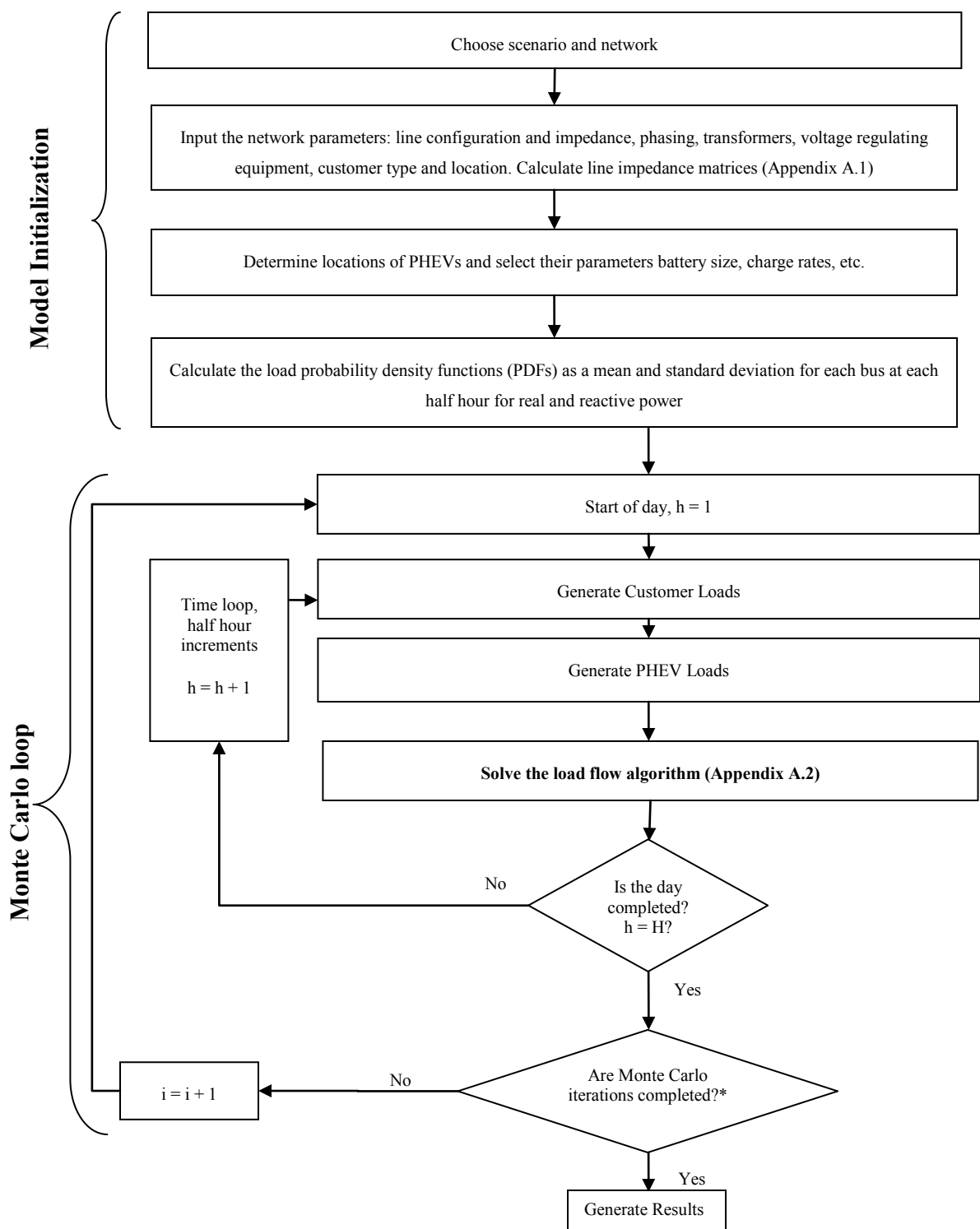
**Figure 3.2. PLF model logic flowchart**

With a scenario and network selected, the next step is to import the parameters that define the network. This includes the locations of all voltage regulating equipment, phasing of the branches, locations and types of customers and structure of the network. This information is then used to calculate generalized line impedance matrices that are used when solving the deterministic load flow algorithm. These calculations are outlined in Appendix A. PHEVs are assigned randomly throughout the network to the residential customers and their battery sizes, home charging rate and other parameters defining their vehicle characteristics are initialized. Probability density functions describing the customer demand at each hour and for each customer are calculated next. With all of the inputs to the model defined, the Monte Carlo (MC) loop is initialized.

The MC loop repeats a single "peak load" day multiple times solving the deterministic steady-state load flow algorithm at a half hour resolution. The MC loop begins by generating the residential and commercial demand on the network based on the probability density functions calculated earlier. The PHEV simulation follows, calculating the number of PHEVs connected both in residential and commercial locations and determining their charging demand on the network. The PHEV simulation also calculates fuel consumption and battery state of charge for any driving events that may occur during a given time period for each vehicle. Once the PHEV load is determined and the complex power demand at each bus of the network has been calculated for that time point, the deterministic load flow algorithm is solved producing voltage and current magnitudes and angles for the buses.

The deterministic load flow algorithm assumes that the complex power supplied to the network is in a steady state and solves for the line currents, bus voltages and phase angles using a forward-backward sweep algorithm outlined in Appendix A.2. The network complex power loss

is calculated following the solution to the load flow. Any transformer/current ratings or bus voltage limits that are exceeded during the simulations are flagged. The MC loop continues the process of generating input data and solving the deterministic load flow algorithm for multiple iterations until a predetermined number of iterations have been reached, determined by a convergence analysis of the means and standard deviations (Section 5.1).

The methods described in this chapter are used to estimate the customer demands and PHEV charging demands at each location in a network. A number of variables are probabilistically determined during model initialization and during the Monte Carlo loop, these variables are summarized in Table 3.1. Customer electricity demands are described by a normal distribution, which produces a demand value ($S_{n,h,i}$) for each half-hour ($h$) and iteration ($i$) at each secondary transformer ($n$) in the network. Similarly, the PHEV simulation model predicts the temporal charging demand for each individual PHEV at residential, office and retail locations on the network. The individual PHEV demands are summed at each secondary transformer for each half hour and iteration of the model ($S_{n,h,i}^{PHEV}$). In the model derivation, superscripts are used for descriptive variables to distinguish between types of loads and customers for example, $S^{PHEV}$ to represent PHEV demand. Subscripts are used for tracking the Monte Carlo model parameters $n$, $h$ and $i$.

**Table 3.1. Summary of probabilistic parameters that are selected throughout the model**

| Probabilistic Parameter | Symbol | When it is selected during the model |
|---|---|---|
| Vehicle trip distance and timing | $D^{trip}$ | PHEV simulation model/Monte Carlo loop |
| Customer loads | $S_{n,h,i}$ | Each half hour/Monte Carlo loop |
| Initial battery SOC for PHEVs at office locations | SOC | Monte Carlo loop |
| Charging demand at retail chargers | $S_{n,h,i}^{PHEV,retail}$ | Each half hour/Monte Carlo loop |
| CD mode efficiency | $\eta^{CD}$ | Each simulated PHEV trip |
| CS mode efficiency | $\eta^{CS}$ | Each simulated PHEV trip |
| Battery size | $B$ | Model initialization |
| Charge rate at home | $CR$ | Model initialization |
| Work start time | $WS$ | Model initialization |
| Work end time | $WE$ | Model initialization |
| Charging at work | $WC$ | Model initialization |
| One-way commuting distance | $D$ | Model initialization |
| Location of residential PHEVs | - | Model initialization |
| Number of installed retail and office chargers | # Chargers | Model initialization |

## 3.3   Network Solution Algorithm

As mentioned, the core of the probabilistic model is a steady-state deterministic three phase load flow algorithm. There are many options when selecting an algorithm for load flow solutions for distribution networks. The traditional approach is to use an algorithm that takes advantage of the radial structure of the network in an iterative fashion. A ladder iterative technique known as the forward/backward sweep (FBS) algorithm was chosen for its simplicity and robustness in radial systems [25]. The details and equations used in this algorithm are shown in Appendix A. A brief description follows.

The first step in the FBS algorithm calculates generalized line impedance matrices that relate sending end and receiving end voltage and current for all of the lines. The generalized matrices can also be used to model the voltage regulators, shunt capacitors or in-line transformers. The algorithm makes use of Kirchhoff's voltage law (KVL) and Kirchhoff's current law (KCL) with the generalized matrices. The iterative process begins at the extreme buses of the network that are the furthest from the substation and assumes that they are at the base voltage of the network for the first iteration. The complex (real and reactive) power is known at all buses in the network so the current in the furthest branches can be determined. This value is then used with KVL to find the voltage at the upstream bus. When the upstream voltage is calculated, the current at the upstream bus is found using KCL. In this manner, all the currents and voltages are calculated stepping forward towards the substation. When the substation is reached, the calculated voltage is compared to the set-point (base) voltage of the substation. If it is within the tolerance of the calculation, then the iteration can stop. If it is not, then the backward sweep begins by resetting the substation voltage to its base value.

The backward sweep calculates new voltage values using the current values calculated during the forward sweep and moving downstream using KVL and KCL until the extreme buses are reached at which time the forward sweep begins again. This forward/backward sweep process is repeated updating the voltages and currents after each sweep. The process continues until the maximum difference in set-point substation voltage and calculated substation voltage converges to a predefined tolerance of $1\times10^{-4}$ per unit of voltage. At this point the voltage and current at each bus and on each line throughout the network is known. The calculations of power loss in the system can then be completed (Appendix A.2). For simplicity in calculations and

reporting, the per-unit (p.u.) system is used for all calculations in this thesis as explained in Appendix B.

## 3.4   Customer Demand Modelling

Determining the power demand on a distribution network is a difficult task due to the stochastic behaviour of the customers connected to it and seasonal changes in both climate and light. An efficient method to predict the 24-hour total load curve at a distribution substation is to sum the load curves corresponding to the various types of customers supplied by the substation [26]. These customer 24-hour load curves for each specific season or day show a small variation around a mean value. Thus, it is common when performing probabilistic load flow studies to assume a normal distribution of load within a time interval for each load bus and customer class on the network [14, 19, 26]. The normally distributed load values are assumed to be independent of time, meaning that load values do not depend on the previous or subsequent load value.

For this thesis, five unique customer classes are identified: apartments, single detached homes (houses), offices, retail and other. The "other" class is used for locations with little to no expected PHEV charging demand such as schools and municipal pumping stations. It is important to separate the customers into unique classes because each exhibits distinct 24 hour load profiles, and the assumptions for vehicle charging and simulation will be different for each class.

The assumption of a normally distributed load is convenient because the distribution is completely described using only the mean and standard deviation of the load at the given hour as shown [14]:

$$f(P_{n,h}) = \frac{1}{\sigma_{n,h}\sqrt{2\pi}} \cdot e^{\frac{-(P_{n,h}-\overline{P_{n,h}})}{2\sigma_{n,h}^2}} \qquad (3.1)$$

where $P_{n,h}$ is the load value, $\overline{P_{n,h}}$ is the mean and $\sigma_{n,h}$ is the standard deviation at each half-hour (*h*) and secondary transformer (*n*). With an average half-hourly load profile and standard deviation, the probability density function (PDF) shown in Equation (3.1) can be used to generate load data within the bounds of each PDF. A brief analysis was performed to validate the assumption of normality of the load when considering various numbers of customers connecting to a single transformer. This analysis, performed in Appendix C, shows that for five or more residential customers connecting to a single transformer, the load at a given hour can be considered to be a normal distribution at the 95% confidence level.

To estimate the PDFs for each bus on the network, a normalized annual load profile for each customer class was used to calculate a mean and standard deviation at each half hour of a day. Normalized profiles are used due to a lack of individual customer class data, or substation level hourly data. The normalized profiles were supplied by BC Hydro from estimates of annual customer demands. To calculate the PDF parameters, a time window representing three high-demand winter months (90 days, mid-November – mid-February) centered on the peak demand day was selected. This peak load period was chosen to represent a worst-case demand scenario. As an example, a normalized mean load profile for a group of single detached homes is shown in Figure 3.3. The half hour increments were found by interpolating linearly between the hours.
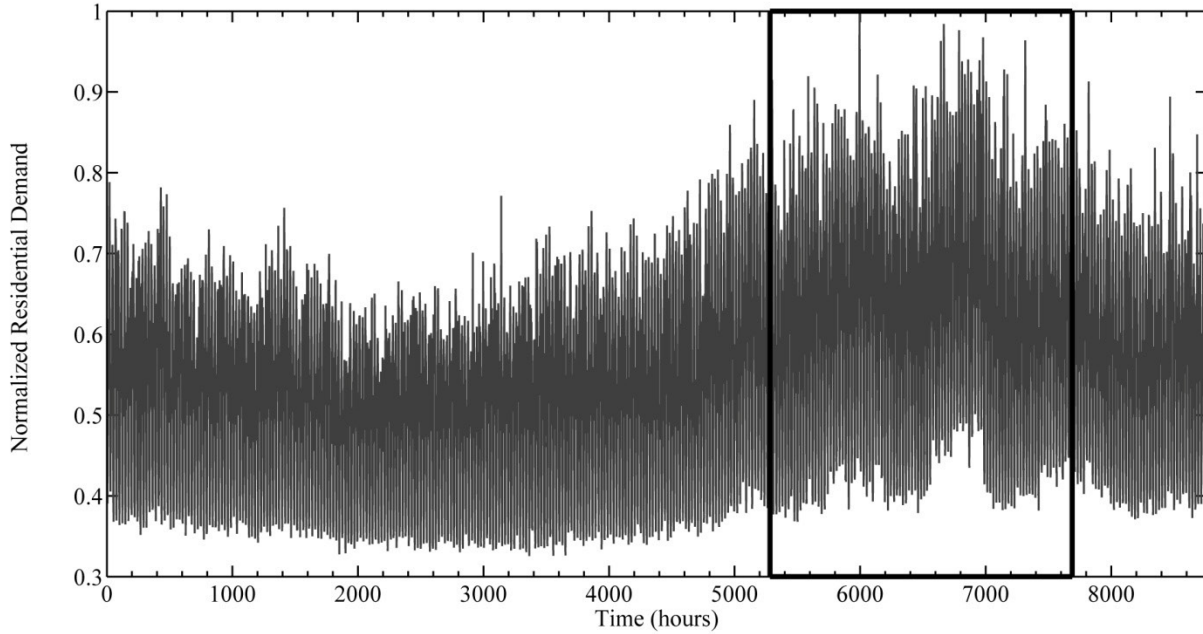
**Figure 3.3. Normalized annual load profile for a group of single detached residences showing the selected time window for calculating probability density function parameters**

The only demand data available that was specific to each network was the customer monthly energy consumption readings and a peak substation demand reading taken monthly by a technician through a field visit to the substation. The method used to estimate the PDF parameters is shown in Figure 3.4.

To simplify the nomenclature used for customer demand modelling, the following conventions are used. Peak values will be denoted with an asterisk, such as $S^*$ to represent peak power demand. Normalized values will be denoted with a dot accent, such as $\dot{S}$. The superscript $c$ is used to represent the customer class where $c$ can have the values: *house, apartment, retail, office* or *other*.
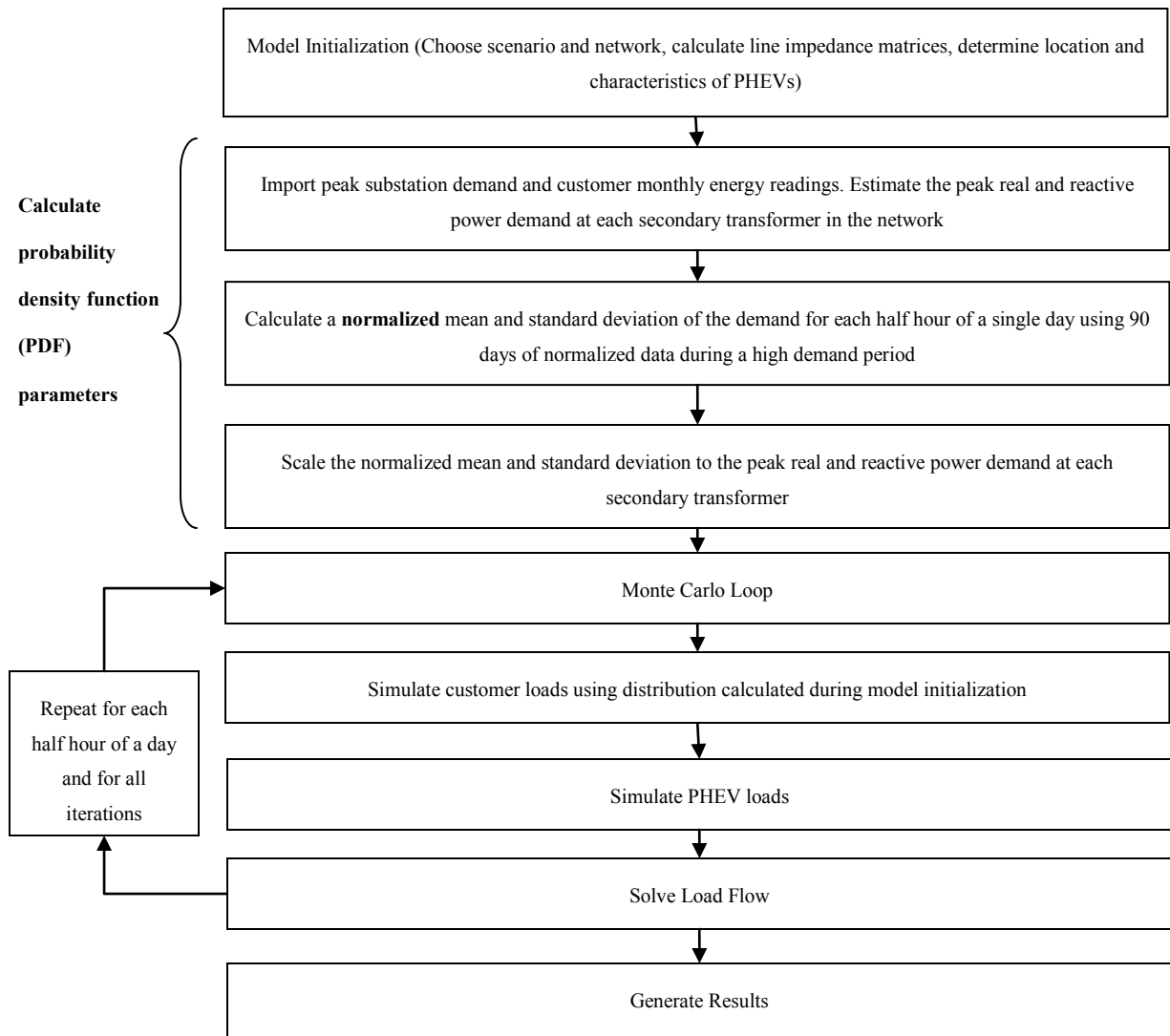
**Figure 3.4. PLF model logic flow chart showing process to calculate probability density function parameters for customer load generation**

Only one type of customer class is connected to each secondary transformer. Thus, the PDFs for individual transformers can be specified without the need to specify a PDF for each individual customer on the network. The following method is used to create PDFs at each half hour for each group of customers attached to a secondary transformer:

1) The peak demand on each secondary transformer is first estimated by dividing the substation peak demand amongst all secondary transformers. The peak substation demand reading ($S^{*,T}$) is allocated to each secondary transformer (*n*) in the network by dividing the energy consumption of each group of customers at a secondary transformer ($E_n$) by the total energy consumption of all the customers in the network ($E^T$) and multiplying by the peak substation demand. This creates a peak demand value ($S_n{}^*$) at each secondary transformer that when summed equals the recorded peak feeder demand as shown in Figure 3.5. This step allocates the peak feeder demand such that customers with higher energy consumption share a larger percentage of the peak load. The peak load at each transformer is:

$$S_n^* = S^{T,*} \cdot \frac{E_n}{E^T}$$

(3.2)
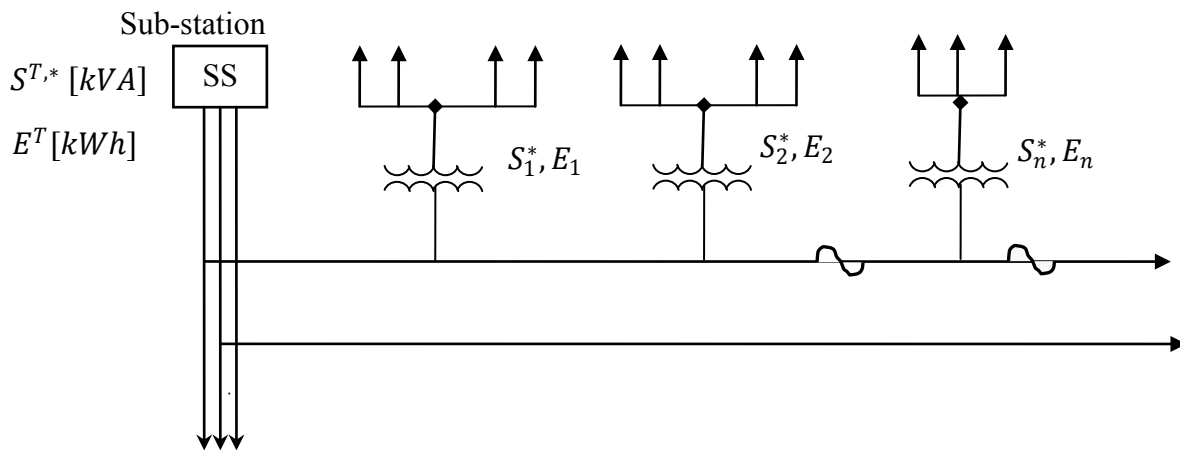


**Figure 3.5. Allocation of peak substation demand to secondary transformers**

2) A power factor (*PF*) estimate equal to 0.94 [27] was used to calculate the real ($P_n^*$) and reactive ($Q_n^*$) components of the peak demand for each customer group:

$$P_n^* = S_n^* \cdot PF \tag{3.3}$$

$$Q_n^* = \sqrt{(S_n^*)^2 - (P_n^*)^2} \tag{3.4}$$

3) Now, the normalized load data, such as that shown in Figure 3.3, is used to calculate normalized means and standard deviations for each half hour of a day. Dot accents are used above variables to represent normalized values. The normalized load data for each half hour ($h$), day ($d$) and customer class ($c$), $\dot{P}_h^{c,d}$, is used to calculate a mean and standard deviation of the normalized load at half hour intervals ($\overline{\dot{P}_h^c}$ and $\dot{\sigma}_h^c$) over a 90 day period. This produces vectors of normalized load half hour means and standard deviations for each customer class for a single day:

$$\overline{\dot{P}_h^c} = \frac{\sum_{d=1}^{90} \dot{P}_h^{c,d}}{90} \quad \forall\, h, c \tag{3.5}$$

$$\dot{\sigma}_h^c = \sqrt{\frac{\sum_{d=1}^{90} (\dot{P}_h^{c,d} - \overline{\dot{P}_h^c})^2}{90}} \quad \forall\, h, c \tag{3.6}$$

4) The normalized means and standard deviations vectors from Equations (3.5) and (3.6) were then scaled for each secondary transformer by multiplying each element of the vectors by the real and reactive peak transformer demand calculated in Equations (3.3) and (3.4):

$$\overline{P_{n,h}^c} = \overline{\dot{P}_h^c} \cdot P_n^* \quad \forall \, h, c, n \tag{3.7}$$

$$\sigma_{n,h}^c = \dot{\sigma}_h^c \cdot P_n^* \quad \forall \, h, c, n \tag{3.8}$$

Equations (3.7) and (3.8) are repeated using the reactive power $(Q_n^*)$ calculated from Equation (3.4) with the same mean and standard deviation $(\overline{\dot{P}_h^c}$ and $\dot{\sigma}_h^c)$. Scaling in this manner preserves the power factor of the load.

This method ensures that the sum of the resulting load profiles of each secondary transformer will represent a "high demand" day in order to reflect a worst-case scenario of network demands. The normalized load profiles $(\dot{P}_h^c)$ for three of the customer classes are shown in Figure 3.6; the retail and "other" load categories have a very similar profile to the office load and are not shown.
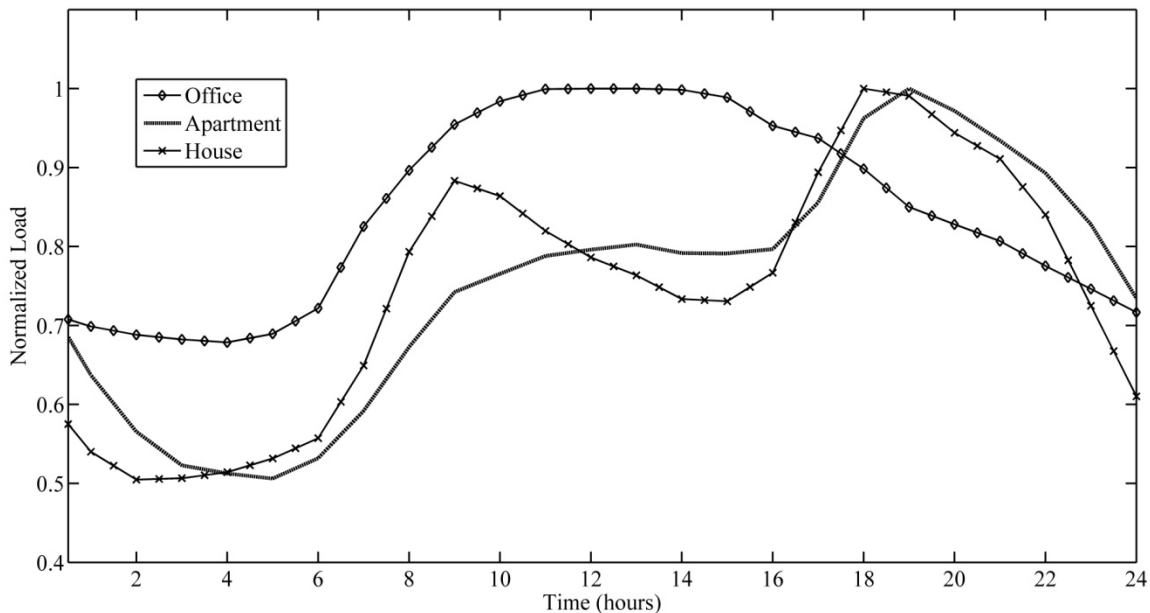


**Figure 3.6. Normalized load profiles for apartment, house and office**

## 3.5    Simulation of PHEV Charging Behaviour

Many difficulties arise when attempting to model the temporal charging demand and predict the technological aspects of PHEVs in future scenarios. First and most importantly, there are currently no PHEVs or EVs in production leading to a wide uncertainty in the types of technologies and market penetrations that will be seen in the coming years. Second, the scale of distribution networks may not warrant an aggregated charging demand modelling approach due to the small number of PHEVs on the networks, especially when examining low PHEV market penetration scenarios. Third, the assumptions for vehicle charging within residential or commercial customer classes will be inherently different. The above points show a need to take a novel approach to modelling PHEV driver's actions while segregating the vehicle simulation model by customer class and considering the uncertainties in PHEV technology.

The following sections describe the major assumptions and simulation techniques used for determining the vehicle charging demand on a network in residential and commercial settings. A separate set of assumptions is used for residential (both homes and apartments), office and retail locations. The residential PHEV model simulates the daily driving behaviour of each individual PHEV owner that resides on the network in a probabilistic manner.

### 3.5.1  PHEV Technology Assumptions and Vehicle Characteristics Selection

The assumed specifications and operating parameters used for PHEV technologies were taken from a recent report on a joint effort between NREL and the US Advanced Battery Consortium (USABC) who attempted to define requirements for energy and power, electric range, cost, volume, weight and calendar life of future PHEV batteries [28]. Their researchers considered two main modes of PHEV operation: charge depleting (CD) and charge sustaining

(CS) modes. CD is an operating strategy in which the vehicle's battery state of charge (SOC) decreases steadily while the vehicle is driving, relying very little, if at all, on the gas engine. The average distance that a PHEV is capable of driving in CD mode when the battery is full is called the all-electric range (AER). In CS mode, the battery SOC may vary slightly but on average is maintained at a certain level by utilizing both engine and battery, an identical operating strategy is used in most hybrid electric vehicles. These types of vehicles are commonly known as extended range electric vehicles (EREV), but are still classified as PHEVs because of the hybridization between gas and electric motor.

The USABC results suggest battery size requirements for specific AERs including energy and gasoline consumption for CD and CS modes. The requirements put forth by the USABC were selected for use as future PHEV specifications in this study because they represent a realistic target for future PHEV batteries. Two main vehicle batteries were highlighted by the USABC – a PHEV-10 and a PHEV-40, meaning PHEVs with 10 and 40 mile AERs, respectively. The characteristics of these vehicles are summarized in Table 3.2. For simplicity in estimating energy consumption, it is assumed that the engine does not turn on during CD mode.

The process for selecting the vehicle characteristics of individual PHEVs is performed before the Monte Carlo loop is initialized as shown in Figure 3.7. During model initialization, the assumed penetration rate ($U^{PR}$) of PHEVs is used to randomly assign vehicles to residential apartments and houses. This is accomplished by stepping through a loop of each individual customer (not customer groups). For each residential customer ($x$), a randomly generated number ($r^x$), uniformly distributed between 0 and 1 is compared to the penetration rate of PHEVs (Table 4.1). If the random number ($r^x$) is less than the penetration rate, then a PHEV will be assigned to that secondary transformer location. Once the vehicles are assigned a location, a full set of

characteristics are assigned to each vehicle. These characteristics remain constant throughout the Monte Carlo Simulations. The selection method described above, where a uniform random number is compared to a probability value to select residential PHEV locations, is used extensively throughout the model to select vehicle characteristics, control the vehicle trips, and select locations for retail and office charging. A flow chart of the method used to select the vehicles and their characteristics is shown in Figure 3.8.

**Table 3.2. PHEV Technology Assumptions**

| Vehicle or Battery Characteristics | PHEV-10 | PHEV-40 |
|---|---|---|
| Total Battery Size, B (kWh)[1] | 4.85 | 16.6 |
| Available Battery Energy for CD mode or grid recharge when empty (kWh)[1] | 3.4 | 11.6 |
| Outlet Recharge Rate, CR @ 120V 15A (kW) [28] | 1.44 | |
| Outlet Recharge Rate, CR @ 240V 40A (kW) [28] | 7.6 | |
| Vehicle's Charger Efficiency (%) | 90 | |
| CD Mode Efficiency (kWh/km) [29] | 0.171-0.249 | 0.180 – 0.264 |
| CS Mode Efficiency ( (L per 100 km) [29] | 4.5 – 4.7 | 4.6 – 4.9 |
| Vehicle Charging Power Factor Estimate | 0.95 | |
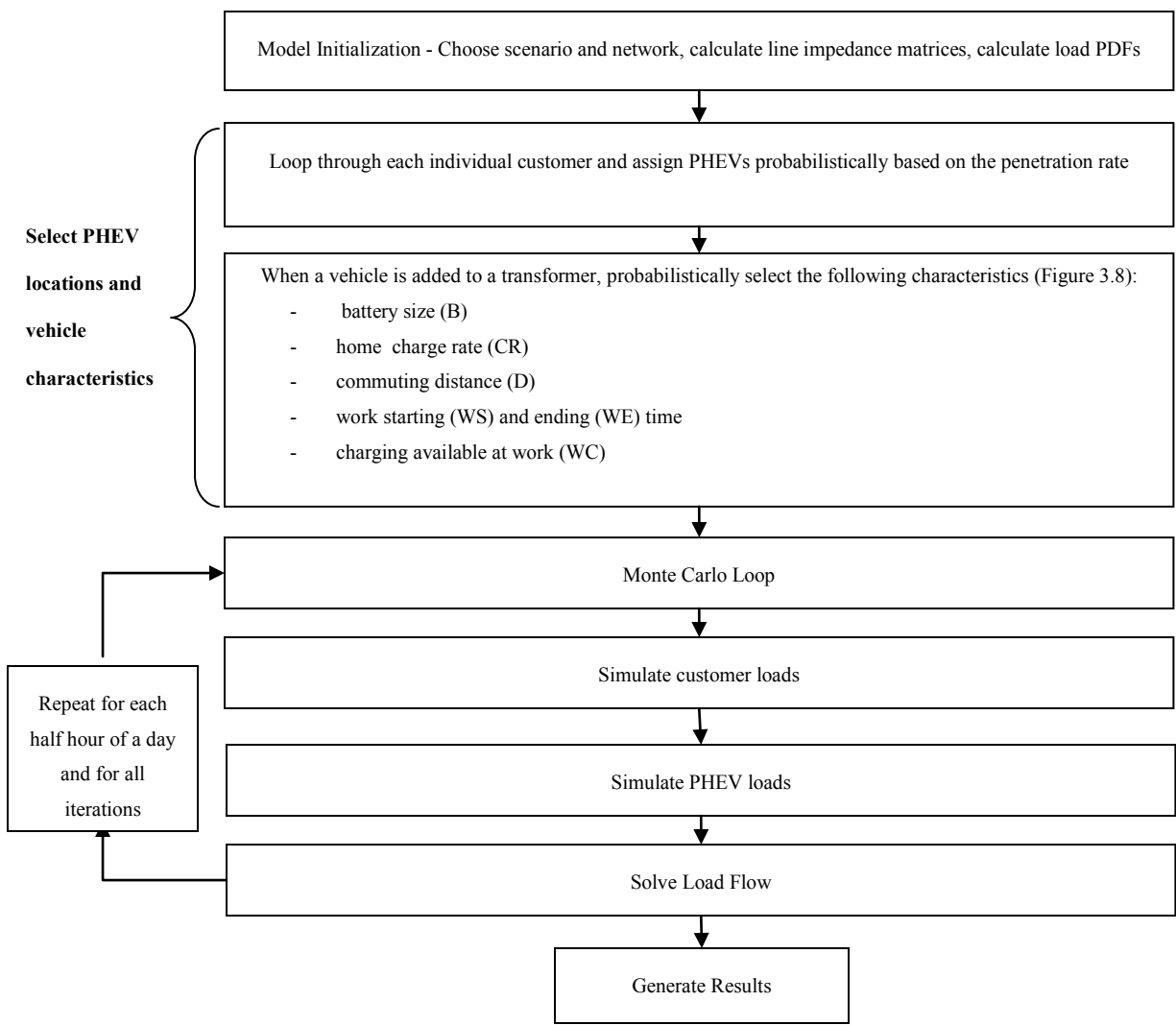
**Figure 3.7. PLF model logic flow chart showing processes to select vehicle characteristics**
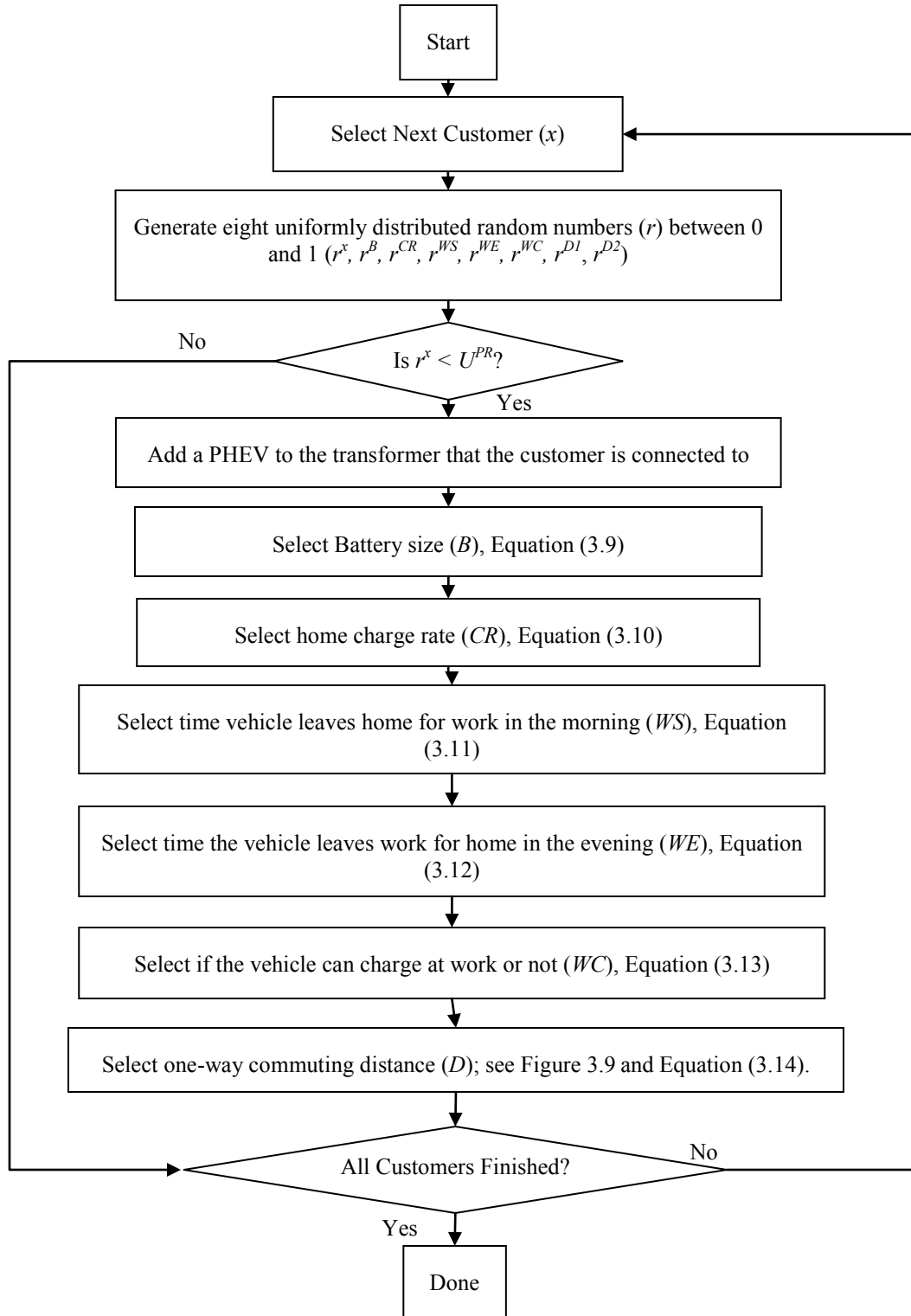
**Figure 3.8. Flow chart for probabilistic selection of individual residential vehicle charactersistics.** *U* **is a probability value. The superscripts are:** *x* **– customer number,** *PR* **– penetration rate,** *B* **– battery size,** *CR* **– charge rate,** *WS* **– Work start time,** *WE* **– work end time,** *WC* **– Work Charging,** *D* **– commuting distance.**

The probabilistic selection method to determine the vehicle characteristics that are used throughout the simulations (Figure 3.8) begins by selecting the battery size ($B$) from the probability value ($U^B$) and the randomly generated number ($r^B$):

$$B = \begin{cases} 4.85 & r^B < U^B \\ 16.6 & r^B \geq U^B \end{cases} \tag{3.9}$$

The charging rate ($CR$) used for home charging is selected next:

$$CR = \begin{cases} 1.44\ kW & r^{CR} < U^{CR} \\ 7.60\ kW & r^{CR} \geq U^{CR} \end{cases} \tag{3.10}$$

The time that the vehicle leaves home for work ($WS$) in the morning is:

$$WS = \begin{cases} 07:00 & r^{WS} < 0.2 \\ 07:30 & 0.2 < r^{WS} \leq 0.4 \\ 08:00 & 0.4 < r^{WS} \leq 0.6 \\ 08:30 & 0.6 < r^{WS} \leq 0.8 \\ 09:00 & r^{WS} > 0.8 \end{cases} \tag{3.11}$$

The $WS$ variable is then used to select the time that the vehicle leaves work for home ($WE$)

$$WE = \begin{cases} WS + 6.5\ hours & r^{WE} < 0.2 \\ WS + 7\ hours & 0.2 < r^{WE} \leq 0.4 \\ WS + 7.5\ hours & 0.4 < r^{WE} \leq 0.6 \\ WS + 8\ hours & 0.6 < r^{WE} \leq 0.8 \\ WS + 8.5\ hours & r^{WE} > 0.8 \end{cases} \tag{3.12}$$

The WE and WS times are fixed for each vehicle throughout the MCS. A binary variable ($WC$) is selected that is equal to one if the vehicle can charge at work and equal to zero otherwise:

$$WC = \begin{cases} 1 & r^{WC} < U^{WC} \\ 0 & r^{WC} \geq U^{WC} \end{cases} \tag{3.13}$$

Finally, the one-way commuting distance that the vehicle will travel each day to work is selected. The cumulative probability of one-way commuting distance shown in Figure 3.9 contains data for the entire province of BC, taken from statistics Canada census 2006 [30]. This data was used to assign a commuting distance to each vehicle by generating a uniform random number ($r^{D1}$) between 0 and 1. If the uniform random number fell within the cumulative probability for each distance range then a second uniform random number ($r^{D2}$) between the ranges of driving distances was generated to assign a distance to each vehicle. For distances of over 30 km, a maximum value of 75 km was chosen as the upper bound for commuting distance range. For example, if the uniform random number was greater than 0.41 and less than 0.65 (i.e within the first "step" of Figure 3.9), a driving distance uniformly distributed between 5 and 10 km would be selected, such as 7.1 km. To select a commuting distance ($D$), within the range [$D^{low}$ $D^{high}$] a uniformly distributed number ($r^{D2}$) between 0 and 1 is used:

$$D = D^{low} + (D^{high} - D^{low}) \cdot r^{D2} \tag{3.14}$$

In any case throughout the model, where a uniform distribution is used to select between ranges of values, Equation (3.14) is used.
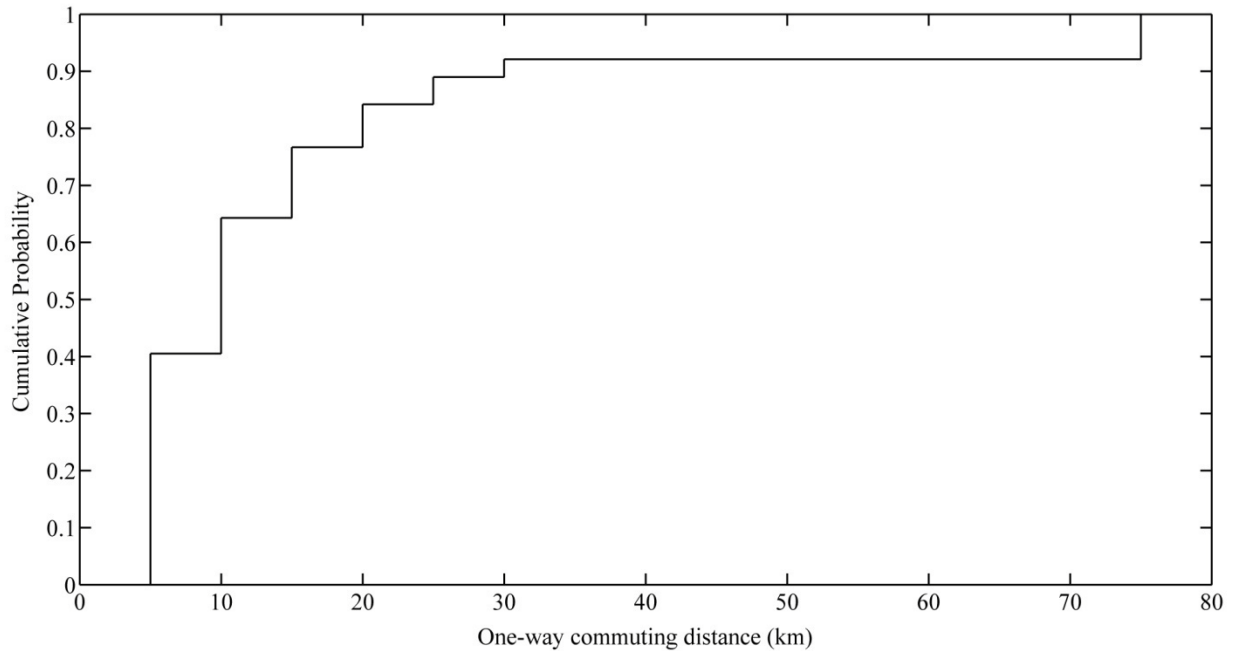
**Figure 3.9. Piecewise cumulative distribution of one-way commuting distances for the province of BC. Source: Statistics Canada [30]**

### 3.5.2 Vehicle Simulation Model for Residential Customers

The residential vehicle simulation model attempts to recreate the stochastic actions of vehicle operators as they commute to work and make trips away from their homes. The vehicle simulation model was designed for the dual purpose of predicting the temporal charging demand of PHEVs and also estimating the gasoline and electricity consumption of individual vehicles. The model assumes that all PHEV owners commute to work each day. This assumption stems from one of the main benefits proposed for PHEVs; that they will allow for a means of travel to and from the workplace using mostly electricity as the fuel [31]. The process for determining vehicle charging demand at residential and commercial locations is shown in Figure 3.10.
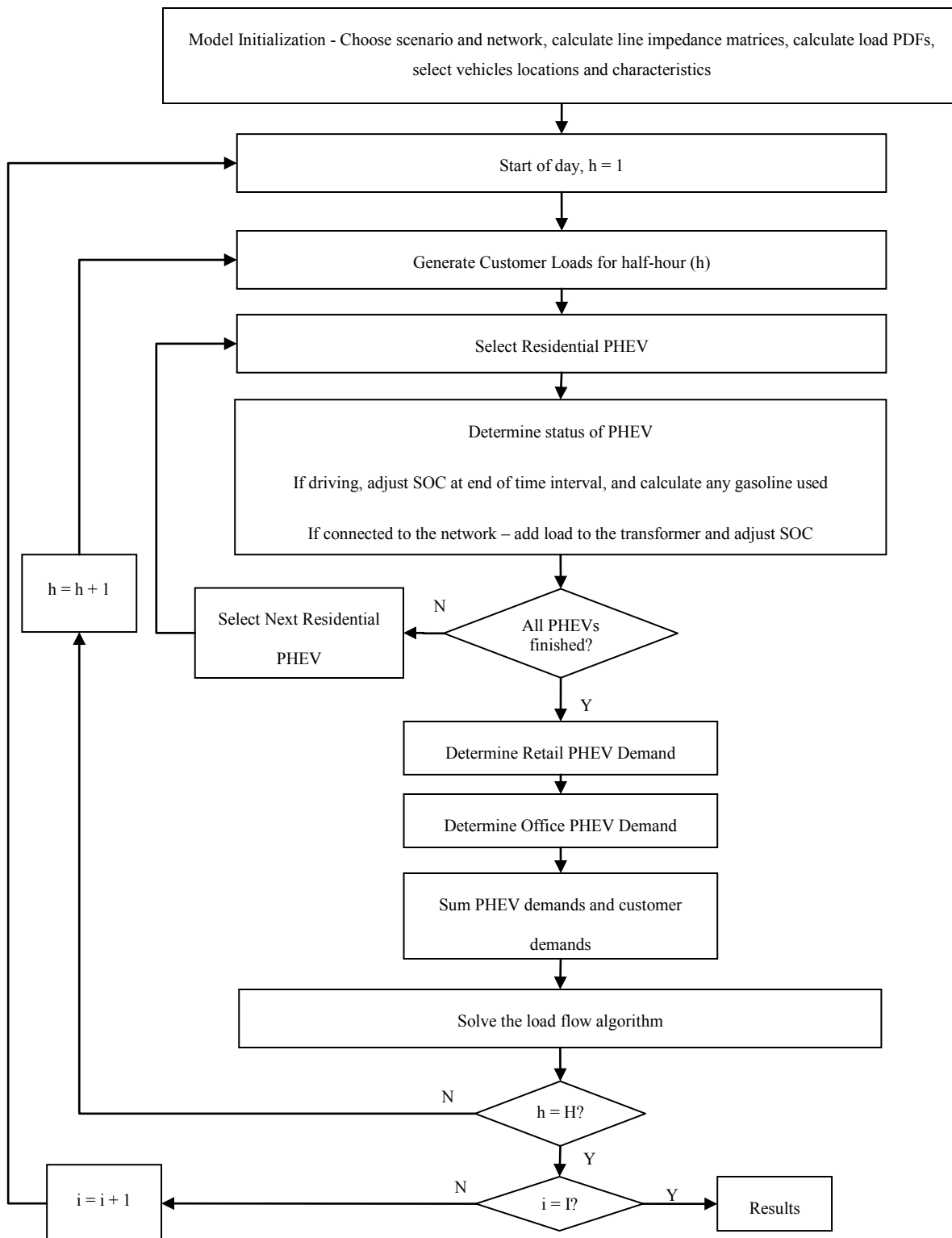
**Figure 3.10 Model logic flow chart showing process for determining vehicle charging demand at residential and commercial locations**

For all simulated vehicle charging considered in this thesis, an uncontrolled charging scenario is assumed. This means that when vehicles are parked at their home base they are always connected to the grid and charging at a constant rate until the battery is fully charged. Charging in an uncontrolled fashion creates a "worst case" scenario of coincidental peak electrical demand and vehicle charging. For the first time point (00:30) of the first iteration of the model, all residential vehicle batteries are assumed to be fully charged and parked at home. For subsequent iterations, all charging loads, vehicle locations and battery SOCs carry over when the next MCS iteration begins. The SOC of each PHEV and the demand for each vehicles charging is tracked throughout the simulation to ensure the battery SOC limits are not exceeded, and to determine the timing of the vehicles electricity demand on the grid.

Each PHEV that resides in a detached home or apartment building on the network is simulated using a set of simple rules that define their actions. There are two trips for each vehicle that must occur during each 24 hour period – commuting to and from work. Apart from these mandatory trips, there are three periods during each day in which trips can be taken. These three non-commuting trip periods are shown in Figure 3.11, which is adapted from a travel demand analysis model presented by Bhat et al. [32] who used surveys of U.S. drivers to estimate the probability ($U$) of a trip occurring within the travel period. For each simulated vehicle, only one trip can occur during each trip period of Figure 3.11, as the data from Bhat et al. showed that two or more trips during each trip period occurred with much lower frequency than a single trip.

At the first time point of each non-commuting period, a decision is made that determines if a vehicle trip occurs based on the probabilities shown in Figure 3.11. If a trip is to occur, the start time, length of time and total distance of this trip is then probabilistically selected. All non-commuting trip distances are assumed to be normally distributed and the mean distance ($\mu^{trip}$)

travelled during these trips is estimated from data in the US National Personal Transportation Survey (NPTS, Table 5.17) [33]. A 15% standard deviation ($\sigma^{trip}$) is assumed for the trip distances.
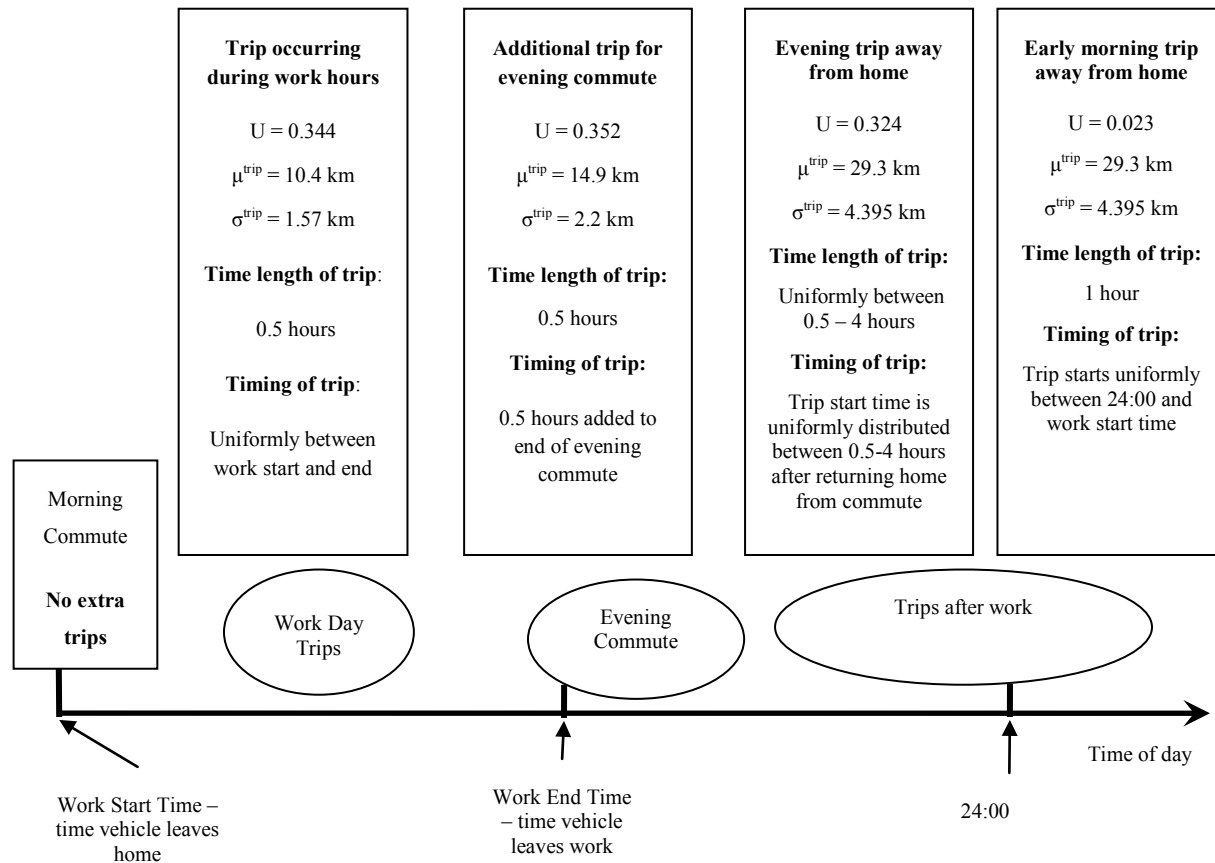


### Daily Vehicle Timeline

**Figure 3.11. Schematic of vehicle simulation timeline and assumptions for driving distances and trip times. Circles represent time periods during the day in which trips can be taken. Probabilities of trips, mean distances and standard deviations of those trips are given in the square boxes along with a description of the trip timing.**

The mean distances and probability values in Figure 3.11 are used in simulating the vehicle trips for both apartments and detached dwellings. The data presented by Bhat et. al [32] showed that additional trips taken during the morning commute happened with a very low probability,

thus no additional morning trips are considered in this analysis. In contrast, a higher percentage of drivers (35.2%) made an additional trip during their evening commute and 32.4% of surveyed drivers made a trip after returning home from work. After midnight and before work, there is a 2.3% probability that a vehicle will take a trip, based on data from the US NPTS (Table 5.20) [33]. This trip is distributed identically to the evening trips; however it lasts for an hour only.

When a PHEV trip is triggered and a driving distance ($D^{trip}$) selected, a value for energy consumption per kilometre is generated for CD mode from the range given in Table 3.2. The CD mode efficiency ($\eta^{CD}$) is used to calculate the amount of energy to withdraw from a vehicles battery ($E^B$):

$$E^B = \eta^{CD} \cdot D^{trip}$$
(3.15)

If $E^B < SOC$, then no gasoline will be used on this trip, and the new battery state of charge ($SOC^{new}$) is calculated as the difference between the $SOC$ and $E^B$:

$$SOC^{new} = SOC - E^B$$
(3.16)

However, if $E_B > SOC$ after calculating Equation 3.15, then the battery will be depleted during the trip and a CS mode efficiency value ($\eta^{CS}$) is generated from Table 3.2. The remaining distance that the vehicle travels on gasoline is estimated ($D^{trip,new}$):

$$D^{trip,new} = D^{trip} - \frac{SOC}{\eta^{CD}}$$
(3.17)

This new distance is used with the charge sustaining efficiency to calculate the amount of gasoline used for that trip:

$$G = D^{trip,new} \cdot \eta^{CS} \tag{3.18}$$

The amount of gasoline (G) and battery energy used for each vehicle trip is stored for the purposes of estimating individual vehicle grid energy consumption and emissions from driving. The process for determining gasoline and battery energy usage for each trip is shown in Figure 3.12.

### 3.5.3 Charging Simulation for Office Customers

To simulate charging demand at office locations ($S_{n,h,i}^{PHEV,office}$) on the network, a simplified approach is taken. First, all office charging is assumed to be performed at 120V (1.44 kW). The probability of an office location providing charging stations is determined during model initialization. This probability value is assumed to be the same as that for the probability of a residential PHEV being able to charge while at work (Table 4.1). To estimate the number of charging stations that each office customer can install, a small percentage of the transformer's kVA capacity is allocated to vehicle charging stations using the "Fraction of capacity for charging" value from Table 4.1:

$$\# \ of \ Chargers = \frac{Fraction \ of \ Capacity \ for \ Charging * Rated \ Capacity \ (kVA)}{Plug \ rating} \tag{3.19}$$

The number of chargers is then rounded to the nearest whole number. The plug rating value in Equation (3.19) is the plug real power (e.g. 1.44 kW) adjusted for a 0.95 power factor. Each installed office charger is assumed to be utilized for vehicle charging during each day.

To estimate the office PHEV charging demand at each installed charger, a vehicle is assumed to arrive with a uniform probability between 07:00 and 09:00 with a SOC uniformly
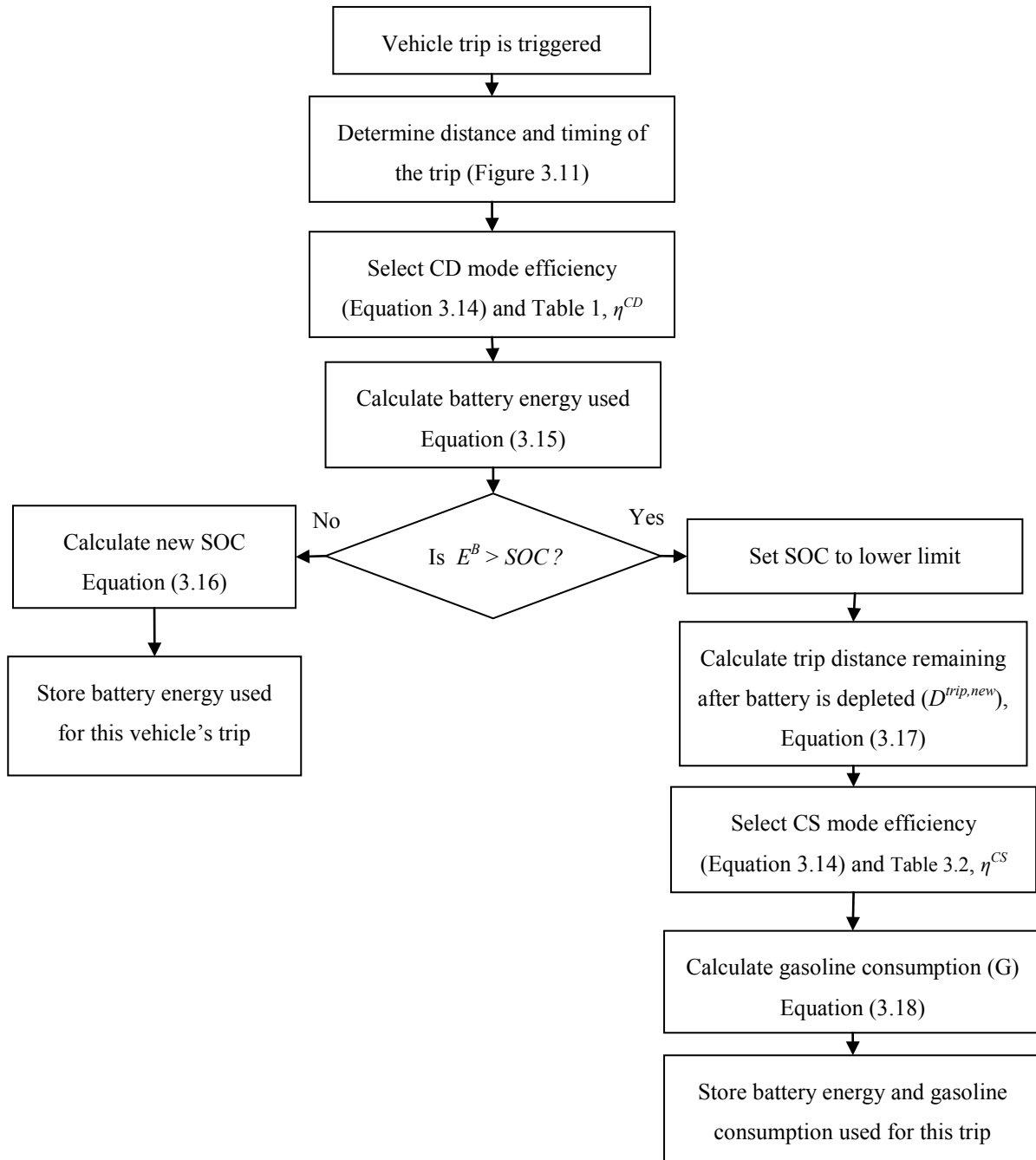
**Figure 3.12. Process to calculate gasoline and battery energy used for each vehicle trip**

distributed between 0 and 50% of its capacity. The vehicle's battery size (kWh) is selected each day upon arrival using the same assumptions for battery technology that are used to select batteries for residential PHEVs. The vehicle is connected immediately upon arriving at work and starts charging. Daytime vehicle trips for office PHEVs use the same set of assumptions as those for the daytime trips of residential PHEVs.

### 3.5.4 Charging Simulation for Retail Customers

Estimating PHEV charging at retail locations requires a different approach than that used for the office or residential vehicle charging simulations. Vehicles connecting to retail charging stations would be doing so for short periods of time while performing small personal tasks such as shopping or eating. This kind of charging is known as "opportunity charging" [22] and is assumed to occur at 240 V (7.6 kW). The probability of a retail location providing charging and the number of chargers at each location are calculated as for the office locations using Equation 3.19. To determine the demand ($S_{n,h,i}^{PHEV,retail}$) and timing of retail charging, traffic volume data from BC was used to calculate a probability distribution of vehicles on the road, shown in Figure 3.13 [34]. Charging events at retail locations were triggered by comparing the probability of vehicle charging ($U_h^{retail}$) from Figure 3.13 to a uniform random number ($r^{retail}$). Charging events at retail locations last only for a half hour.
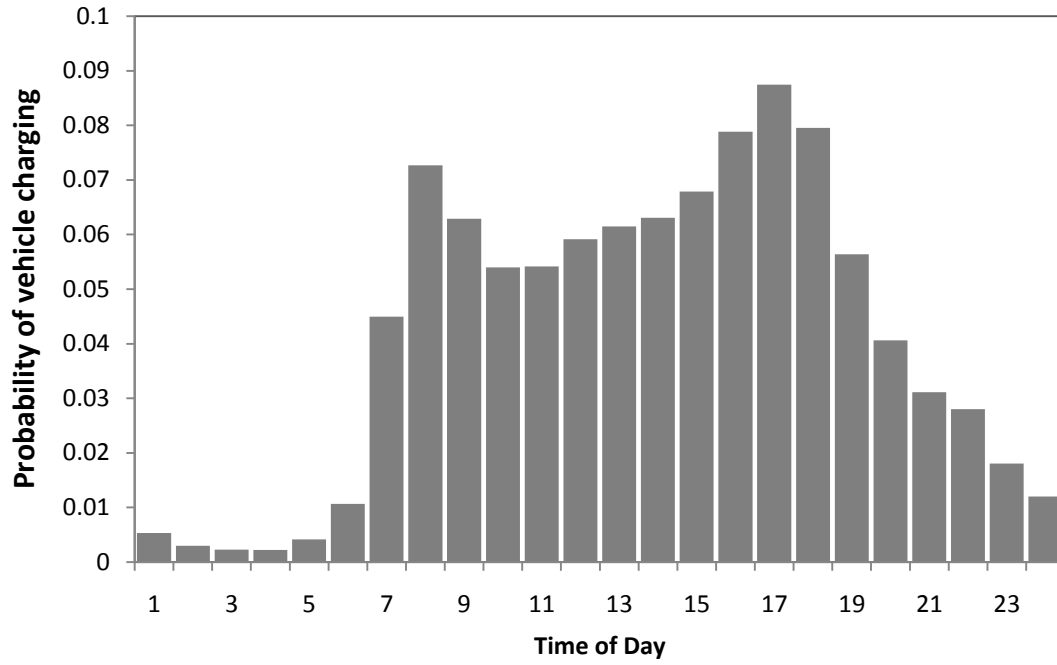
**Figure 3.13. Probability of vehicle charging at retail locations by time of day**

# 4  Scenario Definition and Network Characterization

This chapter provides a summary of three scenarios used as inputs to the MCS model. The scenarios represent increasing penetrations of PHEVs and improved technological advancement of charging infrastructure. Three networks are selected for analysis representing suburban, urban and rural locations. The defining characteristics of each network are presented.

## 4.1  Scenario Definition

The model incorporates three scenarios for investigating the PHEV impacts. The scenarios were created to capture the uncertainty of vehicle technology, charging infrastructure and local penetration of PHEVs. For the purposes of this thesis, PHEV penetration is defined as the probability of a residential customer in the given network owning a PHEV (Figure 3.8, $U_{PR}$). The assumptions for each scenario are summarized in Table 4.1. Scenario 1 ("low scenario") represents a low penetration (5%) of PHEVs where most charging occurs at 120V and there is limited availability of charging stations at office and retail locations. Scenario 2 ("medium scenario") includes a 15% penetration of PHEVs at residential locations with a higher probability of office and retail charging. Scenario 2 also has higher charge rates for homes than Scenario 1. Scenario 3 ("high scenario") has the highest penetration of vehicles considered, with higher charge rates and increased installations of retail and office charge stations. These three scenarios are meant to cover a range of possibilities for PHEVs in the future.

**Table 4.1. Scenario definition for increasing PHEV technological advancement**

| Parameter | Scenario 1 – Low | Scenario 2 – Medium | Scenario 3 – High |
|---|---|---|---|
| Residential PHEV penetration rate ($U^{PR}$) | 0.05 | 0.15 | 0.25 |
| Apartment PHEV penetration rate ($U^{PR,apt}$) | 0.025 | 0.075 | 0.25 |
| Probability of retail location installing chargers | 0.2 | 0.3 | 0.5 |
| Probability of office location installing chargers | 0.2 | 0.5 | 0.6 |
| Fraction of capacity for charging | 0.025 | 0.05 | 0.1 |
| Probability of residence charging at 120V ($U^{CR}$) | 0.75 | 0.25 | 0.1 |
| Probability of a PHEV having a small battery (4.85 kWh), ($U^{B}$) | 0.5 | 0.5 | 0.5 |
| Probability of a residential PHEV owner being able to charge at the workplace ($U^{WC}$) | 0.2 | 0.5 | 0.6 |

## 4.2   Network Characterisation

The variety of customer types and demographics within the small areas served by distribution networks leads to drastically different characteristics between some networks. These characteristics include:

- various levels and types of residential, commercial and industrial loads,

- different amounts of three phase and single phase loads,

- network topology variations including differences between total length and lengths of single and three phase sections,

- different network voltage levels (25.2 kV, 14.4 kV, etc) and substation MVA ratings.

To include the uncertainties and differences in network types, three networks were selected that supply different levels of the four customer types: office, retail, apartment and house. The selected networks are representative of suburban, urban and rural locations. All three networks

are real distribution networks within the provincial grid. The network data was provided by BC Hydro. Figures showing the topology and relative lengths of the networks are included in Appendix D. The defining parameters for each of the network types are shown in Table 4.2 and the customer type distributions by connected capacity are summarized in Figure 4.1.

Table 4.2 contains a parameter called "network capacity", which represents the capacity that is allocated to this network through the substation. It is generally advisable to keep the demand below this level to avoid excessive voltage drops or current overloads. The percentage of capacity values shown in Figure 4.1 are calculated using the rated capacity of the secondary transformers ($S_n^{c,cap}$) for each customer class ($c$):

$$\% \text{ of Capacity} = \frac{\sum_{n=1}^{N} S_n^{c,cap}}{\sum_{n=1}^{N} S_n^{cap}}, \quad \forall\, c = \{house, apartment, office, retail, other\} \qquad (4.1)$$

The urban network contains 51% of its connected capacity as office loads, with a further 7% of the connected capacity coming from retail locations (Figure 4.1). The suburban location serves primarily houses and a few apartment buildings with less than 1% office and retail connected capacity. The rural network also serves primarily houses, however, it also contains small amounts of office, retail and apartment loads. This network is quite typical of rural areas; it contains very long single and three phase sections due to the spread of customers over a wide geographical area, and has a very large amount of connected capacity. It is important to note that the individual customer loads are not distributed evenly by connected capacity (Section 3.2) and thus, Figure 4.1 may not reflect the total demand from each type of customer.

**Table 4.2. Summary of representative network characteristics**

| Parameter | Suburban | Urban | Rural |
|---|---|---|---|
| Total Length (km) | 26.1 | 10.1 | 114.6 |
| Length of Three Phase Sections (km) | 6.3 | 8.1 | 18.3 |
| Length of Single Phase Sections (km) | 19.8 | 2.0 | 96.3 |
| Line-to-Line Voltage (kV) | 25.2 | 12.6 | 25.2 |
| Network Capacity (MVA) | 12 | 6 | 12 |
| Recorded Peak Feeder Demand (MVA) | 9.4 | 3.8 | 11.8 |
| Total Connected Capacity (kVA) | 14, 735 | 7,375 | 24,900 |
| Number of Secondary Transformers | 244 | 59 | 769 |
| Number of Three Phase Transformers | 3 | 11 | 7 |
| Total number of customers | 1983 | 494 | 2169 |
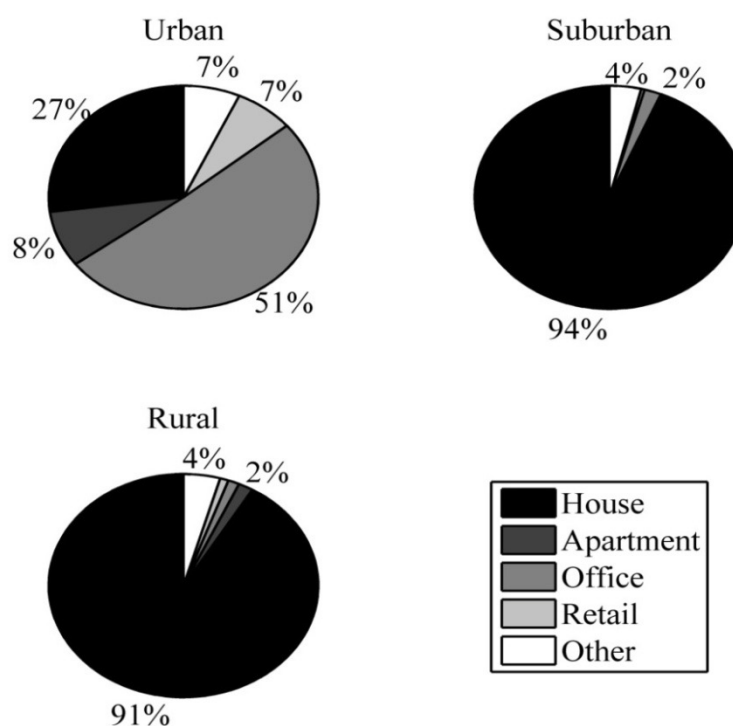


**Figure 4.1. Percentages of total connected capacity of each customer type for the selected networks. Values less than 1% have not been shown**

# 5 Results and Analysis

In this chapter, the results of the model simulations are presented and analyzed. A convergence analysis is first performed and the model inputs are shown summarizing the number of vehicles simulated on the networks for each scenario. The networks are investigated considering three main categories of possible impacts: PHEV demand, bus voltages and transformer overloads. Emissions and gasoline use from individually simulated residential vehicles are calculated.

## 5.1 Convergence Analysis and Model Input Results

The model was first run for 500 iterations to determine a suitable stopping point criterion explained in terms of the number of iterations that could be used for subsequent analyses. The line current entering a single-phase bus at 18:00 hours with PHEV charging is chosen to analyze the evolving mean and standard deviation of the calculated current as the iterations progress. As shown in Figure 5.1, the mean and standard deviation of the value changes with each progressive iteration and approaches a converged value. A value of 350 total iterations is chosen for the model because at this point the mean values have changed less than 0.1% in at least 50 subsequent iterations.
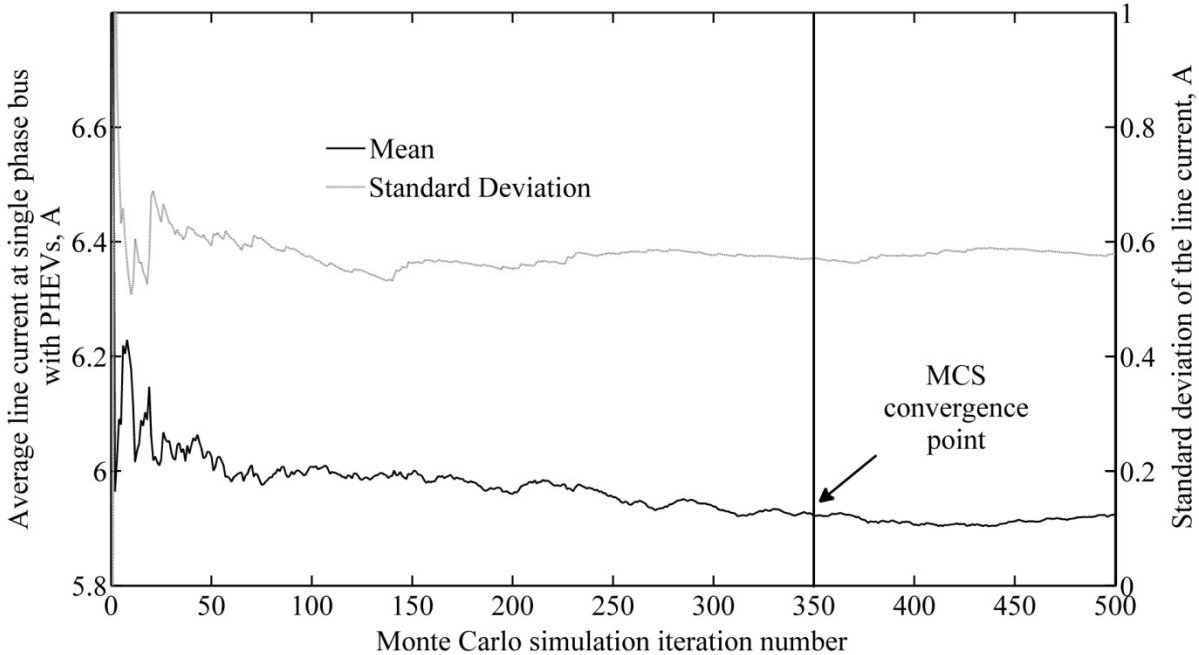
**Figure 5.1. Convergence of the mean and standard deviation for the load at a residential single phase bus with PHEVs at 18:00 hours.**

Initially, a scenario without PHEV charging is run on each network to determine the base network demand. Following this, the three scenarios (Table 4.1) are run on all three networks creating 12 model data sets. A summary of the office and retail chargers and the simulated residential vehicles for each scenario and network is shown in Table 5.1. The values found in Table 5.1 are selected before the MCS iterations begin using the probabilistic methods outlined in Section 3.5, and are constant throughout the given simulation.

**Table 5.1. Categorization of residential vehicles, office and retail charging locations for each scenario and network**

| Parameter | Suburban | | | Urban | | | Rural | | |
|---|---|---|---|---|---|---|---|---|---|
| | L[1] | M | H | L | M | H | L | M | H |
| Total number of office chargers | 0 | 0 | 30 | 16 | 65 | 178 | 5 | 12 | 10 |
| Total number of retail chargers | 0 | 3 | 1 | 5 | 12 | 53 | 4 | 27 | 49 |
| **Residential Vehicle Parameter** | | | | | | | | | |
| Total number of PHEVs simulated | 100 | 296 | 507 | 21 | 62 | 114 | 96 | 292 | 559 |
| Number of 4.85 kWh batteries | 57 | 152 | 251 | 13 | 33 | 44 | 40 | 144 | 300 |
| Number of PHEVs charging at 7.6 kW | 20 | 217 | 454 | 4 | 47 | 99 | 21 | 223 | 496 |

[1] *L – low (scenario 1), M – medium (scenario 2), H – high (scenario 3)*

## 5.2 PHEVs and Network Demand

The total demand on the network *without* PHEV charging, which will be referred to as "network demand" ($S_{h,i}^T$), is calculated for each half hour and averaged over the 350 MCS iterations to produce the "average network demand" ($\overline{S_h^T}$):

$$S_{h,i}^T = \sum_{n=1}^{N} S_{n,h,i} \tag{5.1}$$

$$\overline{S_h^T} = \frac{\sum_{i=1}^{350} S_{h,i}^T}{350}, \quad \forall\, h \tag{5.2}$$

where *N* is the total number of secondary transformers, *i* is the iteration number, *h* is the half-hour interval and *T* represents "total".

For each scenario and network, the demand from PHEV charging at each bus is summed over the entire network at each half-hour. The "average PHEV demand" ($\overline{S_h^{PHEV}}$) is calculated for each scenario and each network as follows:

$$\overline{S_h^{PHEV}} = \frac{\sum_{i=1}^{350}(\sum_{n=1}^{N} S_{n,h,i}^{PHEV})}{350} \quad ... \forall \, h \tag{5.3}$$

The results in Figure 5.2(a-c) show the average PHEV demand in each scenario for the three networks at each time interval. In each of the plots in Figure 5.2, the right hand axis shows the PHEV demand normalized to the demand without PHEVs ($\overline{\dot{S}_h^{PHEV}}$) during each time interval:

$$\overline{\dot{S}_h^{PHEV}} = \frac{S_h^{PHEV}}{S_h^T} \quad ... \forall \, h \tag{5.4}$$

For all of the networks shown in Figure 5.2, a large demand for vehicle charging in the peak period between the hours of 16:00 and 19:00 is evident due to the return of vehicles after their evening commutes. Then, as batteries become fully charged and drivers make evening trips away from their homes, the peak charging diminishes after 19:00 and levels off. The charging continues throughout the evening and early morning hours as vehicles return from evening trips and charge throughout the night. The urban network, Figure 5.2(a), with its higher proportion of office and retail loads, shows an increase in demand during the morning hours from 7:00 to 10:00 caused by vehicles charging at workplaces. A small amount of retail charging at the urban location adds only a small amount to the total PHEV charging demand as demonstrated in Figure 5.3, by separating the PHEV demand into office, retail and residential portions
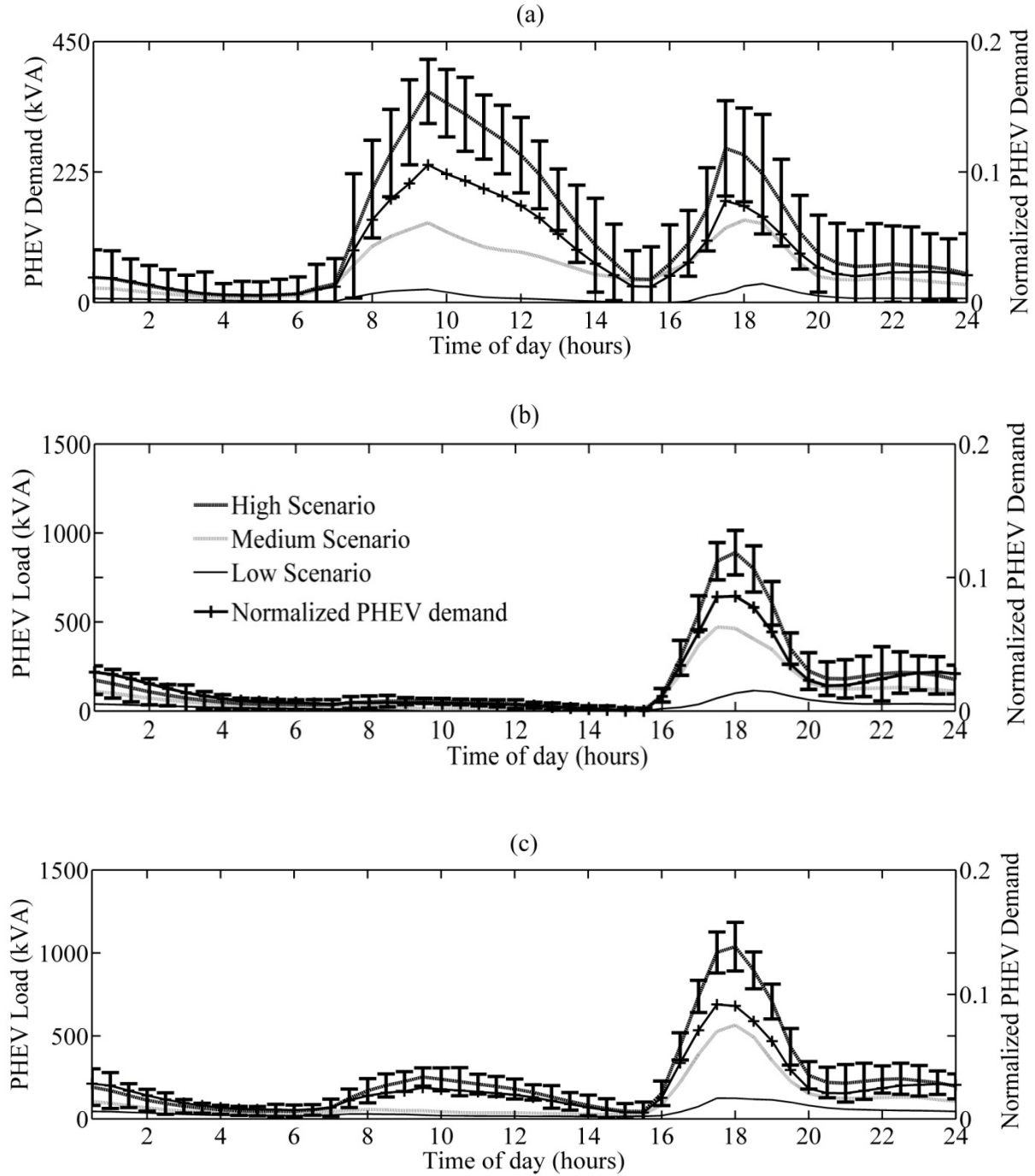
**Figure 5.2. Average PHEV demand for each scenario on (a) urban, (b) suburban and (c) rural networks at each time interval. Error bars show the extreme values of maximum and minimum PHEV demand for the high scenario.**
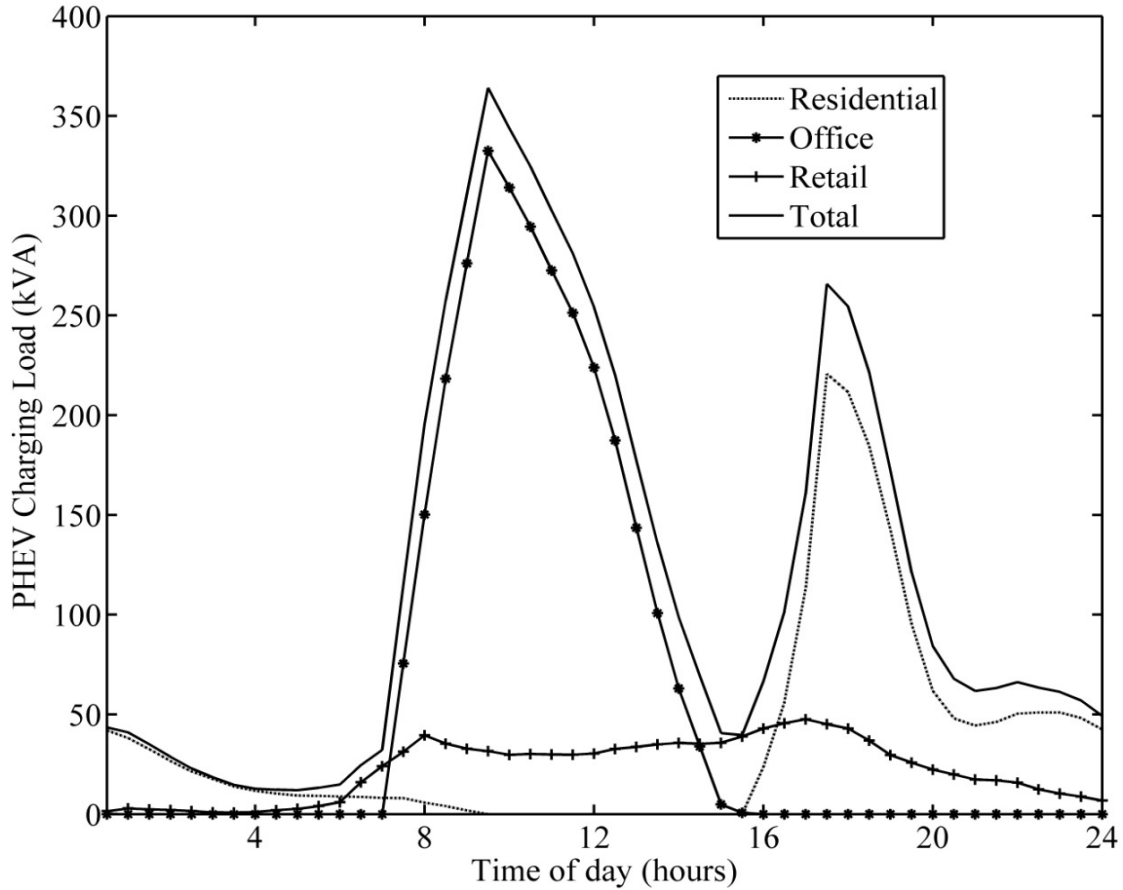
**Figure 5.3. Average PHEV demand for scenario 3 on the urban network showing residential, office, retail and total PHEV demand.**

To further examine the impact of the PHEV demand on the three networks, the network demand and PHEV demand at each bus is summed for each half hour of the MC iterations to find the "average network demand with PHEVs" ($\overline{S_h^{T,PHEV}}$) at each half-hour time interval:

$$\overline{S_h^{T,PHEV}} = \frac{\sum_{i=1}^{350}\sum_{n=1}^{N}(S_{n,h,i} + S_{n,h,i}^{PHEV})}{350}, \quad \forall\, h \tag{5.5}$$

These demand curves are compared to the average network demand without PHEVs (Equation 5.2), and shown in Figure 5.4 for the urban network, Figure 5.5 for the suburban network and

Figure 5.6 for the rural network. The suburban network has a demand curve similar to the rural network and is not shown.

For all of the networks, the low penetration case shows a marginal increase in the network demand evident from the low scenario shown in Figure 5.4 and Figure 5.5. The demand increases significantly during the peak period for the medium and high scenarios, especially in the rural and suburban networks. An increase in the daytime network demand between 9:00 and 15:00 occurs in the urban network due to the charging of PHEVs at large office locations. This creates a different overall load shape than the suburban or rural networks and produces a morning peak as vehicles arrive to work and begin charging. On the rural network, the average network demand exceeds the network capacity during the hours of 18:00 – 19:00.
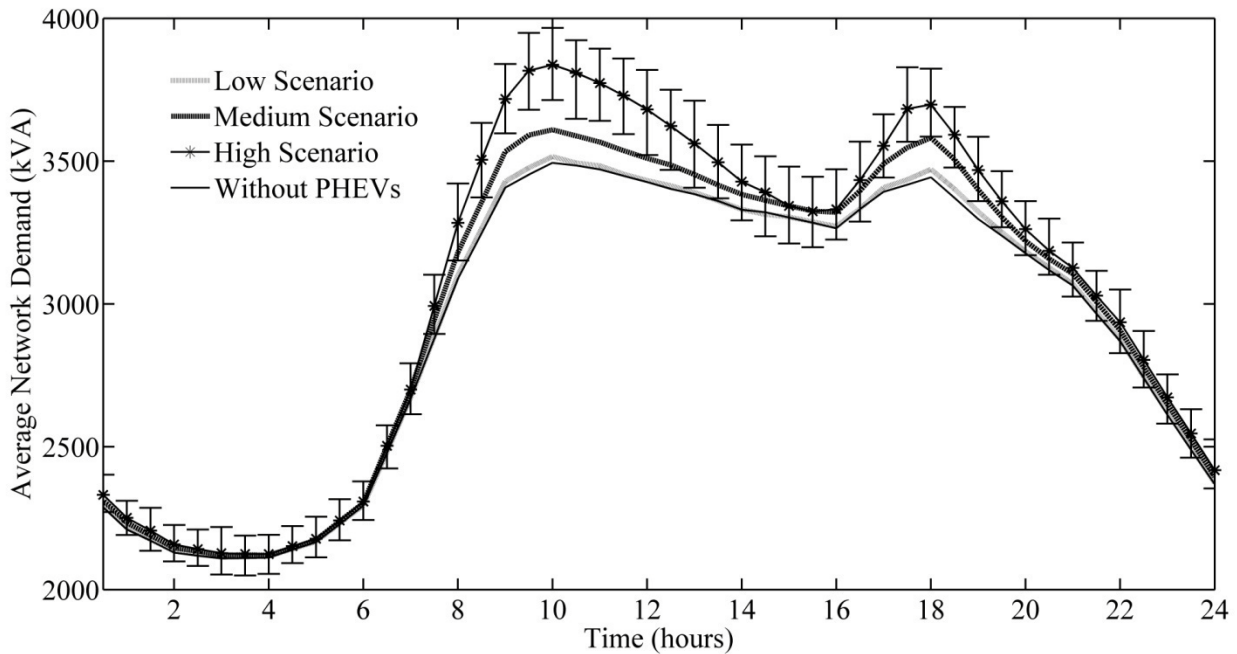


**Figure 5.4. Average network demand for the urban network with PHEVs for all scenarios in each time interval. Error bars show the maximum and minimum values for the high scenario.**
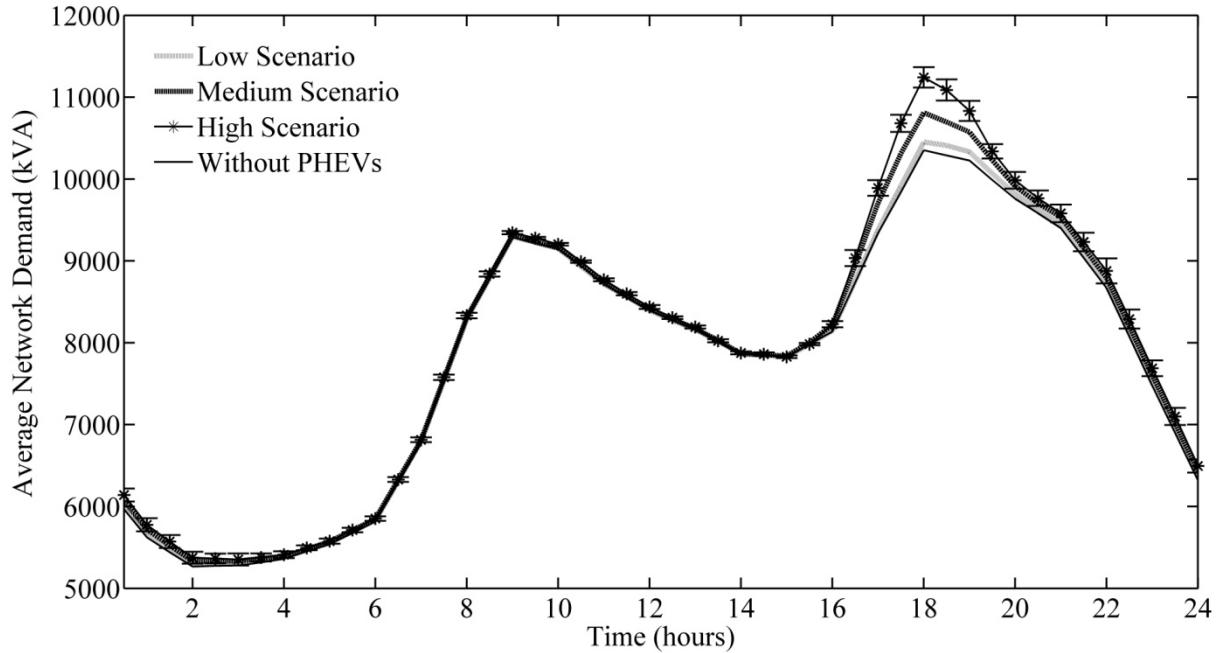
**Figure 5.5. Average network demand for the suburban network. Error bars show the maximum and minimum values for the high scenario.**

Distribution designers and engineers are often concerned with the maximum demand likely to occur on a given network in order to determine the likelihood of faults due to overloading fuses and conductors. In each of Figure 5.4 to Figure 5.6 the average network demand in the high scenario is shown with error bars representing the maximum and minimum demand occurring during each time interval. The maximum demand including PHEVs in the high scenario in each network is 11.45 MVA, 3.966 MVA and 12.72 MVA for the suburban, urban and rural networks respectively. Notably the peak demand for the urban network comes at 10:00 hours, while the peak load for the other two networks occurs at 18:00 hours.

In the rural network the average demand exceeds the network capacity rating for the high scenario (Table 4.2). The other two networks do not exhibit any network capacity overloads. On

the rural network in Figure 5.6, the maximum demand is 10.4% higher than the average demand

without PHEV charging at that time (18:00 hours).
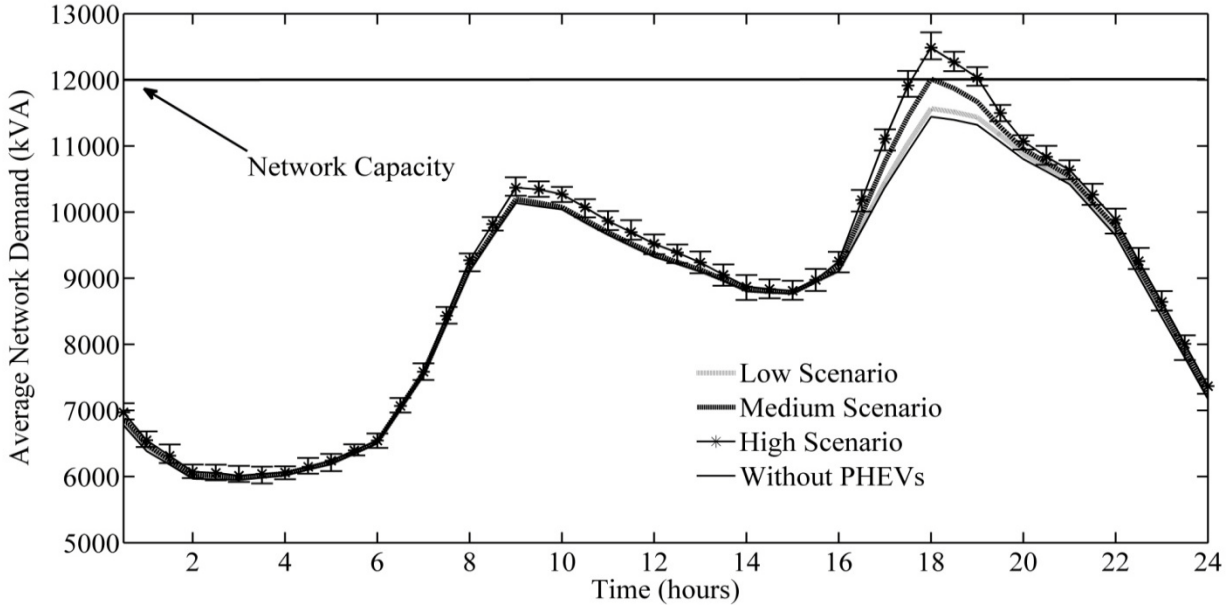


**Figure 5.6. Average network demand on the rural network showing exceedance of the network capacity. Error bars show the maximum and minimum values for the high scenario.**

While the timing of the demand is important to distribution operation, the increase in

energy supplied for PHEV charging is a central aspect for utility planning to estimate growth in

aggregate energy demand. The total energy supplied without PHEV charging ($E_i^T$) and the total

PHEV energy supplied ($E_i^{T,PHEV}$) during each iteration is calculated for every scenario and

network. The calculated energy values are averaged over the iterations and used to calculate the

average percent increase in energy supplied ($\overline{\%\Delta E^T}$) above the case without PHEV charging as

follows:

$$\overline{\%\Delta E^T} = \frac{\sum_{i=1}^{350}\left(\frac{E_i^{T,PHEV}}{E_i^T}\right)}{350} \tag{5.6}$$

These average percent increase in energy values are then compared to the average percent increase in peak demand ($\overline{\%\Delta S^{*,T}}$) as shown in Figure 5.7. The average percent increase in peak demand is calculated by finding the peak network demand at all iterations and calculating the percent increase above the network demand without PHEV charging at that time:

$$\%\Delta S_i^{*,T} = \max\left(\frac{S_{h,i}^{T,PHEV}}{S_{h,i}^T}, \forall\, h\right) \cdot 100\%\, , \forall\, i \tag{5.7}$$

These peak increase values from Equation (5.7) are averaged over the iterations ($i$) to produce a mean percent increase in peak demand for each scenario and network.

An important aspect of charging PHEVs in an uncontrolled fashion is that the peak demand increases at a higher rate than energy as PHEV penetration increases. This result can be seen in Figure 5.7. For example, for the rural network, the increase in energy from PHEV charging rises from 0.47% to 2.76% in the low to the high scenarios, respectively. In comparison, the average percentage increase in peak demand rises from 1.10% to 9.15%.
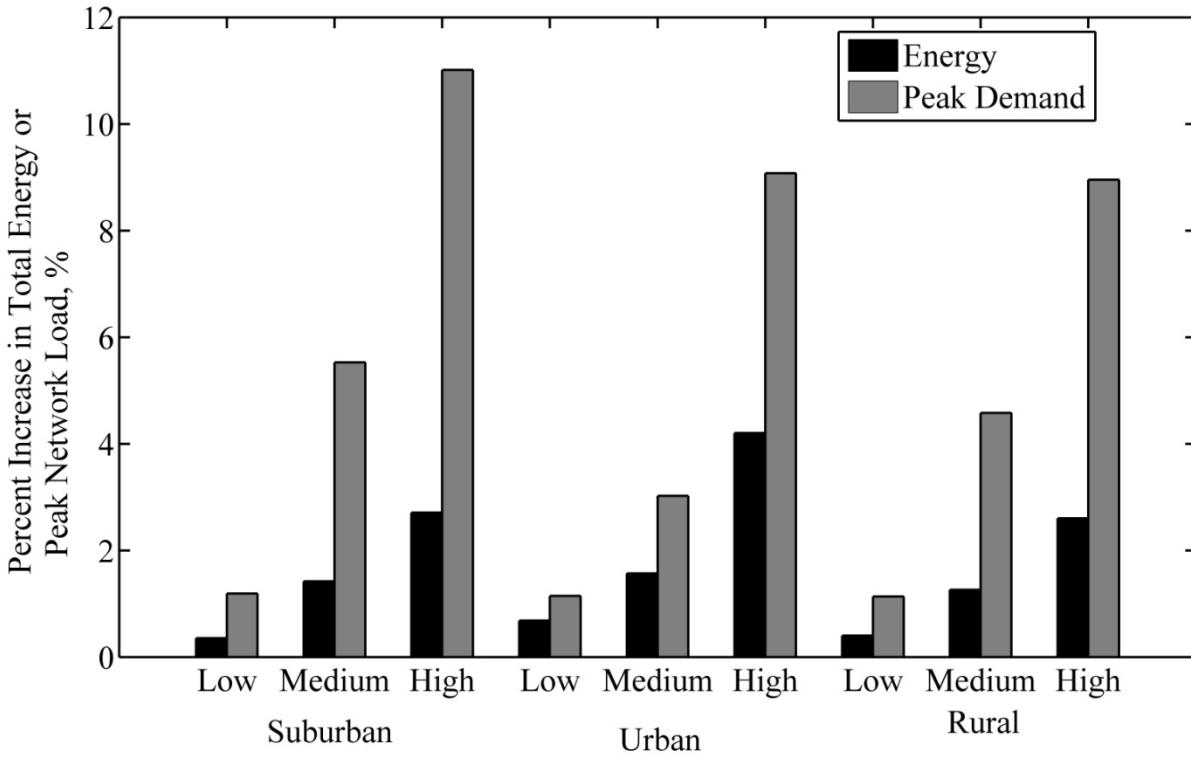
**Figure 5.7. Percentage increases in energy and peak demand for all three networks in all scenarios**

### 5.2.1 Network Losses

Power loss on the networks is calculated using Equation (A.11) in Appendix A for each section (Figure A. 1) and summed over the whole network for each time point. This produces a total network power loss value ($S_{h,i}^{loss,T}$) at each half hour throughout the simulations for every network and scenario:

$$S_{h,i}^{loss,T} = \sum_{k=1}^{K} S_{k,h,i}^{loss} \quad \forall\, h, i \tag{5.8}$$

where k is the section (branch) and K is the total number of sections. Using the total power loss values, daily energy loss ($E_i^{loss}$) on each network is then calculated for each iteration and averaged ($\overline{E^{loss}}$):

$$\overline{E^{loss}} = \frac{\sum_{i=1}^{M} E_i^{loss}}{M} \tag{5.9}$$

where M is the total number of MCS iterations.

Figure 5.8 shows the average percentage increase in energy supplied to each network (Equation 5.6) alongside the average percent increase in energy loss in those networks. The increase in energy loss is calculated for the percent difference between the demand without (*wo*) PHEVs and the demand in the high scenario:

$$\overline{\%\Delta E^{loss}} = \left( \frac{\overline{E^{loss,PHEV}}}{\overline{E^{loss,wo\ PHEV}}} - 1 \right) \cdot 100\% \tag{5.10}$$

The percent increase in energy loss is higher than the percent increase in energy for all of the networks. Specifically in the urban network, energy loss increased by almost 10%. The energy loss in the urban network is highest because of the increases in the morning and evening peak demands. Although the percent increase in energy loss is higher than the percent increase in energy, the absolute values in Figure 5.8 show that the energy supplied for PHEV charging is an order of magnitude above the change in energy loss.
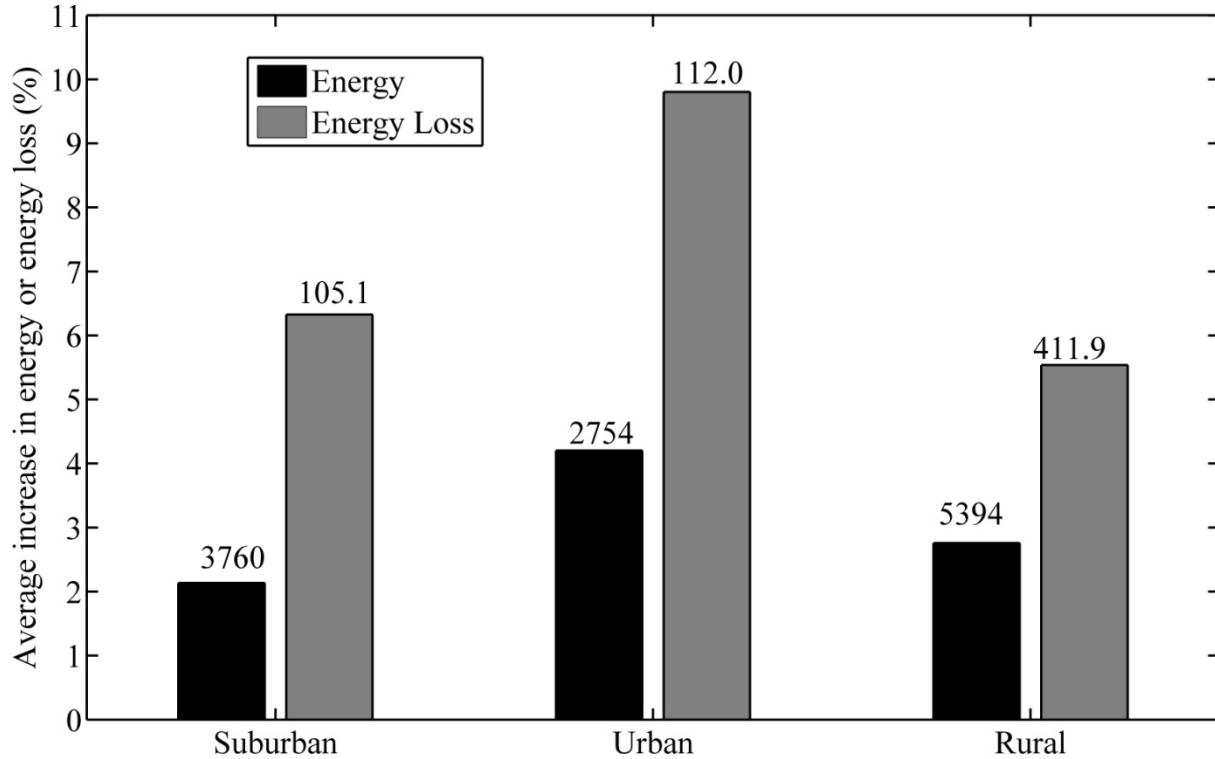
**Figure 5.8. Average percent increase in energy and energy loss for the high scenario compared to the base case without PHEV charging. Absolute changes in energy values are shown above each bar in kWh.**

## 5.3   Voltage drop and Unbalance

Voltage drop is an aspect to consider for reliable operation of a distribution network. Excessively low voltages can cause electrical equipment to malfunction and damage to electric motors [35]. Increasing the impedance on a line causes more power loss, resulting in an increased voltage drop. Thus, as the distance from the source (substation transformer) increases on a network, so does total impedance causing the lowest system voltages to occur at the extreme buses of a network. A generally accepted practice for voltage limits has been set forth by the American National Standards Institute (ANSI), which suggests the following guidelines for voltage magnitudes at the point of utilization (connection of the secondary transformer) [24]:

- Favourable zone: between 1.05 p.u.  and 0.95 p.u. above or below nominal base voltage

- Tolerable zone: between 0.91 p.u. and 0.95 p.u. of nominal voltage

- Extreme (emergency) zone: between 0.90 p.u. and 0.91 p.u. of nominal voltage

Voltages within the favourable zone will allow for satisfactory operation of equipment (motors, lights, computers, etc.) without noticeable problems or damage. The tolerable zone is acceptable for most purposes, and equipment should operate satisfactorily. However, voltages in the tolerable zone may be unacceptable to customers with voltage sensitive equipment, and thus attempts should be made to improve the voltages on the network within this range. The extreme or emergency zone is the last permissible voltage range. When voltages are within the emergency zone, most equipment will continue to function but will do so at a lower level of performance or incur some minor damage. It is recommended that voltages within the emergency zone be improved immediately through the use of a voltage regulator or shunt capacitor.

The voltage results for each network in the high scenario are analyzed for the lowest occurring line-to-neutral voltage on the network and the bus location, phase and hour of this minimum voltage is recorded. This minimum voltage bus is then used to analyze the impact of PHEV charging on network voltage drop by creating histograms to compare the voltage magnitude with and without PHEV charging on the three networks. The histograms are shown in Figure 5.9, Figure 5.10 and Figure 5.11 for the suburban, urban and rural networks respectively. The percentage decrease in average voltage at the minimum voltage buses due to PHEV charging was 0.38%, 0.25% and 0.63% for the suburban, urban and rural networks respectively. The rural network exhibits the largest voltage drops due to the long line lengths in that network, dropping below the favourable zone even in the absence of PHEV charging.  The emergency zone voltage range is not reached in any network.
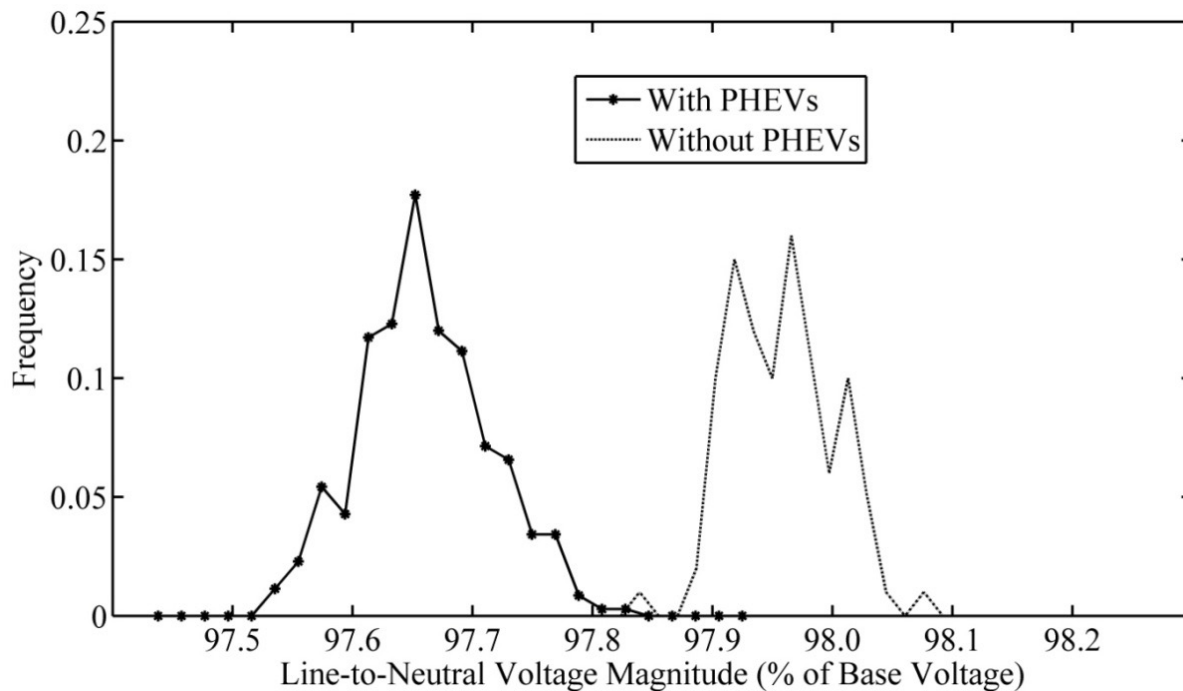
**Figure 5.9. Bus voltage distribution for lowest single phase bus voltage on the suburban network at 18:00 hours**
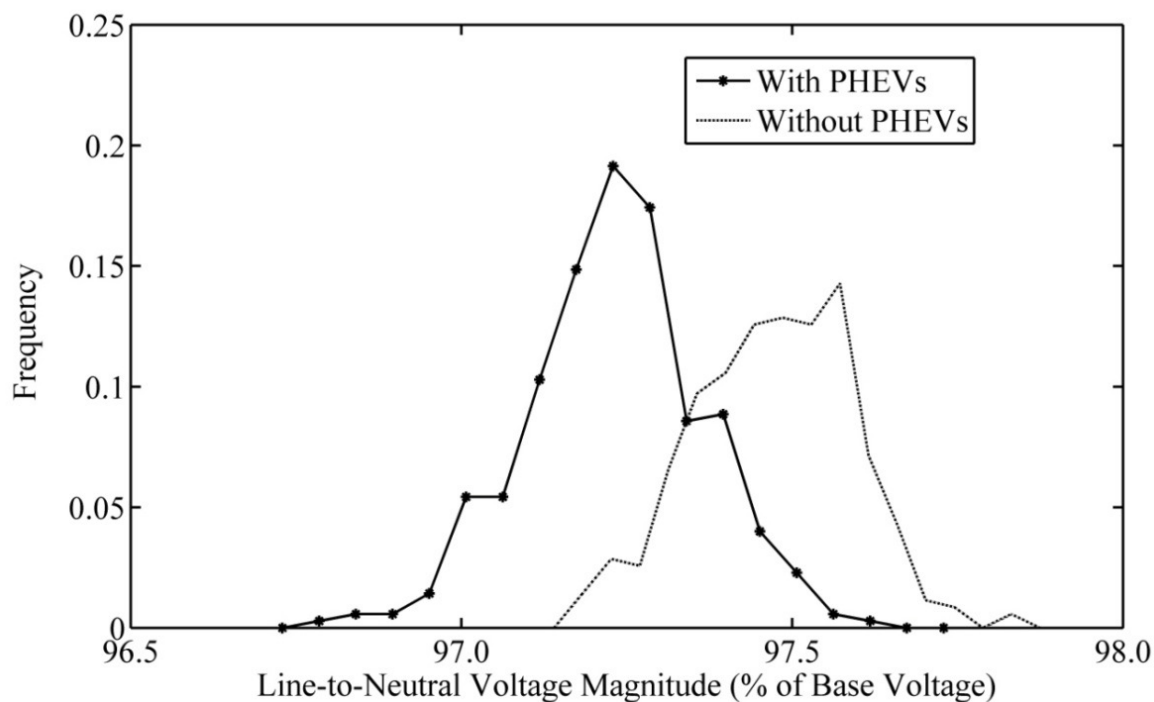


**Figure 5.10. Bus voltage distribution for lowest single phase bus voltage on the urban network at 10:00 hours.**
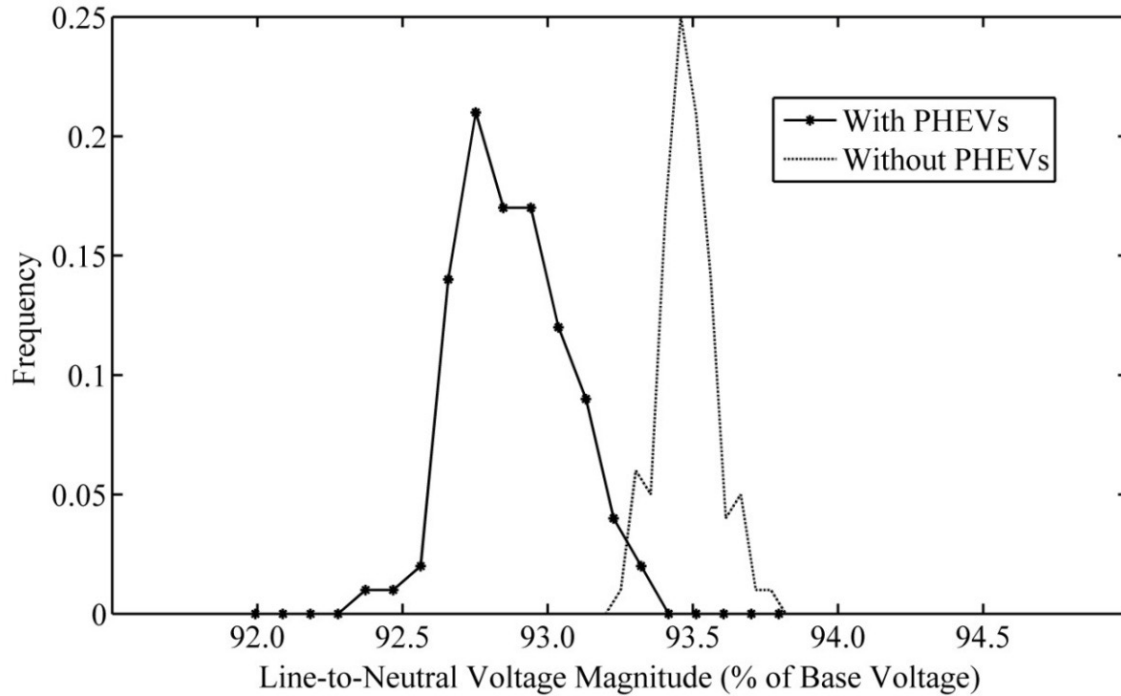
**Figure 5.11. Bus voltage distribution for lowest single phase bus voltage on the rural network at 18:00 hours.**

Apart from voltage drop, voltage unbalances can cause adverse impacts to three phase equipment on a power system such as induction motors, power electronic converters and adjustable speed drives [36]. In an unbalanced condition, a distribution network will incur more losses and will be less stable. The usual method for assessing voltage unbalance is to use the method from the National Electrical Manufacturers Association [24]. To calculate the maximum percent voltage unbalance at a three phase bus ($n$), the line-to-line voltage magnitudes ($V$) are used in the following expression:

$$\% \, Voltage \, Unbalance_n$$

$$= \frac{Maximum \, Deviation \, from \, Mean \, of \, \{V_{ab_n}, V_{bc_n}, V_{ca_n}\}}{Mean \, of \, \{V_{ab_n}, V_{bc_n}, V_{ca_n}\}} \cdot 100\% \qquad (5.11)$$

where a, b and c represent the phases.  It is recommended that electrical supply systems should be designed to limit the maximum voltage unbalance to 3% to avoid the majority of problems for three phase equipment on the network [36].

Voltage unbalance is calculated for each three phase bus on the network by first converting all of the line-to-neutral voltages to line-to-line voltages. Equation (5.11) is used to calculate a percent voltage unbalance at each bus for each hour and iteration. The maximum percent voltage unbalance is shown in Figure 5.12 for each network with and without PHEV charging. In Figure 5.12, the bus with the highest maximum voltage unbalance is selected. The charging of PHEVs causes a slight increase in the maximum unbalance on all three networks, increasing the maximum unbalance to 0.55%, 1.06% and 2.01% for the suburban, urban and rural networks respectively. The limit of 3% maximum voltage unbalance is not reached in any of the networks. The unbalance is highest in the rural network because of the presence of large single phase sections on the network.
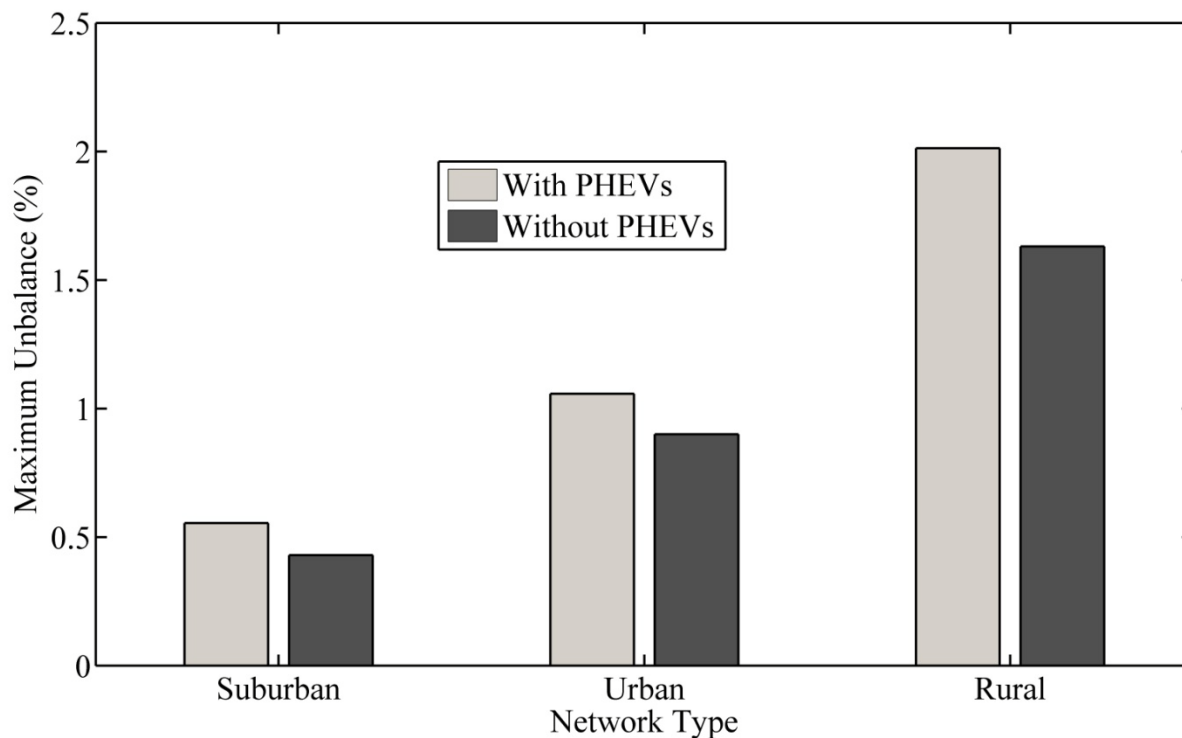
**Figure 5.12. Maximum percent voltage unbalance for a three phase bus on each network**

## 5.4    Transformer Overloads

In the following section, the term overload refers to an exceedance of a transformer's rated power capacity.

### 5.4.1    Transformer Overloading

The overloading of both primary (substation) and secondary transformers is a concern associated with the economical operation of distribution networks. For secondary transformers this is important when considering the upgrade of charging to 240V as numerous households charging PHEVs simultaneously at this level would add a load that is much higher than typical household loads.

To investigate secondary transformer overloading, the number of transformers with an overload above 20% of their rated capacity are counted at each time interval. The value of 20% greater than the rating is chosen because loss of life is not expected to be very significant below this level [37]. The percentage of transformers overloaded at each time step is then averaged over the iterations to produce an average percentage of overloaded transformers for each time step:

$$\overline{\%Overload_h^T} = \frac{\sum_{i=1}^{M}\left(\frac{Total\ Number\ of\ Overloads_{i,h}}{N}\right)}{M}, \forall\ h \tag{5.12}$$

where M is the total number of MCS iterations

Figure 5.13 (a-c) shows the average percentage of overloaded secondary transformers $(\overline{\%Overload_h^T})$ at each time step ($h$) in the high scenario and in the absence of PHEVs for the three networks. The rural network, Figure 5.13 (c), shows a small amount of transformer overloading which increases a small amount when PHEVs are added. The urban network, Figure 5.13 (b), shows almost 10% of the transformers are overloaded in the absence of PHEVs; however, when considering the high scenario, PHEVs do not increase the amount of overloads significantly. The suburban network, Figure 5.13 (a), shows the most secondary transformer overloading accounting for nearly 25% of all the transformers in the network at 18:00 hours in the high scenario. The suburban network also has the highest increase in transformer overloading when PHEVs were added.
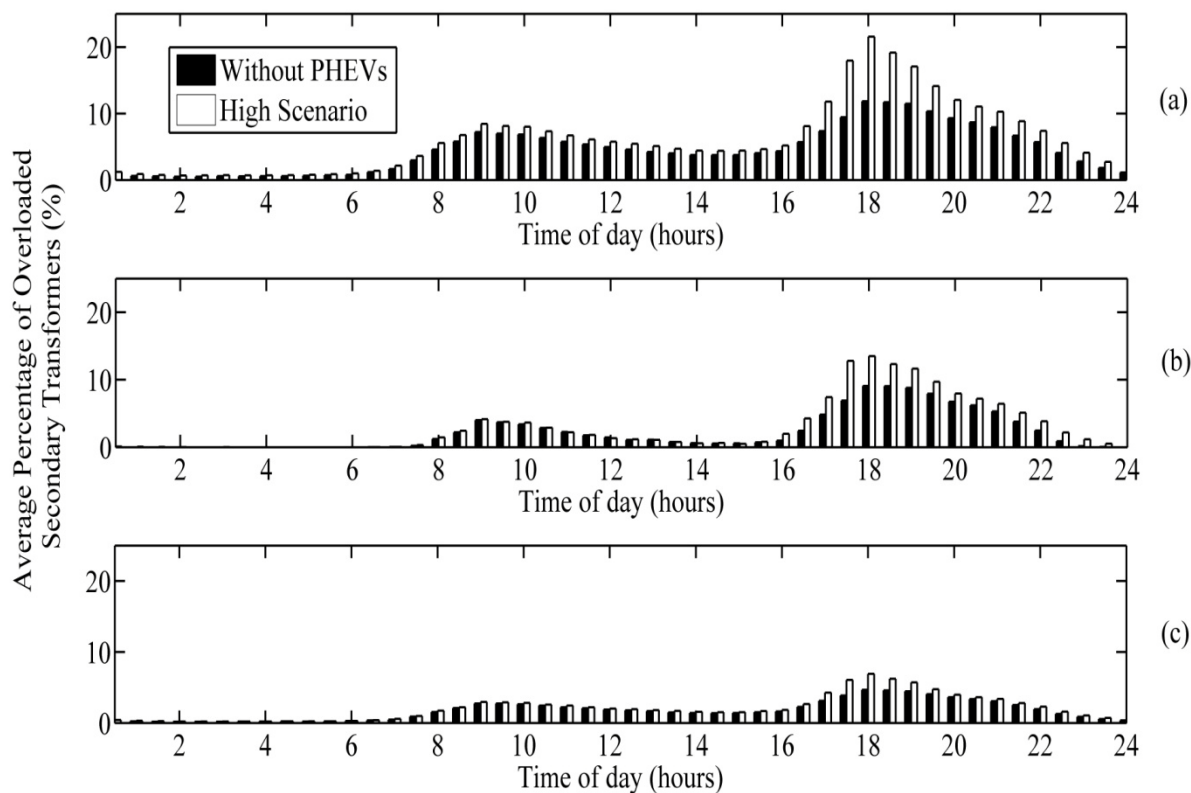
**Figure 5.13. Average percentage of overloaded secondary transformers with and without PHEV charging for (a) suburban, (b) urban and (c) rural networks for the high scenario**

### 5.4.2   Transformer Insulation Loss of Life

The overloaded transformer percentages (Figure 5.13) provide an estimate of the number of transformers that have some degree of overloading; however, it does not provide information about the impact on the lifetime of the transformers caused by overloading. During transformer operation the core material and tape insulation on the windings heats up and degrades slightly. Under normal operation the lifetime of the transformer insulation can be greater than 20 years, but overloading will decrease this expected lifetime.

The IEEE standard C57.91-1995 provides a guide to loading mineral oil immersed transformers and a method for estimating the insulation loss of life associated with overloading

of these transformers [37]. The loss of life is a function of the degree and duration of the overload as well as the ambient temperature of the surroundings and the design of the transformer. The method used to estimate the percent insulation loss of life is summarized in Appendix E. The definition of normal life is based on retaining 25% tensile strength of the insulation material for continuous operation of a transformer at rated capacity and a "hottest spot" insulation temperature of 110 ºC. This definition leads to an estimated lifetime of 180,000 hours or 20.55 years. For a 24 hour period of operation at rated capacity and hottest spot temperature of 110 ºC, the daily percent loss of life is estimated to be 0.018% per day. Calculated loss-of-life values below 0.018% will extend the life of the transformer beyond its expected lifetime.

The standard C57.91-1995 is applicable to a wide range of transformer sizes and can be used to estimate the percent loss of life on secondary transformers. To analyze transformer insulation loss of life, three overloaded secondary transformers from the suburban network are used for the calculations. Two of the transformers used for the calculation have a 25 kVA rated capacity, while the other has a 50 kVA rated capacity. The characteristics of these three transformers are shown in Table 5.2

The calculations are made using the average load supplied to each transformer for a 24 hour period $(\overline{S_{n,h}})$. The manufacturer specifications used for the individual transformer calculations are found in Appendix E. The percent loss of life, shown in Figure 5.14, is calculated for the three transformers assuming constant daily ambient temperatures of 5ºC and 25ºC to represent loading in the winter and summer respectively.

**Table 5.2. Summary of characteristics for loss of life calculations on three secondary transformers**

| Parameter | Transformer 1 | Transformer 2 | Transformer 3 |
|---|---|---|---|
| Rated Capacity (kVA) | **25** | **50** | **25** |
| Ratio of peak transformer load to rated capacity | 1.86 | 1.78 | 1.36 |
| Duration of overload (hours) | 15.5 | 17 | 6.5 |
| Number of Customers connected | 6 | 9 | 7 |
| Number of PEVs at 120V | 0 | 1 | 0 |
| Number of PEVs at 240V | 2 | 4 | 1 |

The transformer loss of life increases exponentially with the hottest spot insulation temperature (Appendix E). Transformers 1 and 2 show the highest average loadings of 186% and 178% of rated capacity, respectively. They also have the longest duration of overloads (Table 5.2). This leads to very high percent loss of life for both of these transformers when compared to the expected loss of life (0.018% per day). If repeated overloading of transformers 1 and 2 were to occur for a long period of time, the cumulative loss of life would be significant.

Transformers 1 and 2 are excessively overloaded, especially in the presence of PHEVs. However, transformer 3 shows a lower peak overload and shorter duration of overload than the other two transformers and thus its loss of life is significantly lower. The calculated loss of life for transformer 3 is below the expected loss of life, even though it is loaded up to 136% of its rated capacity. The results in Figure 5.14 provide strong evidence that there is negligible loss of life for a transformer that is subjected to an overload that is less than 20% above its rated

capacity. The vast majority of the overloaded transformers on this network (Figure 5.13) exhibit overloads between 20-30% above their rated capacity where loss of life is not significant.

In the transformer loss of life calculation, the ambient temperature has a linear effect on the hottest spot temperature. Thus, for a given transformer loading profile, higher ambient temperature can significantly increase the transformer loss of life.
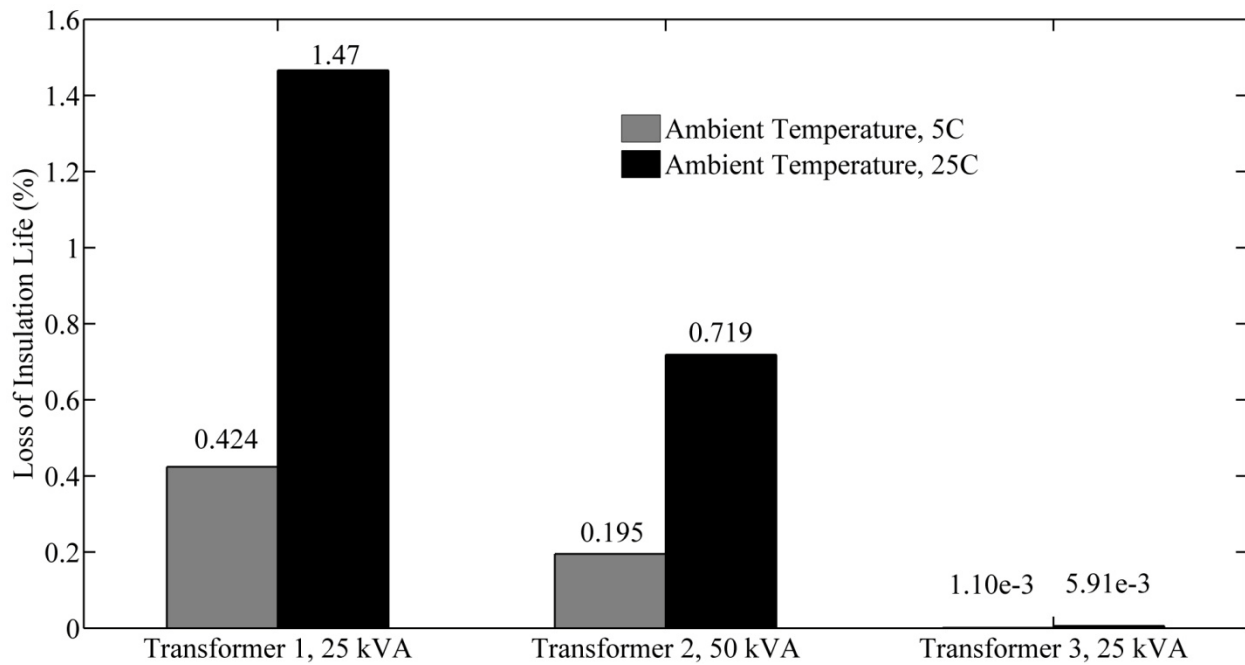


**Figure 5.14. Average percent loss of life for one day considering three secondary transformers from the suburban network at 5⁰C and 25⁰C ambient temperature. Values are shown above the bars.**

## 5.5 Vehicle Simulation Results and GHG Analysis

For all vehicle results considered in this section, the vehicles from the rural network are used. The assumptions determining the vehicles behaviour during the simulations do not change

for a scenario or network, so the network and scenario with the most vehicles is chosen for the analysis.

For the residential vehicles, the energy derived from the grid (grid energy) and the gasoline consumed for each vehicle trip is tracked for the entire simulation. The average gasoline use is calculated for each vehicle on a per day basis by averaging over the iterations. Figure 5.15 shows a histogram of average daily gasoline use. As expected, daily gasoline consumption is higher for vehicles in the low scenario due to the lower availability of charging locations away from home. For the high scenario in Figure 5.15, 78% of vehicles do not use any gasoline for the entire simulation, compared to 56.2% and 33.3% in the medium and low scenarios, respectively.
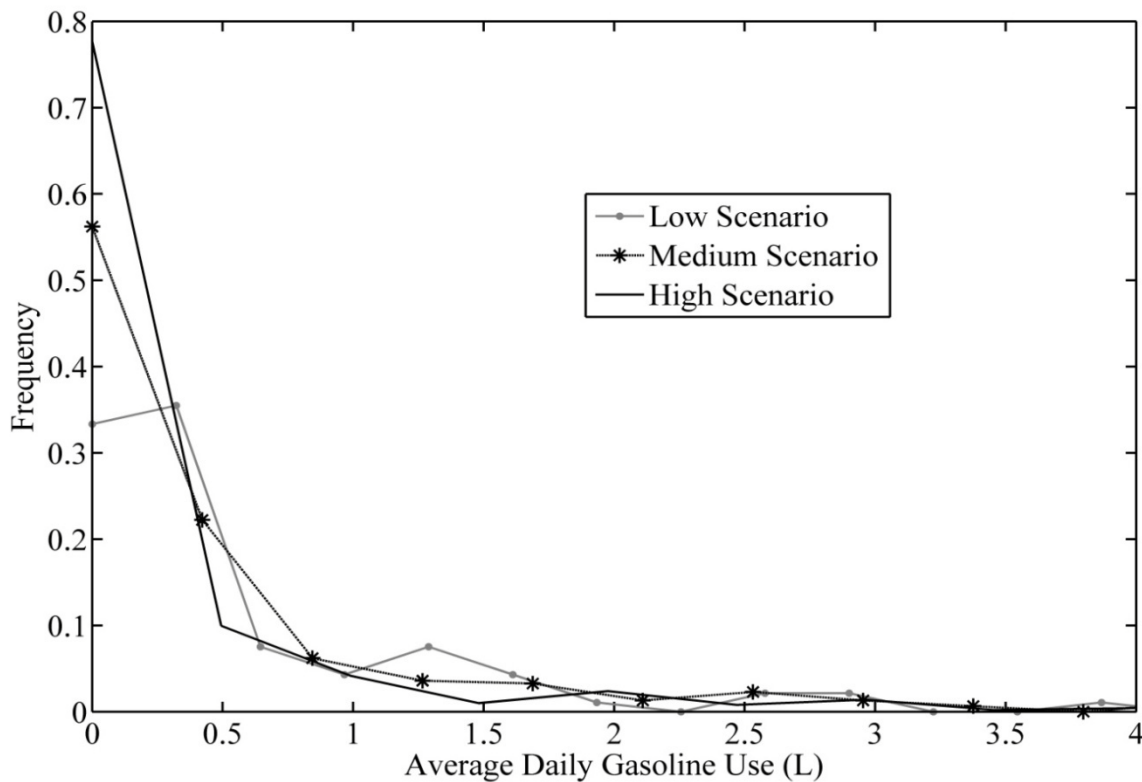


**Figure 5.15. Distribution of average gasoline consumption per day for all vehicles in the rural network**

To investigate the relationship between energy, gasoline and commuting distance, the average daily grid energy and gasoline used for each vehicle is plotted against one-way commuting distance in four different combinations of battery size and home charging rate as shown in Figure 5.16 (a-d). The low, medium and high scenario vehicles are pooled together in Figure 5.16. This can be done because the simulation of residential vehicles does not change between scenarios, only the technology and number of vehicles changes.

In each of Figure 5.16 (a-d) the grid energy and gasoline use trends show a distinct bifurcation at a specific commuting distance at which one trend levels off near the battery capacity, while the other levels off at double the battery capacity. The upper trend representing double the battery size is caused by vehicles which can charge at their workplace. Also, above a threshold commuting distance, a linear trend in gasoline consumption is seen as commuting distance increases. This threshold is increased for those vehicles with the ability to charge at the workplace. When commuting distances are small, there is very little if any gasoline consumption.

In both Figure 5.16 (a) and (b), all of the small battery vehicles have an average daily gasoline use above zero. However, at low commuting distances the gasoline use is very low. Comparing between Figure 5.16 (a) and (b) shows that home charging at 240V (7.6 kW) has little to no effect on gasoline consumption or grid energy used for small battery vehicles. The bifurcation point between PHEVs with no workplace charging and those with workplace charging occurs at a one-way commuting distance of approximately 5 km.

The larger batteries, Figure 5.16 (c) and (d), use significantly less gasoline and more grid energy than the smaller battery vehicles. The larger battery vehicles use no gasoline if their commuting distance is below a threshold of approximately 20 km. Comparing between Figure

5.16 (c) and (d), the ability for home charging at 240V does not appear to affect the gasoline consumption or grid energy used per day.

An interesting trend in Figure 5.16 is seen by comparing the gasoline usage between the small batteries and large batteries in Figure 5.16 (b) and (d), respectively. In Figure 5.16 (b) the gasoline consumption lines run nearly parallel after the bifurcation point, suggesting that the ability to charge small batteries at work has little effect on daily gasoline usage if the commuting distance is high. However, in Figure 5.16(d) the gasoline consumptions lines are further apart after the bifurcation point showing that even for very high commuting distances, larger battery PHEVs can significantly reduce gasoline usage, especially if they can charge at their workplace.
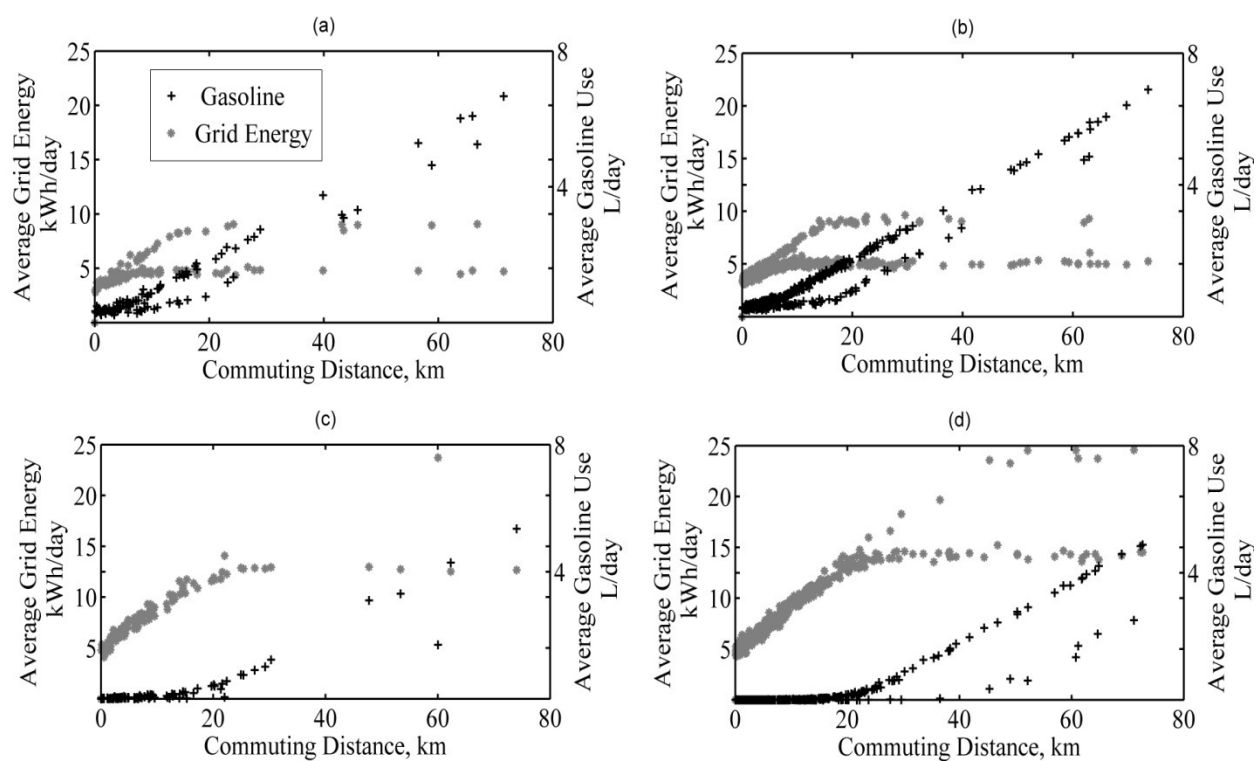


**Figure 5.16. Average daily energy and gasoline usage verses commuting distance for combinations of battery sizes and charging rates. (a) 4.85 kWh batteries, 1.44 kW charge rate, (b) 4.85 kWh batteries, 7.6 kW charge rate, (c) 16.6 kWh batteries, 1.44 kW charge rate and (d) 16.6 kWh batteries, 7.6 kW charge rate.**

Emissions from vehicle operation are often cited as a major reason for widespread adoption of electric vehicle technologies. Emissions from the grid in BC are significantly lower than other jurisdictions due to the high proportion of hydro electric power dominating the generation mixture. In 2008, BC hydro reported an average emission intensity of 22 $tCO_2e$/GWh [38], a value significantly lower than the Canadian average of 217 $tCO_2e$/GWh [39]. Using the BC hydro reported emissions intensity (22 $tCO_2e$/GWh) and a value of 9.254 kg $CO_2e$ per gallon of gasoline [39], average daily emissions are calculated using the same vehicles as in Figure 5.16. The combined gasoline and grid energy average daily emissions are plotted in Figure 5.17 against the average daily distance driven for each vehicle.
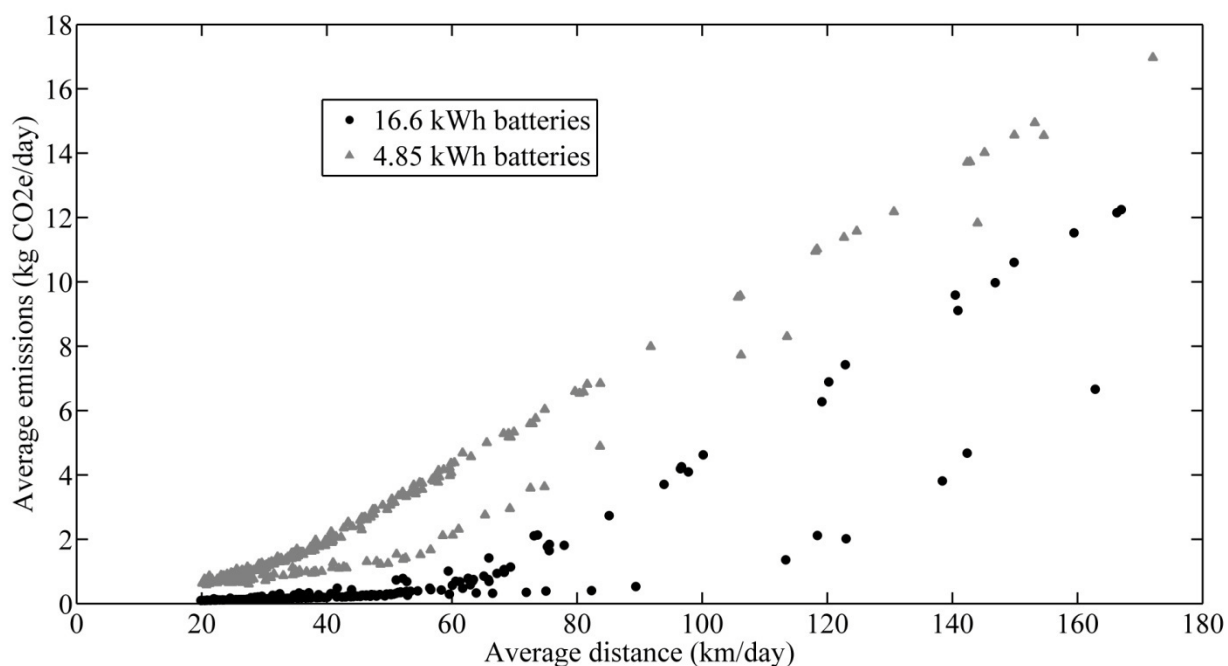


**Figure 5.17. Scatter plot of average emissions verses the average daily distance.**

The scatter plot of average emissions in Figure 5.17 shows that vehicle emissions increase rapidly as vehicles drive further and use more gasoline. Emissions are lower for the larger

batteries because they derive more energy from the grid than the smaller batteries. The larger battery vehicles are more likely to drive solely on electricity and a large proportion obtained more than 90% of their kilometres from grid energy. The average emissions rate for the larger batteries is 0.38 $kgCO_2e$/day, while the small batteries have an average of 1.31 $kgCO_2e$/day. These averages are quite low due to the small commuting distances used as inputs to the model and can be seen by the clustering of points around the low ranges of average distance in Figure 5.17.

# 6 Discussion

This chapter begins with a discussion of the impact of PHEV charging on network demand and the implications for each type of network. Next, the results from the voltage drop and unbalance analysis are discussed followed by a thorough treatment of the consequences of transformer overloading and loss of life. Emissions results are summarized and a discussion of the impact of generation mixture on emissions in BC is given.

## 6.1 Network Demand

The coincidence between peak electricity demand and vehicles returning home from daily commutes is one of the main near-term concerns for utilities when considering electric vehicles. Model results show that as vehicles return home and begin charging, they can cause a large increase in the peak demand on a network (Figure 5.7). In the suburban and urban networks, the peak simulated network demand is not high enough to cause overloading above the suggested network capacity. Thus, increased peak demand from PHEV charging does not appear to be a significant concern for the reliable supply of power, even for high PHEV penetrations of up to 25%.

For the rural network, the measured peak demand (Table 4.2) is near the suggested network capacity. As a result, PHEV penetrations in excess of 15% on this network cause overloads and excessive voltage drops during high demand days.

As PHEVs numbers grow, the peak demand may increase at a higher rate than the increase in energy supplied to the network due to PHEV charging (Figure 5.7). The peak demand increases more than energy growth because of a wider assumed availability of 240V chargers at residences. A further result of a higher peak demand is that the energy loss in the networks

increases more than the energy growth because of the losses being a function of the square of the current (Equation A.12). Economically this is undesirable because more energy needs to be generated to meet the incremental demand. This result is a further example of the need for vehicle charging control.

PHEV demand at retail and office locations differs significantly from residential PHEV demands. The urban network exhibits an increase in the demand during the daytime hours creating a morning peak on this network (Figure 5.4). Areas with high office loads, such as the urban network, may exhibit similar morning peak demands if workplaces are willing to install charging locations for their employees. A network with a high level of retail demand was not considered (see Figure 4.1). It is uncertain whether the charging demand at retail locations will be significant, as vehicles will connect for only short periods of time and the demand might be spread more evenly throughout the day. Charging stations installed on streets, retail locations and workplaces will mean less aggregate gasoline usage and lower vehicle emissions for PHEV operators who can take advantage of these stations.

In terms of total network demand, the possible implications of large penetrations of PHEVs charging in an uncontrolled fashion are higher voltage drops, lines current overloading and the possible exceedance of the network capacity. These impacts are all difficult and costly to remedy and can reduce the reliability of power supply. In any jurisdiction, networks that exhibit total demands near their capacity are at higher risk for some of these possible detrimental impacts.

Control over vehicle charging will be important in the future for shifting the vehicle charging demand into the off-peak hours. Even with charging control, it is likely that some owners will still want to charge during the peak period in order to make trips during the evening

without the need to use gasoline. Also, if PHEV owners have larger batteries and are charging at 120V, the amount of time needed to charge their battery may require them to charge during the peak period.

In the near term it is suggested that a program be started to keep track of the location and type of electric vehicles sold throughout a jurisdiction. This type of program will help to determine the networks that are at highest risk for some of the adverse impacts considered in this study and could help with a transition to control of vehicle charging or integration of vehicles into a smart metering infrastructure. Identifying the possible networks or areas where high penetrations of PHEVs could occur will be important for predicting impacts on these areas.

## 6.2    Voltage Drop and Unbalance

Maximum voltage drops on the suburban and urban networks remain within the favourable zone for all of the scenarios considered, as shown in Figure 5.9 and Figure 5.10. This is mainly due to the shorter feeder length and lower peak demands when comparing these networks to the rural network (Table 4.2). Voltage drop is an issue for the rural network because of the long line length. The maximum voltage drops calculated on the rural network are in the tolerable zone as shown in Figure 5.11. Thus, further voltage regulation may be needed on this network in the near future, most likely in the form of a shunt capacitor or voltage regulator.

In the model, the substation transformer was considered as a constant voltage source, when in fact, substation transformers are equipped with load tap changers that can raise the base network voltage by altering the turns ratio of the transformer windings. By increasing the base voltage by 5%, the minimum voltage drop of 0.93 p.u. encountered on the rural network could be

improved to bring it into the favourable zone. This is possible because the voltage standards allow for voltages greater than 5% above the nominal level for the favourable zone.

Rural networks often exhibit higher voltage drops and lower reliability when compared to smaller networks because of the large areas that they supply power to [17]. Uncontrolled PHEV charging on rural networks will further lower the voltages found on these networks and they may require reinforcing if PHEV penetration is significant. Alternatively, there is an opportunity to use PHEVs for voltage support in a vehicle-to-grid (V2G) scheme on these networks. Thus, rural networks could be used as demonstration or pilot projects as a means of introducing V2G in a jurisdiction.

## 6.3   Overloading and Transformer Loss of Life

The overloading of secondary transformers is highest for the suburban network. Almost 10% of the transformers are overloaded without any vehicles charging. When PHEV are considered in the high scenario, the total percentage of overloaded transformers reaches nearly 25% as shown in Figure 5.13 (a). The rural and urban networks do not show a significant increase in transformer overloading even for the high penetration scenarios (Figure 5.13 (b) and (c)).

In the suburban network, the total connected capacity (the sum of all secondary transformers' rated capacities) is much lower when compared to the rural network (Table 4.2). However, both networks have the same total network capacity and voltage level. This means that on the suburban network there are more customers sharing fewer transformers leading to the higher rates of overloading. In the suburban network, customers are closer together and thus, it may be economical to connect more customers to fewer transformers. In the rural network, customers are spread out over larger distances and generally more transformers are used for fewer customers.

This is done to avoid lengthy secondary wiring sections where voltage drop and losses are higher. In the urban network, there is a substantial amount of demand connected to large three phase secondary transformers serving larger customers such as apartments and offices. Three-phase secondary transformers are more expensive to install and maintain than the pole-mounted single phase type. Consequently, these transformers are generally over-sized to accommodate load growth leading to fewer overloads on the urban network when compared to the suburban network. Overloads on the urban network mostly occur on single phase transformers.

Single-phase secondary transformers are of standardized size and can be easily replaced to minimize the effects of transformer overloading. For example, an overloaded 50 kVA transformer could be replaced with a 75 kVA transformer. This 50 kVA transformer could then be used to replace an overloaded 25 kVA transformer. In this manner the economical loss of transformer life is diminished and secondary transformers of lower ratings can be slowly swapped out as needed.

During model initialization, the power demand on each transformer in the network is estimated from customer energy consumption readings (Figure 3.5). In practice, the demand on a given secondary transformer is unknown. Thus, a method to identify overloaded transformers could be implemented to ensure that the properly sized transformers are used for all customer groups. This type of program could help to reduce the impact of PHEV charging on secondary transformer lifetimes, especially if other networks have similarly overloaded transformers as the suburban network does. If future smart grid technologies are installed correctly on a network, overloaded transformers could be easily identified and monitored.

The simulation results for transformer insulation loss of life (Figure 5.14) show that the ambient temperature of the surroundings can have a large impact on the lifetime of a transformer. This may be especially evident in jurisdictions with high summer peak loads. In a jurisdiction where the peak demand occurs in the winter months, transformer insulation may last longer due to the lower temperatures. Specifically, in BC, the annual peak demand is often correlated to the coldest day of the year.

Transformers that are experiencing overloads without PHEV charging can have their lifetime significantly reduced if PHEVs are added, which is evident from Figure 5.14. This is particularly true if large numbers of PHEVs are charging at the 240V level. However, the loss of life is not significant for short time duration overloads in the range of 20-30% above the rated capacity of the transformer. Thus, identifying the transformers with excessively high overloading is necessary.

## 6.4   Emissions

Total emissions from PHEV operation are lower for large battery vehicles as shown in Figure 5.17. As the average distance driven increases, the emissions rise rapidly due to a higher use of gasoline. Thus, replacing gasoline use with grid energy could have large benefits in terms of reducing transportation sector emissions, particularly in grids with low emission rates such as BC.

The emissions are calculated by assuming constant emission intensity for grid energy. In reality, the emissions depend upon how generation is allocated to the generation assets and the amount of power being imported. In BC, electricity may be imported during the low demand

hours when the price for imported power is lowest. Generation during the low demand hours in neighbouring jurisdictions, specifically Alberta, may contain a large fraction of coal generation, leading to higher emission rates. If large amounts of vehicles are charging in the off-peak hours this could increase the emissions from these vehicles. The amount of power imported is generally low compared to the amount generated domestically and thus, emissions may not increase dramatically. Further study is needed in this area to properly determine the emissions increase caused by this effect.

Large penetrations of PHEVs could alter both the economics of grid operation and the emissions intensity. The effect of PHEVs on the dispatch of generation and, thus, the emissions and costs of electricity is a region-specific problem that must be investigated for entire electrical systems through the use of optimal power flow algorithms. The results of this type of study may lead to optimal charging scenarios for vehicles that consider the emissions produced during charging rather than simply considering the timing of charging. For the sole purpose of reliable operation of the distribution network, vehicle charging during the off-peak hours would be ideal.

## 6.5 Electric Vehicle Technologies and the Future Smart Grid

Electric vehicles represent a paradigm shift for both the transportation sector and utilities. As electric vehicles increase in numbers, more electricity will be generated and less gasoline used, affecting aspects of both sectors positively and negatively. As an example of a negative impact, when gasoline is replaced by electricity, tax revenue from gasoline sales will diminish and this revenue will need to come from another source, the most likely candidate being electricity price increases. This could eventually reduce the price benefit of electric vehicles for vehicle owners.

The transition to an electrified transportation sector will require careful planning and sound policy. Electrifying the transportation sector will also create new and unique business and employment opportunities. Balancing the positive and negative impacts of electric vehicles will be important for maximizing the social, economic and environmental benefits. Smart grid technologies are a promising approach to both control vehicle charging and add an element of active control and measurement to distribution networks. Currently, a widespread smart grid program is being undertaken by many utilities in an effort to increase the efficiency of the grid and to gain more insight into the operation of the distribution networks.

Integration of PHEVs with smart grid technologies will be important to realize the maximum benefit of PHEVs to vehicle owners and lessen the negative impact of vehicle charging. The integration of PHEVs and smart grid technologies could also help in the transition to Vehicle-to-grid (V2G) schemes, where vehicles could act as distributed storage mechanisms and supply power back to the grid. V2G schemes have been proposed as a means of increasing the penetration of renewable generation [2]; however, this aspect requires more investigation on a region-specific level to determine feasibility.

The control and pricing of PHEV charging are two aspects that could play a major role in impacting their market penetration. The control method could be direct control from the utility, where the vehicle responds to a real-time price or wireless control signal. Control could also occur indirectly through incentives or onboard vehicle charge controllers. Also, a mechanism would need to be in place to ensure payment for vehicle charging at workplace and quick charge locations is transferred to the vehicle owner where appropriate. Regardless of how charging is performed or priced, methods of controlling charging times and rates should be implemented well before PHEVs become widespread.

# 7  Conclusions and Recommendations

## 7.1  Study Objective and Summary of Methodology

The objective of this study is to investigate the impacts of plug-in hybrid electric vehicles on distribution networks. The impacts considered on the networks are: total network demand, energy supplied, energy lost, voltage drop, voltage unbalance, and transformer loss of life. Estimated GHG emissions from vehicle operation are calculated to determine the environmental benefit of PHEVs.

The objective is achieved through creation of a probabilistic load flow model based on Monte Carlo simulations (MCS) in which a probabilistic model of customer demand is combined with probabilistic models of uncontrolled PHEV charging at residences, offices and retail locations. The MCS procedure consists of repetitive deterministic solutions to a load flow algorithm supplying the random variables of customer demand and PHEV load. Simulations are performed repeating a peak demand day in order to determine the incremental impacts of PHEVs to a worst-case customer demand scenario. Three-phase distribution networks within the BC grid are selected with distinct demographic and topological aspects to represent suburban, urban and rural areas. Three scenarios are created to investigate increasing PHEV penetration and technology advancement (low, medium and high scenarios). The three phase network incorporates three phase and single phase sections as well as voltage control equipment.

## 7.2 Key Findings

### 7.2.1 PHEVs and Network Demand

All of the networks exhibit an increase in peak demand due to the charging of PHEVs by vehicle owners returning home from evening commutes. For the rural network, the peak demand exceeds the network capacity rating when PHEV penetrations are above 15%. The suburban and urban networks do not exhibit network overload, and can safely accommodate PHEV penetrations up to 25%. This is mainly due to the existing (recorded) peak demand being much higher on the rural network than on the other two networks. A morning peak occurs at 10:00 on the urban network from the charging of PHEVs at offices.

When progressing from the low scenario to the high scenario, the peak network demand increases at a higher rate than the energy supplied to the network for PHEV charging. Energy loss on the networks is also found to increase at a higher rate than the energy supplied, meaning that more energy would need to be generated to meet the incremental demand.

### 7.2.2 Voltage drop and unbalance

The suburban and rural networks did not exhibit voltage drops below the favourable zone. The rural network exhibits the largest voltage drop of the three networks; however, the voltages do not drop below the extreme zone at any time. The rural network may require some form of voltage regulation to improve the voltages on the extreme buses.

PHEV charging increases the maximum voltage unbalance on all of the networks. However; the maximum unbalance does not exceed the 3% suggested threshold. Voltage unbalance should not be a specific area of concern when considering PHEV charging.

### 7.2.3 Transformer Loss of Life

The suburban network shows a large increase in the number of overloaded transformers for the high PHEV penetration scenario. The high number of transformer overloads is due to the fact that this network has more customers that connect to lower rated transformers and thus the risk of overloading is higher. The overloading increases as vehicles are added to the network, especially with more PHEVs charging at 240V.

Transformer loss of life is calculated for three secondary transformers that show significant levels of overloading. The 25 kVA transformer charging 2 PHEVs at 240V shows the largest percent loss of life. Transformers subjected to short duration overloads that are less than 30% of their rated capacity should not experience significant loss of life.

### 7.2.4 PHEV Operation and Emissions

Energy and gasoline usage are tracked for all simulated PHEVs owned by residential customers. When charging infrastructure is limited away from vehicles' home base, PHEVs charge only once per day, increasing the amount of gasoline they use. When charging infrastructure is more available for PHEV owners, it allows them to charge their batteries more than once per day leading to a higher proportion of miles derived from electricity, effectively reducing emissions. The home charge rate, whether 120V or 240V, did not significantly affect the amount of energy that vehicles obtained from the grid. Vehicles with larger batteries were more likely to drive solely on electricity than their smaller battery counterparts. Despite a lower efficiency, large battery vehicles have lower average emissions because of their ability to drive more on electricity.

## 7.3    Conclusions

The networks in this study are representative of the types of networks found within the provincial grid and throughout most of North America. For small penetrations of PHEVs daily operation of the networks are not significantly affected. For networks that do not have peak demands near their capacity, the uncontrolled charging of vehicles does not create significant problems in terms of reliable operation of these networks. However, networks that currently have demands near their capacity are the most likely places that PHEV charging could have adverse impacts.

The introduction of PHEVs to a residential network where the loads on secondary transformers are already close to their capacity will increase the rate of transformer overloads and decrease their expected lifetime. This impact will be amplified if large numbers of PHEV owners upgrade their home charging outlets to 240V. Secondary transformer overloading can be mitigated through a transformer swapping program, however, the transformers that are at risk of being overloaded need to be properly identified first. Smart metering technology can be used to identify overloaded transformers.

Integrating PHEVs with smart grid technologies will allow for higher penetrations of PHEVs because the charging may be shifted to the low demand hours. This can be accomplished without adding significant network infrastructure, even on already stressed networks. The variety of impacts investigated in this thesis shows that an integrated approach to distribution system management is needed that can incorporate real-time measurement of parameters of interest through a smart metering program and high level modelling of networks.

### 7.4 Recommendations for future work

Some improvements to the model are recommended. First and foremost, a survey of vehicle commuters in BC could help to improve the commuting distance statistics as the current data includes all commuters, not solely those driving vehicles. Better estimates of the distance and timing of non-commuting vehicle trips in periods throughout the day would also help to improve the vehicle simulation portion of the model. These improvements would likely change the emissions from vehicles and the daily energy supplied for vehicle charging; however, changing the vehicle simulation inputs may not have a significant impact on the timing of the PHEV demand.

Network load modelling could be improved through better estimates of the temporal demand at the substations. This could aid in better estimating the demand on secondary transformers throughout a network. Further analysis should be undertaken to examine secondary transformer overloading on other suburban type networks to see if this trend could be widespread.

An issue associated with distribution networks that was not considered in this thesis is the potential impact that electric vehicle charging may have on the total harmonic distortion within a network. High harmonic distortion levels can cause excessive harmonic currents leading to higher levels of voltage distortion. Staats et al. [40] examined the impact of electric vehicle charging at a bus within a distribution network in a probabilistic manner. Their findings suggest that total harmonic distortion may be a limiting factor for electric vehicle penetration in certain situations. This study was performed a decade ago on the previous generation of vehicle chargers

and a similar study using newer vehicle chargers could help to determine if the total harmonic distortion from vehicle charging would be significant in the networks studied above.

For PHEV analysis on a larger scale, an agent based model that simulates the actions of large amounts of PHEV drivers as they travel throughout the province could be used to determine energy flows and emissions on a broader scale. An agent based model simulates the actions and interactions of autonomous individuals within a system to determine their aggregate effects on a whole system [41]. This type of modelling approach has been used for determining electric vehicle impacts on energy flows within a transmission grid on the large scale [42]. A similar approach could be tailored to locations in BC or North America for determining the overall impact to generation, transmission and the transportation sector in a jurisdiction. This may be a difficult task however, due to the lack of detailed statistics needed for input to these types of models.

# 8 Bibliography

[1] Province of British Columbia. Climate action plan. Province of British Columbia: Victoria, 2008. Available: http://www.livesmartbc.ca/attachments/climateaction_plan_web.pdf.

[2] T. H. Bradley and A. A. Frank. Design, demonstrations and sustainability impact assessments for plug-in hybrid electric vehicles. *Renewable and Sustainable Energy Reviews 13(1),* pp. 115-128, 2009.

[3] C. H. Stephan and J. Sullivan. Environmental and energy implications of plug-in hybrid-electric vehicles. *Environ. Sci. Technol. 42(4),* pp. 1185-1190, 2008.

[4] Electric Power Research Institute. Environmental assessment of plug-in hybrid electric vehicles vol. 1: nationwide greenhouse gas emissions, 2007.

[5] W. Kempton and J. Tomić. Vehicle-to-grid power fundamentals: Calculating capacity and net revenue. *Journal of Power Sources, 144(1),* pp. 268-279, 2005.

[6] P. Denholm and W. Short. An evaluation of utility system benefits of optimally dispatched plug-in hybrid electric vehicles. National Renewable Energy Laboratory, 2006.

[7] W. Kempton and J. Tomić. Vehicle-to-grid power implementation: From stabilizing the grid to supporting large-scale renewable energy. *Journal of Power Sources, 144(1),* pp. 280-294, 2005.

[8] Rowand M. The electric utility business case. Presented at Plug-in 2008, San Jose, CA.

[9] V. H. Méndez, J. Rivier, J. I. d. l. Fuente, T. Gómez, J. Arceluz, J. Marín and A. Madurga. Impact of distributed generation on distribution investment deferral. *International Journal of Electrical Power & Energy Systems 28(4),* pp. 244-252, 2006.

[10] A. Vojdani. Smart integration. *Power and Energy Magazine, IEEE 6(6),* pp. 71-79, 2008.

[11] J. A. P. Lopes, N. Hatziargyriou, J. Mutale, P. Djapic and N. Jenkins. Integrating distributed generation into electric power systems: A review of drivers, challenges and opportunities. *Electric Power Systems Research 77(9),* pp. 1189-1203, 2007.

[12] T. Ackermann, G. Andersson and L. Söder., Distributed generation: A definition. *Electric Power Systems Research, 57(3),* pp. 195-204, 2001.

[13] H. B. Chowdhury. "Load-flow analysis in power systems," in *Handbook of Electric Power Calculations* (3rd ed.), New York: McGraw-Hill, 2004, pp. 11.1-11.16, 2001.

[14] S. Conti and S. Raiti. Probabilistic load flow using Monte Carlo techniques for distribution networks with photovoltaic generators. *Solar Energy, 81(12),* pp. 1473-1481, 2007.

[15] D. H. O. McQueen. Application of a Monte Carlo simulation method for predicting voltage regulation on low-voltage networks. *Power Systems, IEEE Transactions on 20(1),* pp. 279-285 2005.

[16] W. El-Khattam, Y. G. Hegazy and M. M. A. Salama. Investigating distributed generation systems performance using monte carlo simulation. *Power Systems, IEEE Transactions on 21(2),* pp. 524-532, 2006

[17] D. Aming, A. Rajapakse, T. Molinski and E. Innes. A technique for evaluating the reliability improvement due to energy storage systems. *Electrical and Computer Engineering CCECE 2007. Canadian Conference on* pp. 413-416, 2007.

[18] L. D. Bellomo and G. Olivier. Harmonic distortion analysis software combining EMTP and monte carlo method. *Math. Comput. Simul. 71(4-6),* pp. 299-309, 2006.

[19] P. Caramia, G. Carpinelli, P. Varilone and P. Verde. Probabilistic three-phase load flow. *International Journal of Electrical Power & Energy Systems, 21(1),* pp. 55-69, 1999.

[20] P. Caramia, G. Carpinelli, M. Pagano and P. Varilone. Probabilistic three-phase load flow for unbalanced electrical distribution systems with wind farms. *IET Renewable Power Generation 1(2),* pp. 115-22, 2007.

[21] K. Parks, P. Denholm and T. Markel. Costs and emissions associated with plug-in hybrid electric vehicle charging in the xcel energy colorado service territory. National Renewable Energy Laboratory, TP-640-41410, 2007

[22] M. Kintner-Meyer, K. Schneider and R. Pratt. Impacts assessment of plug-in hybrid electric vehicles on electric utilities and regional US power grids part 1: Technical analysis. Pacific Northwest National Laboratory, 2007.

[23] S. K. Kurani, R. R. Heffner and T. S. Turrentine. Driving plug-in hybrid electric vehicles: Reports from US drivers of HEVs converted to PHEVs, circa 2006-07. Institute of Transportation Studies, UC Davis, 2007.

[24] T. Gonen. *Electric Power Distribution System Engineering.* McGraw-Hill College, 1985.

[25] W. H. Kersting. *Distribution System Modeling and Analysis.* (2nd ed.) CRC Press, 2007.

[26] N. D. Hatziargyriou. Probabilistic load flow in distribution systems containing dispersed wind power generation. *Power Systems, IEEE Transactions on 8(1),* pp. 159-165, 1993.

[27] C. Micu. Personal Communication. *BC Hydro Distribution Engineering*, May 2009.

[28] A. Pesaran. Battery requirements for plug-in hybrid electric vehicles: Analysis and rationale. Presented at 23rd International Electric Vehicles Symposium and Exposition, 2008. Available: http://www.nrel.gov/vehiclesandfuels/energystorage/publications.html

[29] K. Morrow, D. Karner and J. Francfort. Plug-in hybrid electric vehicle charging infrastructure review. US Department of Energy, Tech. Rep. INL/EXT-0815058, 2008.

[30] Statistics Canada. Census. *Catalogue Number 97-561-XCB2006010,* 2006.

[31] M. Conner. Plug-in hybrid vehicles can greatly impact emissions and petroleum dependency. *EDN 52(17),* pp. 16-16, 2006.

[32] C. R. Bhat and S. K. Singh. A comprehensive daily activity-travel generation model system for workers. *Transportation Research Part A: Policy and Practice 34(1),* pp. 1-22, 2000.

[33] Oak Ridge National Laboratory. 1995 national personal transportation survey databook. Tech. Rep. ORNL/TM-2001/248, 2001.

[34] British Columbia Ministry of Transportation. Traffic data program, 2009. Available: http://www.th.gov.bc.ca/trafficdata/tradas/mainmap.asp

[35] S. Conti. Distributed generation in LV distribution networks: Voltage and thermal constraints. *Power Tech Conference Proceedings, 2003 IEEE Bologna 2*pp. 6 pp. Vol.2, 2003.

[36] A. von Jouanne and B. Banerjee. Assessment of voltage unbalance. *Power Delivery, IEEE Transactions on 16(4),* pp. 782-790, 2001.

[37] IEEE Std C57.91-1995. IEEE guide for loading mineral-oil-immersed transformers, 1996.

[38] BC Hydro. 2008 annual report. 2008. Available: http://www.bchydro.com/about/company_information/reports/annual_report.html

[39] Environment Canada. National inventory report – greenhouse gas sources and sinks in Canada. 2007.

[40] P. T. Staats, W. M. Grady, A. Arapostathis and R. S. Thallam. A statistical analysis of the effect of electric vehicle battery charging on distribution system harmonic voltages. *Power Delivery, IEEE Transactions on 13(2),* pp. 640-646, 1998.

[41] L. Zhang and D. Levinson. Agent-based approach to travel demand modeling: Exploratory analysis. *Transportation Research Board, Journal of 1898(1),* pp. 28-36, 2004.

[42] M. Galus, R. Waraich, M. Balmer, G. Andersson and K.W. Axhausen. A framework for investigating the impact of PHEVs. in *International Advanced Mobility Forum (IAMF),* Geneva Switzerland*,* 2009.

[43] T. Chen. Evaluation of line loss under load unbalance using the complex unbalance factor. *Generation, Transmission and Distribution, IEE Proceedings- 142(2),* pp. 173-178, 1995.

[44] W. D. Stevenson. *Elements of Power System Analysis.* (4th ed.) McGraw-Hill, 1982.

[45] NIST/SEMATECH. "Chi-square goodness of fit test", in *e-Handbook of Statistical Methods,* 2009. Available: www.itl.nist.gov/div898/handbook/.

# Appendix A. Forward Backward Sweep Algorithm for Three Phase Unbalanced Radial Load Flow Solution

This section describes the forward-backward sweep (FBS) method used to obtain load flow solutions and has been adapted from Kersting, 2001 [25].

## A.1. Generalized Line Model

The first step to initialize the algorithm is to introduce a generic three phase line segment model that can be used to represent every type of line encountered. The usual representation is a PI model as shown in Figure A1.
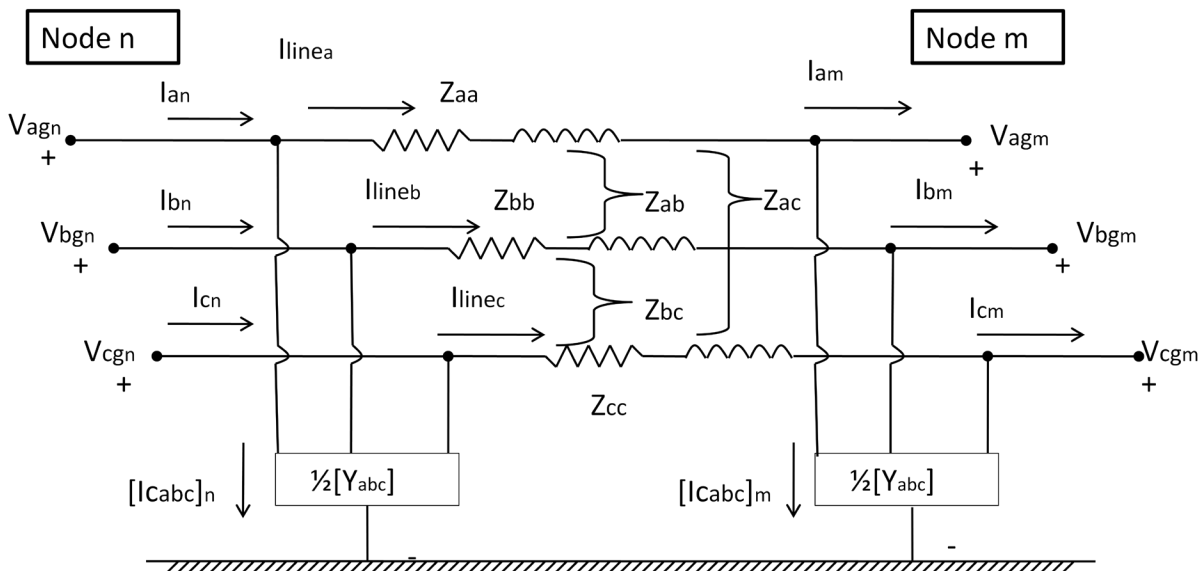


**Figure A. 1. Generic Three Phase Line**

The notation used throughout the derivation is explained as follows:

- The notation a, b and c represents the individual phases, g represents the ground or neutral

- The sending node is designated $n$, the receiving node is $m$

- Zaa is the self-impedance of the line for phase a

- Zab is the mutual impedance of the line between phase a and b

- Vag$_n$ is the line-to-neutral voltage for phase a at node n.

- [Yabc] is the 3x3 admittance matrix for the line segment containing self and mutual admittances of the line (eq. (A1))

- Iline$_a$ is the line current between node n and m

- Ia$_n$ is the node current at node n

Applying Kirchoff's Current Law (KCL) to Figure A.1 at node m leads to:

$$
\begin{bmatrix} Iline_a \\ Iline_b \\ Iline_c \end{bmatrix}_n = \begin{bmatrix} I_a \\ I_b \\ I_c \end{bmatrix}_m + 1/2 \cdot \begin{bmatrix} Y_{aa} & Y_{ab} & Y_{ac} \\ Y_{ba} & Y_{bb} & Y_{bc} \\ Y_{ca} & Y_{cb} & Y_{cc} \end{bmatrix} \cdot \begin{bmatrix} V_{ag} \\ V_{bg} \\ V_{cg} \end{bmatrix}_m \tag{A.1}
$$

Or, in condensed matrix notation:

$$
[Iline_{abc}]_n = [I_{abc}]_m + \frac{1}{2} \cdot [Y_{abc}] \cdot [VLG_{abc}]_m \tag{A.2}
$$

where VLG is line to ground voltage. Applying Kirchoff's Voltage law (KVL) to Figure A.1 yields:

$$
[VLG_{abc}]_n = [VLG_{abc}]_m + [Z_{abc}] \cdot [Iline_{abc}]_m \tag{A.3}
$$

By substituting Equation (A.2) into Equation (A.3), rearranging and collecting terms, three equations can be found that relate the line to ground voltages ([VLG$_{abc}$]$_n$, [VLG$_{abc}$]$_m$) and node currents ([I$_{abc}$]$_n$, [I$_{abc}$]$_m$) to determine the voltage and current in a line section using generalized matrices as follows:

$$[VLG_{abc}]_n = [a][VLG_{abc}]_m + [b][I_{abc}]_m \tag{A.4}$$

$$[I_{abc}]_n = [c][VLG_{abc}]_m + [a][I_{abc}]_m \tag{A.5}$$

$$[VLG_{abc}]_m = [A][VLG_{abc}]_n - [B][I_{abc}]_m \tag{A.6}$$

$$[a] = [ID] + \frac{1}{2}[Z_{abc}][Y_{abc}], [b] = [Z_{abc}] \tag{A.7}$$

$$[c] = [Y_{abc}] + \frac{1}{4}[Y_{abc}][Z_{abc}][Y_{abc}] \tag{A.8}$$

$$[A] = [a]^{-1}, \qquad [B] = [a]^{-1}[b] \tag{A.9}$$

where [ID] is the 3x3 identity matrix and [a], [b], [c], [A] and [B] are the generalized line matrices. These matrices depend only on the impedance and admittance of the line segment being considered and as such are constant throughout the calculations. The equations derived above are for a three phase line segment and can be easily extended to single or two phase sections by replacing the corresponding rows and columns of non-existent phases of the impedance and admittance matrices with zeros.

## A.2. Forward-Backward Sweep Algorithm

The forward-backward sweep FBS algorithm presented here makes a few simplifying assumptions. First, the substation voltage level is assumed to be set at a constant level throughout the algorithm. All loads are complex containing real and reactive components, and assumed to be in steady-state throughout the power flow solution. Secondary transformers generally have low impedances and are not included in the calculations, thus all loads are assumed to be spot loads occurring on the primary side of the network.

The FBS algorithm begins by assuming that the voltages at the terminal (end-point) buses are equivalent to the source or substation voltage. Then the end node current (node $m$) can be calculated as:

$$[I_{abc}]_m = \left( \frac{[S_{abc}]_m}{[VLG_{abc}]_m} \right)^*$$

(A.10)

where the * represents the complex conjugate and $[S_{abc}]_n$ is the three phase complex power at bus $m$. Then, applying Equation (A.4) using the current in each branch $[I_{abc}]_n$, calculated from Equation (A.10) the voltage at the upstream bus is found.  This upstream voltage is then used to calculate the current at the upstream bus by applying Equation (A.5).

If a bus is a junction where two or more branches extend from, then both the downstream voltages need to be determined before using Equations (A.4) and (A.5). In this fashion, the bus voltages and currents are calculated stepping line by line towards the substation bus. The calculated substation bus voltage is compared to the actual known voltage of the substation and, if it is within the tolerance of the solution ($1 \times 10^{-4}$), then the algorithm is considered to be converged. If the calculation must continue, the backward sweep begins.

The backward sweep works in the opposite direction to the forward sweep. It begins by using the known set-point voltage at the substation and proceeds to calculate the downstream bus voltage using the line currents calculated during the forward sweep. The backward sweep uses Equation (A.6) to update the downstream voltages at each bus and steps through all the buses until the terminal nodes have been reached. When all the end node voltages have been calculated, the forward sweep can begin again starting with the end nodes and using the updated voltages from the backward sweep. The whole process is repeated alternating between forward and backward sweeps until convergence is reached.

After the FBS solution has converged, the power loss in the network can be calculated as well as the current flowing in the neutral wire due to the imbalance of the loads. Complex power loss, $S_{loss}$, can be calculated when the currents and voltages are known by calculating the difference in voltage between sending and receiving end, multiplied by the complex conjugate of the current in the branch [43]:

$$[Sloss]_m = ([V_{abc}]_n - [V_{abc}]_m) \cdot [I_{abc}]_n{}^* \tag{A.11}$$

The power loss in each branch can then be summed over all the branches in the network to estimate the total network power loss.

# Appendix B. The Per-unit System of Calculations

It is convenient and customary to use the per-unit (p.u.) system when performing load flow calculations and examining electrical power systems. The per-unit value of a quantity is defined as the ratio of the quantity to its base value expressed as a decimal [44]. In a three phase distribution system, the selection of two base variables determines the base values of the other two variables (current, voltage, complex power or impedance). The bases values given are usually the line-to-line Voltage (kVLL) and complex power (MVA) total over three phases.

The following equations can be used to calculate the other base quantities:

$$Base\ current\ (A) = \frac{1000 * base\ power\ MVA\ (3phase)}{\sqrt{3} * Base\ Voltage, kV\ line - line} \tag{B.1}$$

$$Base\ Voltage\ line - ground\ (kV) = \frac{base\ Voltage, kV\ line - line}{\sqrt{3}} \tag{B.2}$$

$$Base\ Impedance\ (\Omega) = \frac{(Base\ Voltage, kV\ line - line)^2}{base\ MVA\ (3\ phase)} \tag{B.3}$$

At the start of the load flow solution all variables are converted into p.u. quantities, then all calculations can precede without the need to check units.

# Appendix C. Hypothesis Testing for Normal Distribution of Residential Loads

This section describes the process used to validate the assumption that the load within an hour is normally distributed for a group of customers. In order to make the validation, a series of secondary transformer level readings were used for groups of 2 to 20 residential single detached dwelling customers. The readings were taken at 15 minute intervals for a period of one month.

A chi-squared goodness-of-fit test [45] is used to test the null hypothesis that some data is a random sample from a normal distribution with the mean and standard deviation estimated from the sample. The alternative, i.e. rejection of the null hypothesis occurs when the data is not from a normal distribution at the given confidence level, in our case 95%. The transformer data was grouped by the 15 minute intervals over the entire month. This lead to 96 vectors (every 15 minutes for 24 hours) of transformer data with 30 data points in each vector, for each group of customers considered. The chi-square test was then performed for each of these data vectors. The total number of rejections of the null hypothesis was counted for each customer and compared to the total sample. Figure C.1 shows the frequency of rejection of the null hypothesis at the 95% confidence level for the range of customers considered.

Figure C.1 shows that for groups of customers greater than 5, only a small percentage of the samples (<10%) rejected the null hypothesis that the data was normally distributed. The assumption that the load is normally distributed within an hour for each group of customers should then be valid, as it is rare for the networks considered in this study that the number of customers connected to a transformer is less than 5.
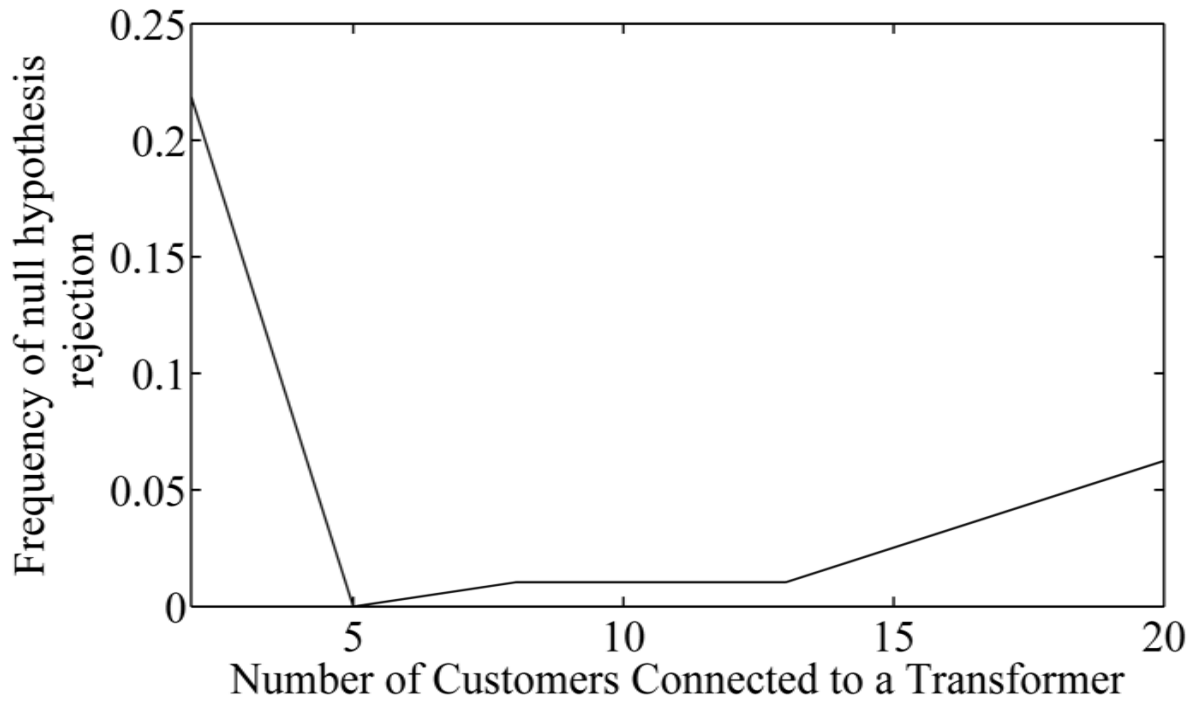
**Figure C.1. Frequency of chi-square test null hypothesis rejection for various sized groups of residential customers, 95% confidence level**

# Appendix D. Topology and Length of Selected Networks

This section contains Figures D.1, D.2 and D.3 showing the topology and relative distance of the
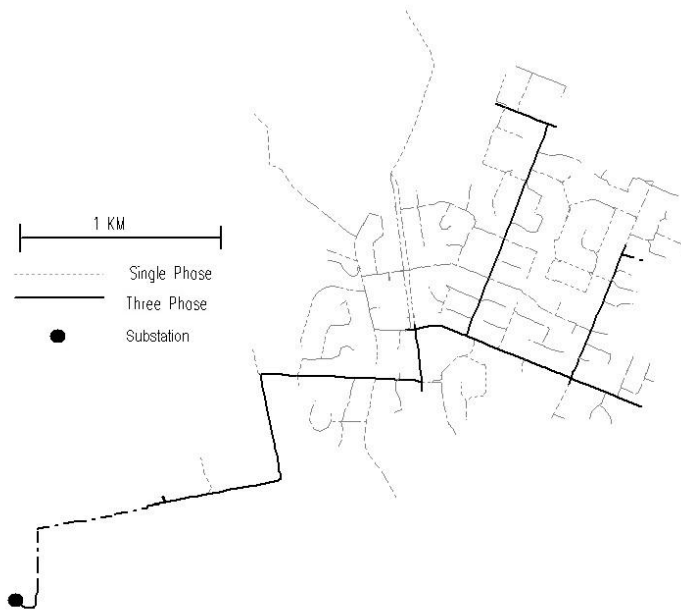
suburban, urban and rural locations.



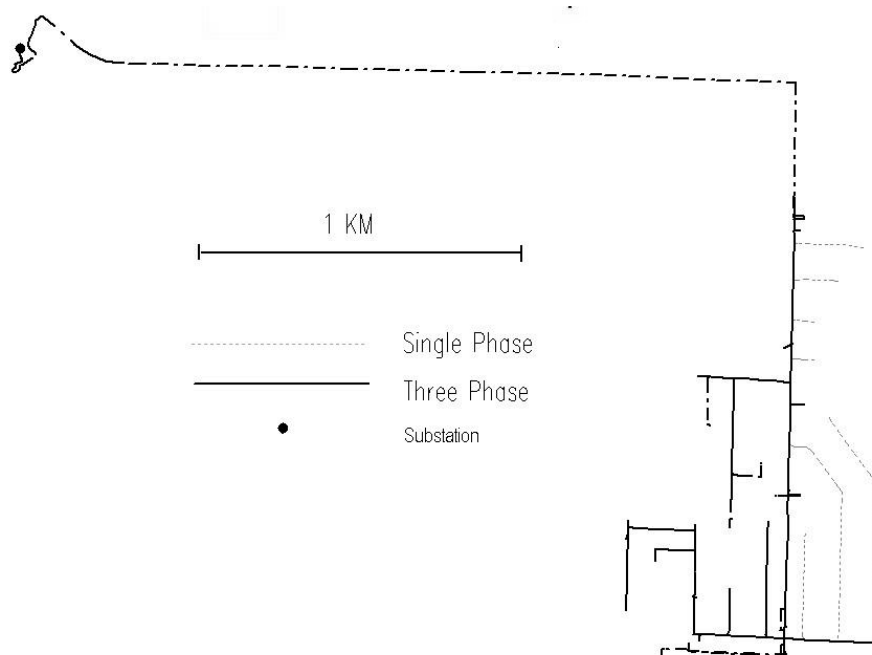**Figure D. 1. Suburban Network (BCHydro code: GTP2546)**

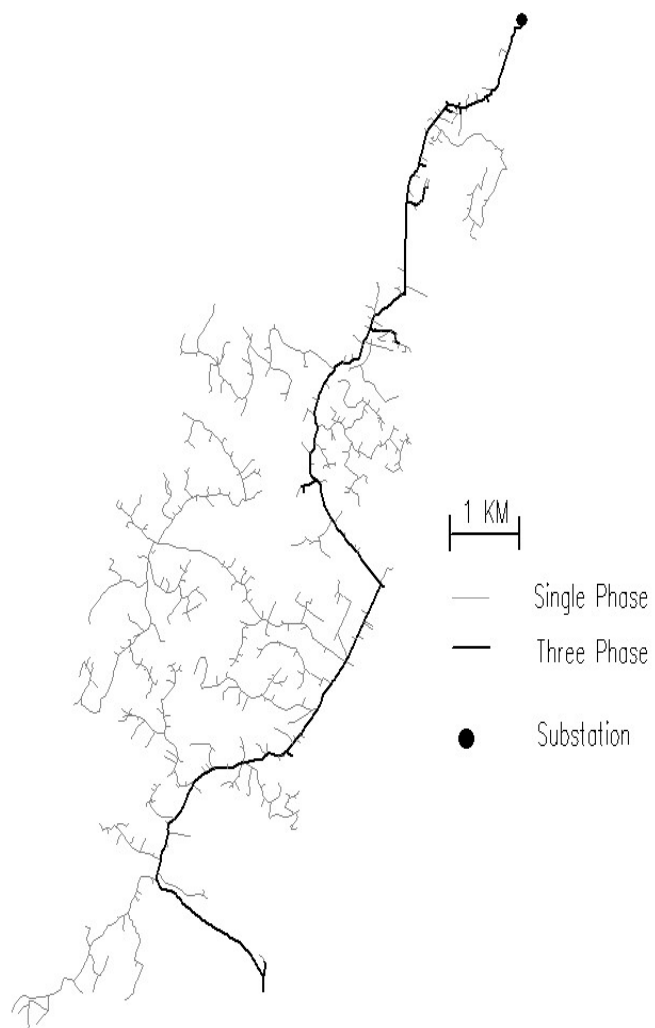**Figure D. 2 Urban Feeder (BCH code: SPG12F112)**

**Figure D. 3 Rural Network (BCHydro code: CLD2573)**

# Appendix E. Summary of Transformer Insulation Loss of Life Calculations

The IEEE standard C57.91-1995 [37] sets forth a guide for loading of mineral oil immersed transformers in order to estimate the risk associated with application of loads in excess of nameplate ratings of distribution and substation (power) transformers. The standard sets a guideline for calculating the ageing of insulation material due to high temperatures caused by overloading a transformer. The calculations and input data used for the calculations in Section 5.5.2 are summarized below.

## E.1 Definitions and Equivalent Ageing

Deterioration of insulation material is a time function of the temperature, moisture content and oxygen content. Usually, oxygen content and moisture content are ignored when considering deterioration calculations and insulation temperature is the only factor considered as it contributes the most deterioration. The temperature distribution within a transformer is not uniform and the part of the insulation that is at the highest temperature will undergo the most deterioration, this is called the "hottest-spot" temperature. First a number of definitions will be made:

[1] **Average winding temperature rise:** The arithmetic difference between the average winding temperature of the hottest winding and the ambient temperature. Typically this value is 65°C at rated load.

[2] **Hottest spot temperature:** The part of the insulation that is at the highest temperature that undergoes the most deterioration.

**[3] Hottest spot temperature rise:** The arithmetic difference between the hottest-spot temperature and the top-oil temperature.

**[4] Top-oil rise:** The arithmetic difference between hottest oil temperature and ambient temperature for a given load.

**[5] Normal Life:** The lifetime of a transformer's insulation when operating with a 65°C average winding temperature rise, 110°C hottest-spot temperature and an ambient temperature of 30°C. The expected lifetime of a transformer operating in this way with an end of life criterion being 25% retained tensile strength of insulation is 180,000 hours or 20.55 years.

From experimentally determined evidence, the per unit transformer insulation life curve follows an Arrhenius reaction rate theory based on hottest spot temperature $T_H$:

$$\text{Per unit life} = 9.80\text{x}10^{-18}e^{\left(\frac{1500}{T_H+273}\right)} \tag{E.1}$$

Using the definition of per unit life, for a given load and temperature, an ageing acceleration factor ($F_{AA}$) can be calculated:

$$F_{AA} = e^{\left(\frac{1500}{383}-\frac{1500}{T_H+273}\right)} \tag{E.2}$$

Then, for a hottest spot temperature of 110°C, the ageing acceleration factor calculated in Equation (E.2) will give a value of 1. For hottest spot temperatures above 110°C, the $F_{AA}$ will be greater than 1; for temperatures below 110°C, $F_{AA}$ will be below 1.

Equation (E.2) can be used to calculate the equivalent ageing of a transformer in hours. The equivalent ageing ($F_{EQA}$) at the reference temperature (110°C) that will be consumed in a given time period for a given temperature and load cycle is:

$$F_{EQA} = \frac{\sum_{h=1}^{N} F_{AA,h} \Delta t_h}{\sum_{h=1}^{N} \Delta t_h} \tag{E.3}$$

where h is the index of the time interval, N is the total number of time intervals (48) and $\Delta t_h$ is the time interval (0.5 hours). Now, percent loss of life can be calculated by dividing $F_{EQA}$ by the total expected lifetime at the reference temperature (180,000 hours) and multiplying by 100:

$$\% \text{ Loss of life} = \frac{F_{EQA} \cdot t \cdot 100}{180,000} \tag{E.4}$$

Other reference lifetimes can be used; however, 180,000 hours was selected as it is the longest expected lifetime considered in standard C57.91.

## E.2 Calculation of Temperatures

To evaluate a transformers loss of life by using Equations (E.2) – (E.4), a hottest spot temperature must first be calculated for a given load cycle and ambient temperature. The hottest spot temperature is assumed to consist of three components: Ambient temperature ($T_A$), top-oil rise over ambient ($\Delta T_{TO}$) and winding hot-spot rise over top oil ($\Delta T_H$):

$$T_H = T_A + \Delta T_{TO} + \Delta T_H \tag{E.5}$$

The temperature calculations assume a constant ambient temperature. First, the equations relating to the top-oil rise will be examined. The top-oil temperature rise is given by the following exponential expression:

$$\Delta T_{TO,h} = \left(\Delta T_{TO,U} - \Delta T_{TO,h-1}\right) \cdot \left(1 - e^{-\frac{1}{\tau_{TO}}}\right) + \Delta T_{TO,h-1} \tag{E.6}$$

where $\Delta T_{TO,U}$ is the ultimate top-oil rise, $\Delta T_{TO,h}$ is the top oil rise for the interval h and $\tau_{TO}$ is the top-oil time constant. The initial top-oil rise for the first time interval considered is:

$$\Delta T_{TO,h=1} = \Delta T_{TO,R} \left(\frac{K_{h=1}^{2} R + 1}{R + 1}\right)^{n} \tag{E.7}$$

where $\Delta T_{TO,R}$ is the top oil rise at rated load, $K_h$ is the ratio of the load at h to the rated load, R is the ratio of load loss at rated load to no-load loss, and n is an experimentally determined constant that accounts for changes in resistance with changes in load. The ultimate top oil rise is found using Equation (E.7) with the maximum value of $K_h$. The top-oil time constant at rated load is calculated from a thermal capacity of the transformer (C), the top-oil rise at rated load ($\Delta T_{TO,R}$) and the total loss at rated load ($L_{T,R}$):

$$\tau_{TO,R} = \frac{\Delta T_{TO,R} C}{L_{T,R}} \tag{E.8}$$

The top-oil time constant is:

$$\tau_{TO} = \tau_{TO,R} \left( \frac{\frac{\Delta T_{TO,U}}{\Delta T_{TO,R}} - \frac{\Delta T_{TO,h}}{\Delta T_{TO,R}}}{\left(\frac{\Delta T_{TO,U}}{\Delta T_{TO,R}}\right)^{1/n} - \left(\frac{\Delta T_{TO,h}}{\Delta T_{TO,R}}\right)^{1/n}} \right) \qquad (E.9)$$

Thermal capacity of the transformer can be estimated empirically using the weight of core and coil assembly ($W_c$, kg), weight of tank and fittings ($W_t$, kg) and volume of oil ($V_{oil}$, L):

$$C = 0.0272 W_c + 0.01814 W_t + 5.034 V_{oil} \qquad (E.10)$$

To complete the calculation of Equation (E.5), the winding hot spot temperature rise is needed:

$$\Delta T_{H,h} = \left(\Delta T_{H,U} - \Delta T_{H,h-1}\right)\left(1 - e^{-t/\tau_w}\right) + \Delta T_{H,h-1} \qquad (E.11)$$

where $\Delta T_{H,h}$ is the hot-spot temperature rise (over top-oil), $\Delta T_{H,U}$ is the ultimate (maximum) hot-spot temperature rise, and $\tau_w$ is the winding time constant. The initial hot-spot rise over top-oil is given by:

$$\Delta T_{H,i} = \Delta T_{H,R} K_h^{2m} \qquad (E.12)$$

where $\Delta T_{H,R}$ is the hot-spot rise at rated load, $K_h$ is the ratio of load to rated load at each interval, m is an experimentally determined exponent. The ultimate hot-spot rise over top-oil is found using Equation (E.12) with the maximum value of $K_h$. Finally, the rated value of hot-spot rise over top oil $\Delta T_{H,R}$, is given by:

$$\Delta T_{H,R} = \Delta T_{H/A,R} - \Delta T_{TO,R} \qquad (E.13)$$

The value $\Delta T_{H/A,R}$ is the hot-spot rise over ambient temperature at the rated load which is assumed to be 80 °C.

## E.3 Summary of Transformer Constants for Loss of Life Calculations

The constants needed to calculate the temperature and equivalent ageing of the transformers considered in this thesis are shown in Table E.1.

**Table E. 1. Constants used for transformer loss of life calculations**

| Parameter | 25 kVA transformer | 50 kVA transformer |
|---|---|---|
| $L_{T,R}$ (W) | 336 | 605 |
| $W_C$ (kg) | 126 | 204 |
| $W_T$ (kg) | 54 | 88 |
| $V_{oil}$ (L) | 40 | 84 |
| R | 4.870 | 5.762 |
| n/m | 0.8 | 0.8 |
| $\tau_w$ (hours) | 0.05 (h) | 0.05 |
| $\Delta T_{TO,R}$ (°C) | 50.9 | 50.9 |